National Library of Canada
Canadian Theses Service
Ottawa, Canada
K1A 0N4

Bibliothèque nationale du Canada
Services des thèses canadiennes

CANADIAN THESES

THÈSES CANADIENNES

NOTICE

The quality of this microfiche is heavily dependent upon the quality of the original thesis submitted for microfilming. Every effort has been made to ensure the highest quality of reproduction possible.

If pages are missing, contact the university which granted the degree.

Some pages may have indistinct print especially if the original pages were typed with a poor typewriter ribbon or if the university sent us an inferior photocopy.

Previously copyrighted materials (journal articles, published tests, etc.) are not filmed.

Reproduction in full or in part of this film is governed by the Canadian Copyright Act, R.S.C. 1970, c. C-30. Please read the authorization forms which accompany this thesis.

AVIS

La qualité de cette microfiche dépend grandement de la qualité de la thèse soumise au microfilmage. Nous avons tout fait pour assurer une qualité supérieure de reproduction.

S'il manque des pages, veuillez communiquer avec l'université qui a conféré le grade.

La qualité d'impression de certaines pages peut laisser à désirer, surtout si les pages originales ont été dactylographiées à l'aide d'un ruban usé ou si l'université nous a fait parvenir une photocopie de qualité inférieure.

Les documents qui font déjà l'objet d'un droit d'auteur (articles de revue, examens publiés, etc.) ne sont pas microfilmés.

La reproduction, même partielle, de ce microfilm est soumise à la Loi canadienne sur le droit d'auteur, SRC 1970, c. C-30. Veuillez prendre connaissance des formules d'autorisation qui accompagnent cette thèse.

THIS DISSERTATION
HAS BEEN MICROFILMED
EXACTLY AS RECEIVED

LA THÈSE A ÉTÉ
MICROFILMÉE TELLE QUE
NOUS L'AVONS REÇUE

NL 339 (r. 86/01)

Canada

THE UNIVERSITY OF ALBERTA

Mineralogic, Fluid Inclusions and Isotopic Investigations of the Great Bear Lake Silver Deposits, Northwest Territories

by

(C) Amarendra Changkakoti

A THESIS

SUBMITTED TO THE FACULTY OF GRADUATE STUDIES AND RESEARCH

IN PARTIAL FULFILMENT OF THE REQUIREMENTS FOR THE DEGREE

OF Doctor of Philosophy

Department of Geology

EDMONTON, ALBERTA

Fall, 1985

National Library of Canada | Bibliothèque nationale du Canada

Ottawa, Canada
K1A 0N4

58

TC –

ISBN 0-315-22924-1

CANADIAN THESES ON MICROFICHE SERVICE – SERVICE DES THÈSES CANADIENNES SUR MICROFICHE

PERMISION TO MICROFILM – AUTORISATION DE MICROFILMER

• Please print or type – Écrire en lettres moulées ou dactylographier

AUTHOR – AUTEUR

Full Name of Author – Nom complet de l'auteur

AMARENDRA CHANGKAKOTI

Date of Birth – Date de naissance
01/02/54

Canadian Citizen – Citoyen canadien
☐ Yes / Oui ☑ No / Non

Country of Birth – Lieu de naissance
KOHIMA, INDIA

Permanent Address – Résidence fixe
C/O MR. B.N. CHANGKAKOTI
MILANPUR ROAD
BAMUNIMAIDAM, GAUHATI-781021
INDIA

THESIS – THÈSE

Title of Thesis – Titre de la thèse

MINERALOGIC, FLUID INCLUSIONS AND ISOTOPIC INVESTIGATIONS OF THE GREAT BEAR LAKE SILVER DEPOSITS, NORTHWEST TERRITORIES

PH.D.

Degree for which thesis was presented
Grade pour lequel cette thèse fut présentée
PH.D.

Year this degree conferred
Année d'obtention de ce grade
1985

University – Université
ALBERTA.

Name of Supervisor – Nom du directeur de thèse
DR. R.D. MORTON

AUTHORIZATION – AUTORISATION

Permission is hereby granted to the NATIONAL LIBRARY OF CANADA to **microfilm** this thesis and to **lend** or **sell copies of the film.**

The author reserves other publication rights, and neither the thesis nor extensive extracts from it may be printed or otherwise reproduced without the author's written permission.

L'autorisation est, par la présente, accordée à la BIBLIOTHÈQUE NATIONALE DU CANADA de **microfilmer** cette thèse et de **prêter** ou de **vendre des exemplaires du film.**

L'auteur se réserve les autres droits de publication; ni la thèse ni de longs extraits de celle-ci ne doivent être imprimés ou autrement reproduits sans l'autorisation écrite de l'auteur.

ATTACH FORM TO THESIS – VEUILLEZ JOINDRE CE FORMULAIRE À LA THÈSE

Signature
Amarendra Changkakoti

Date
15/10/85

NL-91 (r. 84/03)

Canada

THE UNIVERSITY OF ALBERTA

RELEASE FORM

NAME OF AUTHOR Amarendra Changkakoti

TITLE OF THESIS Mineralogic, Fluid Inclusions and Isotopic Investigations of the Great Bear Lake Silver Deposits, Northwest Territories

DEGREE FOR WHICH THESIS WAS PRESENTED Doctor of Philosophy

YEAR THIS DEGREE GRANTED Fall, 1985

Permission is hereby granted to THE UNIVERSITY OF ALBERTA LIBRARY to reproduce single copies of this thesis and to lend or sell such copies for private, scholarly or scientific research purposes only.

The author reserves other publication rights, and neither the thesis nor extensive extracts from it may be printed or otherwise reproduced without the author's written permission.

(SIGNED) Changkakoti

PERMANENT ADDRESS:

C/O. MR. B N. CHANGKAKOTI
MILANPUR ROAD, BAMUNIMAIDAM
GAUHATI - 781021, INDIA

DATED 15th Oct 1985.

THE UNIVERSITY OF ALBERTA

FACULTY OF GRADUATE STUDIES AND RESEARCH

The undersigned certify that they have read, and recommend to the Faculty of Graduate Studies and Research, for acceptance, a thesis entitled Mineralogic, Fluid Inclusions and Isotopic Investigations of the Great Bear Lake Silver Deposits, Northwest Territories submitted by Amarendra Changkakoti in partial fulfilment of the requirements for the degree of Doctor of Philosophy.

.....

Supervisor

.....

.....

.....

.....

External Examiner

Date... 15th October 1985...

Dedication

I dedicate this thesis to my parents and swami.

ABSTRACT

The silver deposits of the Great Bear Lake region occur within two sectors, the Echo Bay sector and the Camsell River sector. The veins are hosted by volcano-sedimentary and intrusive rocks. Native silver, arsenides, sulpharsenides, native bismuth, sulfides, sulphosalts, hematite, uraninite, quartz, calcite, dolomite and fluorite were identified in the veins. Electron microprobe analyses revealed regional variations in the concentration of mercury in native silver, and in the concentration of arsenic in nickeline, cobaltite and gersdorffite.

Fluid inclusion studies of gangue minerals from different paragenetic stages suggest a wide range in salinity and temperature for the hydrothermal fluids. The salinities of the fluids range from about 15 to 35 wt.% NaCl equivalent. The homogenization temperatures range from 150° to 250°C for stage I fluids; 220° to 480°C for stage II fluids; 250° to 350°C for stage III fluids; 150° to 250°C for stage IV fluids and 90° to 250°C for stage V fluids. The coexistence of saturated and unsaturated inclusions in stages II and III minerals suggest that the hydrothermal fluids were boiling or effervescing. The coexistence of saturated and unsaturated inclusions in stages II and III minerals may be due to effervescence of a less saline fluid, whilst for stages IV and V it may be due to mixing of a highly saline fluid with a less saline fluid, or due to alternation of hydrostatic and lithostatic pressures at the time of trapping of the inclusions.

Stable isotopic studies show a wide range in $\delta^{18}O$ (6.8 to 22.5 per mil, SMOW) and $\delta^{13}C$ (-2.7 to -13.3 per mil, PDB) values of the carbonates. The $\delta^{18}O$ values of quartz range from 6.63 to 17.25 per mil (SMOW). The δD values of inclusion water in quartz, calcite, dolomite and nickeline vary from -48.7 to -135.6 per mil (SMOW), The δD values of present day waters from the region vary from -146.5 to -165.2 per mil (SMOW). The calculated oxygen isotopic compositions of the hydrothermal fluids vary from 5.6 to 10.0 per mil (SMOW) for stages I, II and III fluids, and -1.1 to 4.2 per mil (SMOW) for stages IV and V fluids, thereby indicating initial magmatic fluids and the influence of a subsequent fluid which was probably a mixture of

magmatic-, meteoric- or sea-water. The $\delta^{13}C$ values (-3.1 to -8.6 per mil, PDB) of the hydrothermal fluids suggest a magmatic source for the earlier generation carbonates.

Lead isotope data of vein carbonates, galena and chalcopyrite indicate a mineralization age of around 1500 Ma. Lead isotope data of sulfides and lead and strontium isotope data of carbonates suggest a multi-source derivation of Pb and Sr in the vein minerals.

The metals were transported by moderate to high salinity hydrothermal fluids as complexes. Uranium was either transported as carbonate or hydroxyl complexes, whilst the other metals were probably transported mainly as chloride complexes. The metals were deposited in dilatant zones due to decrease in temperature, pressure, boiling or mixing of different types of fluids.

Acknowledgments

The author is indebted to Dr. R.D. Morton for suggesting the thesis area and for his guidance and support during the course of the work. Financial support by Dr. J. Gray during the final stages of research is gratefully acknowledged. Dr. W. Padgham of the Department of Indian Affairs and Northern Development, Yellowknife, arranged finances for field work.

Field work was also supported by the Echo Bay Mines Limited, and Terra Mining and Exploration Limited. The collecting of a complete suite of specimens would not have been possible without the most generous cooperation of Dr. E. Buhlmann of Terra Mining and Exploration Ltd., Mr. G. Woollett of Trigg, Woollett Olson Consulting Limited, and the geological staff of both Terra Mining and Exploration Ltd. and the Echo Bay Mines Ltd..

Mr. S. Launspach helped with the electron microprobe analyses and data reduction. The electron microprobe facilities were generously supported by an NSERC grant # A4254 to Dr. D.G.W. Smith. Dr. H. Baadsgaard assisted with the lead isotope analyses of the sulphides. Particular thanks are extended to Mr. D.K. Ghosh and Mr. D. Krstic for analyzing the carbonate samples for lead and strontium isotopes, to Dr. C.J. Yonge for teaching the basic techniques of stable isotope analysis, to Dr. K. Muehlenbachs for analyzing the quartz samples for oxygen isotopes, to Mr. H.K. Sarma for helping with the computing, to Mr. L. Tober for helping with the hydrogen mass spectrometer, and to Mr. F. Dimitrov for drafting some of the diagrams.

Special thanks are extended to Miss F. Hennessey, Mr. A. Sen, Mr. B. Ramani, Mr. E. Persaud, Mr. J. Walker, Mr. and Mrs. Rao, Mrs. Kumar and Ananda Baba for their help and encouragement in the compilation of this thesis.

Table of Contents

Chapter		Page
1.	INTRODUCTION	1
	1.1 Introduction	2
	1.2 Previous Work	4
	1.3 Present Investigation	5
2.	REGIONAL GEOLOGIC SETTING OF THE SILVER DEPOSITS OF THE NORTHWEST TERRITORIES	7
	2.1 Introduction	8
	2.1.1 The Wopmay Orogen	8
	2.1.2 The Amundsen Basin	10
	2.2 The Great Bear Batholith	10
	2.2.1 Intrusive Rocks of the Batholithic Complex	12
	2.2.2 Structural Features of the Batholithic Complex	14
	2.2.3 Giant Quartz Veins	14
	2.2.4 Non-Granitic Intrusions	15
	2.2.5 Metamorphism	15
3.	THE SILVER DEPOSITS	17
	3.1 Introduction	18
	3.2 The Echo Bay Sector	18
	3.2.1 The Eldorado Deposit	18
	3.2.2 The Contact Lake Deposit	22
	3.2.3 The Echo Bay Deposit	22
	3.2.4 The El Bonanza Deposit	23
	3.3 The Camsell River Sector	23
	3.3.1 The Terra Deposit	23
	3.3.2 The Norex Deposit	25
	3.3.3 The Smallwood Deposit	26

3.3.4 The Northrim Deposit 26

4. ORE- AND GANGUE- MINERALOGY 27

4.1 Introduction 28

4.2 Mineralogy of the Veins 28

4.3 Arsenides 28

4.3.1 Monoarsenides 29

4.3.1.1 Nickeline (NiAs) 29

4.3.2 Metal-Rich Arsenides 35

4.3.2.1 Maucherite ($Ni_{11}As_8$) 35

4.3.3 Diarsenides 35

4.3.3.1 Safflorite ($CoAs_2$) 38

4.3.3.2 Loellingite ($FeAs_2$) 43

4.3.3.3 Rammelsbergite ($NiAs_2$) 44

4.3.3.4 Pararammelsbergite ($NiAs_2$) 45

4.3.4 Triarsenides 48

4.3.4.1 Skutterudite ($CoAs_{3\pm x}$) 50

4.3.5 Sulpharsenides 54

4.3.5.1 Cobaltite (CoAsS) 54

4.3.5.2 Gersdorffite (NiAsS) 59

4.3.5.3 Arsenopyrite (FeAsS) 63

4.4 Native Silver 66

4.4.1 Composition of Native Silver 66

4.4.2 Classification of Native Silver 69

4.4.2.1 Aurian Silver 69

4.4.2.2 Mercurian Silver 69

4.4.2.3 Cuprian Silver 70

4.4.2.4 Arsenian Silver 70

4.4.2.5 Antimonian Silver 70
4.4.3 Electron Microprobe Analyses of Native Silver 71
4.5 Native Bismuth 71
4.6 Sulphosalts 75
4.7 Oxides 77
4.7.1 Uraninite 77
4.7.2 Hematite 77
4.7.3 Magnetite 78
4.8 Sulphides 78
4.9 Gangue Minerals 80
4.10 Secondary Minerals 81
4.11 Interpretations of Ore Textures 82
4.11.1 Replacement Texture 82
4.11.2 Dendrites and Rosettes 82
4.11.3 Other Textures 85
4.12 Parageneses 87
5. FLUID INCLUSION STUDY 95
5.1 Introduction 96
5.2 Fluid Inclusion Studies in the Great Bear Lake Silver Deposits 96
5.3 Petrographic Descriptions of the Inclusions 97
5.3.1 Classification of Inclusions 97
5.3.2 Types of Inclusions 98
5.4 Salinities of the Hydrothermal Fluids 104
5.5 Temperatures of the Hydrothermal Fluids 106
5.6 Density of the Hydrothermal Fluids 112
5.7 Conclusions 112
6. OXYGEN-, HYDROGEN- AND CARBON- ISOTOPE GEOCHEMISTRY 115

6.1 Introduction 116
6.2 Results 117
6.2.1 $^{18}O/^{16}O$ ratios of the carbonates and quartz 117
6.2.2 D/H ratios of the hydrothermal fluids and present day waters 125
6.2.3 $^{13}C/^{12}C$ ratios of carbonates 125
6.2.4 Oxygen isotopic composition of the hydrothermal fluids 125
6.2.5 Carbon isotopic composition of the hydrothermal fluids 127
6.3 Discussion 128
7. LEAD- AND STRONTIUM- ISOTOPE GEOCHEMISTRY 132
7.1 Introduction 133
7.2 Lead Isotope Study 133
7.2.1 Results and Interpretations of Lead Data 133
7.3 Strontium Isotope Study 138
7.4 Rubidium-Strontium Isotope Study in the Great Bear Lake Region 139
7.4.1 Results and Interpretations of Strontium Data 139
8. TRANSPORT AND DEPOSITION OF METALS 143
8.1 Introduction 144
8.2 Environment of Ore Deposition in the Great Bear Lake Silver Deposits 145
9. GENESIS OF THE DEPOSITS 156
9.1 Introduction 157
9.2 The Ag - Co - Ni - As ± Bi ± U Association 157
9.3 A Brief Review on the Geneses of the Great Bear Lake Silver Deposits 158
9.4 Genesis of the Deposits 161
10. CONCLUSIONS 166
11. REFERENCES 170
12. APPENDIX I 201
12.1 Electron Microprobe Analyses of the Arsenides and Native Silver 202

12.2 Fluid Inclusion Analyses 202

12.3 Oxygen-, Carbon- and Hydrogen- Isotope Analyses 203

12.3.1 Oxygen and carbon isotope ratios 203

12.3.2 Hydrogen isotope ratios 204

12.4 Lead and Strontium Isotope Analyses 204

13. APPENDIX II 208

List of Tables

Table 1. Electron microprobe analyses of nickelines from the Great Bear Lake silver deposits, N.W.T. 32

Table 2. Electron microprobe analyses of maucherites from the Great Bear Lake silver deposits, N.W.T. 36

Table 3. Electron microprobe analyses of safflorites from the Great Bear Lake silver deposits, N.W.T. 41

Table 4. Electron microprobe analyses of loellingites from the Great Bear Lake silver deposits, N.W.T. 44

Table 5. Electron microprobe analyses of rammelsbergites from the Great Bear Lake silver deposits, N.W.T. 46

Table 6. Electron microprobe analyses of pararammelsbergites from the Great Bear Lake silver deposits, N.W.T. 49

Table 7. Electron microprobe analyses of skutterudites from the Great Bear Lake silver deposits, N.W.T. 51

Table 8. Electron microprobe analyses of cobaltites from the Great Bear Lake silver deposits, N.W.T. 55

Table 9. Electron microprobe analyses of gersdorffites from the Great Bear Lake silver deposits, N.W.T. 61

Table 10. Electron microprobe analyses of arsenopyrites from the Great Bear Lake silver deposits, N.W.T. 65

Table 11. Electron microprobe analyses of native silvers from the Great Bear Lake silver deposits, N.W.T. 72

Table 12. Temperature and salinity data for hydrothermal fluids in the Great Bear Lake silver deposits, N.W.T. 107

Table 13. Isotopic data for hydrothermal minerals and fluids in the Great Bear Lake silver deposits, Northwest Territories 118

Table 14. Lead isotope data for hydrothermal minerals in the Great Bear Lake silver deposits, N.W.T. 134

Table 15. Rubidium and strontium isotope data for hydrothermal minerals in the Great Bear Lake silver deposits, N.W.T. 140

Table 16. Reactions used in the construction of the phase diagrams 147

List of Figures

Figure 1. Location of the silver deposits 3

Figure 2. Regional geology of the Wopmay Orogen and adjacent areas (modified after Hildebrand, 1983) 9

Figure 3. Intrusive rocks of the Great Bear Magmatic Zone (modified after Hoffman and McGlynn, 1977) 13

Figure 4. Location and geology of the silver deposits in the Echo Bay sector (modified after Hoffman *et al.* 1976) 19

Figure 5. Cross-section through the Eldorado mine showing the different vein zones (modified after Campbell, 1957) 21

Figure 6. Location and geology of the silver deposits in the Camsell River sector (modified after Hildebrand, 1983) 24

Figure 7. Variations of As+S+Sb : Ni+Co ratios of nickelines in the ores of the Great Bear Lake silver deposits 34

Figure 8. Compositional limits of natural diarsenides. H - Holmes (1947). R - Roseboom (1963). R & B - Radcliffe and Berry (1968) 37

Figure 9. Compositional variations of the diarsenides in the ores of the Great Bear Lake silver deposits 39

Figure 10. Compositional variations of skutterudites in the ores of the Great Bear Lake silver deposits 53

Figure 11. Compositional variations of the sulpharsenides in the ores of the Great Bear Lake silver deposits 57

Figure 12. Variations of As+Sb : S ratios of cobaltites in the ores of the Great Bear Lake silver deposits 58

Figure 13. Variations of As+Sb : S ratios of gersdorffites in the ores of the Great Bear Lake silver deposits 64

Figure 14. Ternary plot of Ag-Hg-Sb showing the variations of native silver in the ores of the Great Bear Lake silver deposits 74

Figure 15. Paragenesis of the Terra deposit 88

Figure 16. Paragenesis of the Norex deposit 89

Figure 17. Paragenesis of the Northrim deposit 90

Figure 18. Paragenesis of the Smallwood deposit 91

Figure 19. Paragenesis of the Eldorado deposit 92

Figure 20. Paragenesis of the Contact Lake deposit 93

Figure 21. Paragenesis of the Echo Bay deposit 94

Figure 22. Relationship between homogenization temperature and different stages of mineralization in the Great Bear Lake silver deposits 114

Figure 23. Carbon and oxygen isotopic composition of carbonates from the veins of the Camsell River sector deposits 123

Figure 24. Carbon and oxygen isotopic composition of carbonates from the veins of the Echo Bay sector deposits 124

Figure 25. Plot of δD vs $\delta^{18}O$ values of hydrothermal fluids and present day surface and mine waters in the Great Bear Lake region. The δD of fluid inclusion waters in nickeline is plotted on the δD axis because $\delta^{18}O$ value is not available. Open circle - Calcite. Closed circle - Quartz. Open triangle - Dolomite. Closed square - Nickeline 129

Figure 26. $^{207}Pb/^{204}Pb$ vs $^{206}Pb/^{204}Pb$ plot for hydrothermal minerals in the Great Bear Lake silver deposits. Gn - Galena. Cp - Chalcopyrite. C - Carbonates 136

Figure 27. $^{87}Sr/^{86}Sr$ vs $^{87}Rb/^{86}Sr$ plot for hydrothermal carbonates in the Great Bear Lake silver deposits 141

Figure 28. An fO_2 - fS_2 diagram for the system Fe-S-O at 200°C. 149

Figure 29. An fO_2 - pH diagram for the system UO_2 - CO_2 - H_2O at 150°C..... 150

Figure 30. An fO_2 - pH diagram for the system UO_2 - CO_2 - H_2O at 200°C..... 151

Figure 31. A model illustrating the origin of the Great Bear Lake silver deposits. 165

List of Plates

Plate 1. Dendrites of native silver rimmed by nickeline (pinkish) and rammelsbergite (bluish grey). P.P.L. 200X 30

Plate 2. Nickeline (pinkish) rimmed by complex intergrowth of gersdorffite (grey), rammelsbergite (bluish grey) and cobaltite (pinkish grey). Normarsky phase interference contrast. 200X 30

Plate 3. Inclusions of native silver in safflorite stars. P.P.L. 200X 40

Plate 4. A dendrite of native silver rimmed by rammelsbergite. P.P.L. 200X 40

Plate 5. Intergrowths of gersdorffite (grey), arsenian gersdorffite (bluish grey) and nickeline (pinkish) being replaced by native bismuth (pale brownish). P.P.L. 200X 60

Plate 6. Idiomorphic (diamond-shaped) and sub-idiomorphic grains of arsenopyrite within gangue (black). P.P.L. 200X 60

Plate 7. Interstitial grains of native silver within quartz. P.P.L. 200X 67

Plate 8. Native silver replacing nickeline along fractures. P.P.L. 100X 67

Plate 9. Nickeline replacing earlier generation of native silver. P.P.L. 200X 68

Plate 10. Pseudomorph of acanthite (bluish) after native silver. The pinkish mineral is chalcopyrite. P.P.L. 100X 68

Plate 11. Native bismuth replacing skutterudite along fractures. P.P.L. 100X 76

Plate 12. Bismuthinite (grey) selectively replacing native bismuth (creamy). The enclosing mineral is safflorite. P.P.L. 200X 76

Plate 13. Chalcopyrite replacing earlier generation pyrite along fractures. P.P.L. 200X 79

Plate 14. Native bismuth (creamy) which fills cleavage planes of calcite is being replaced by bismuthinite (light grey). P.P.L. 100X 79

Plate 15. Native bismuth replacing massive skutterudite. P.P.L. 200X 83

Plate 16. Inclusions of native bismuth (pale brownish) within gersdorffite. The sub-idiomorphic grain is skutterudite. P.P.L. 100X 83

Plate 17. Native silver rimmed by carbonates and arsenides. P.P.L. 100X 84

Plate 18. Dendrites of carbonates rimmed by arsenides. P.P.L. 100X 84

Plate 19. Native silver rimmed by complex intergrowth of arsenides. Note the differences in relief of the arsenide phases. Normarsky phase interference contrast. 200X 86

Plate 20. Inclusions of arsenopyrite in a groundmass of bismuthinite, safflorite and native bismuth. P.P.L. 50X 86

Plate 21. A primary inclusion in quartz containing a liquid phase, a vapour phase and unidentified radiating daughter crystals 99

Plate 22. Primary two phase (vapour-rich) inclusions in quartz intimately associated with the arsenides 99

Plate 23. A primary three phase inclusion in quartz 100

Plate 24. A primary two phase inclusion in dolomite 100

Plate 25. A primary two phase inclusion in dolomite 101

Plate 26. A primary two phase inclusion in quartz 101

Plate 27. A primary two phase inclusion in dolomite 102

Plate 28. A primary two phase inclusion in calcite 102

Plate 29. A primary three phase inclusion in dolomite 103

Plate 30. A primary inclusion in fluorite containing a liquid phase, CO_2 and a halite daughter crystal 103

Plate 31. The crushing stage for extracting fluid inclusion waters 205

Plate 32. The hydrogen extraction line 206

1. INTRODUCTION

1.1 Introduction

The silver-bearing vein deposits of the Great Bear Lake region are located approximately 400 km north-northwest of Yellowknife in the Northwest Territories. The silver deposits occur within two separate sectors, namely, the Echo Bay sector in the north and the Camsell sector, about 50 km to the south (Fig. 1).

The deposits are best accessible by air. During the winter, heavy equipment, fuel, and other supplies are trucked into the mines by a winter road from Yellowknife. Heavy equipment could also be shipped from Fort McMurray down the Slave and McKenzie river system, Great Bear River and Great Bear Lake (Mursky, 1973).

The topography is rugged, with a maximum elevation of around 400 m above the level of the Great Bear Lake. The elevated regions are generally represented by resistant intrusive porphyries and granitic rocks, while the depressions are represented by recessive volcanic and sedimentary rocks. Glacial lakes are numerous in the region. The climate is sub-arctic with long winters and short summers.

The occurrence of mineralization in the Great Bear Lake region was first reported by J. McIntosh Bell of the Geological Survey of Canada in 1900. In 1929 Gilbert Labine and E.G. St. Paul visited the area described by Bell, and in the following year, Labine staked claims on the property which later became the Port Radium mine of Eldorado Mining and Refining Limited. They also staked claims in the southern sector, namely, the Camsell River area.

Underground operations at Port Radium started in 1932, and production started in 1934. The mine produced both uranium oxide and silver. However, the mine was closed down in 1940. It reopened in 1942 to produce uranium for strategic purposes and the company was turned into a Crown corporation in 1944 by the federal government. The mine was closed down in September 1960 when the ore reserves were exhausted.

Cominco staked the Echo Bay property in 1930 and development work was carried out until 1941. Echo Bay Mines Limited took over the property in 1964 and produced silver until its closure in 1982. The Eldorado (Port Radium), Contact Lake and El Bonanza mines were also

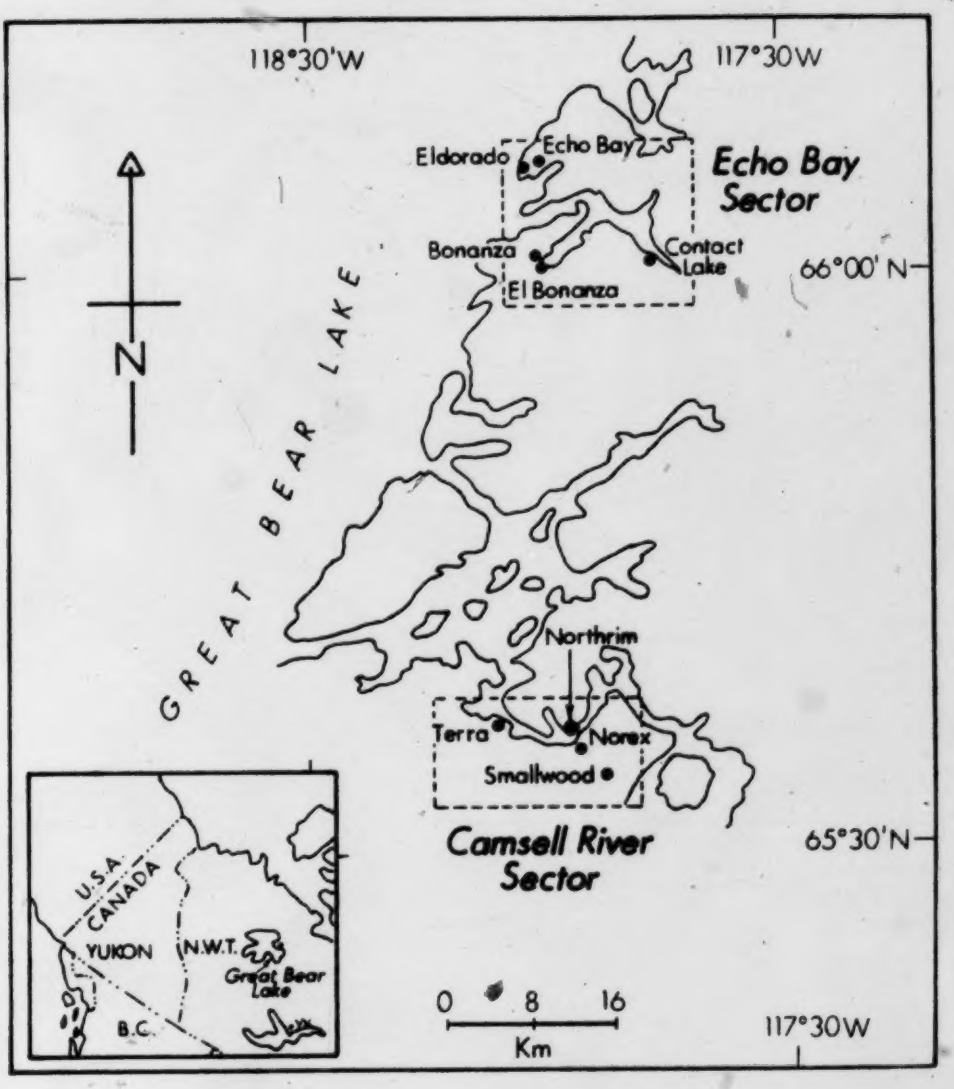

Figure 1. Location of the silver deposits.

under the management of the Echo Bay Mines Limited until their closure in 1982.

The Camsell River sector, about 50 km south of the Echo Bay sector did not receive much attention until the mid-sixties. Various companies were carrying out exploration and mining in the region until the late seventies when Terra Mining and Exploration Limited took over all the important properties in the region and continues producing silver to this day.

1.2 Previous Work

Since the first report on the occurrence of mineralization in the region in 1900, many workers have carried out investigations in the region. The first scientific report was that of Labine in 1929. Some of the earlier reports on the region are given in Kidd (1931, 1932), Kidd and Haycock (1935), Robinson (1933), Parsons (1948), Feniak (1947), Campbell (1955) and Jory (1964). Recent studies on the region may be found in Robinson (1971), Fraser *et al.* (1972), Badham (1973), Shegelski (1973), Mursky (1973), Hoffman (1973, 1978, 1980, 1982), Hoffman and Bell (1975), Hoffman *et al.* (1976), Hoffman and McGlynn (1977), Withers (1979), Hildebrand (1981, 1982, 1983, 1984).

There have been different views on the origin of the silver-bearing deposits of the region. A detailed description of the various views are given in a later section. Robinson (1971) and Robinson and Ohmoto (1973) proposed, from results of an isotopic study of the carbonates and of the late stage sulphides of the Echo Bay deposit, that heated sea water was responsible for forming that deposit. Robinson and Badham (1974) also put forward a similar hypothesis for the other deposits of the region. Shegelski (1973), Shegelski and Scott (1975) and Badham (1973, 1975), in contrast, proposed a magmatic origin for the Terra and other deposits of the Camsell River region. Hoffman *et al.* (1976) and Hildebrand (1983) favoured a magmatic origin for the deposits. Withers (1979) supported the 'lateral secretion' hypothesis of Robinson (1971).

1.3 Present Investigation

It was obvious from the earlier reports on the different deposits of the region that there was still scope for further detailed investigation to shed new light on the genesis of the deposits. Hence the present investigation was undertaken. The main objectives of the project were as follows :

(i) Detailed investigation of the mineralogy of the veins from all the deposits.

(ii) Detailed fluid inclusion investigation of gangue minerals from the veins to determine the temperature, pressure and composition of the hydrothermal fluids responsible for depositing the metals in the veins.

(iii) Detailed oxygen and carbon isotopic investigation of the vein minerals and hydrogen isotope study of waters extracted from fluid inclusions to determine the nature and origins of the hydrothermal fluids.

(iv) To determine the environment of deposition of native silver and associated minerals from the analytical data and available thermodynamic data.

(v) To propose a new and more firmly based genetic model of the deposits.

In addition, a preliminary lead and strontium isotopic study of the vein minerals was undertaken to see if new insights could be gained on the genesis of the deposits.

Since extensive research has been done on the structure, geochemistry, and petrology of the rocks of the region since the 1930s, it was decided not to deal with this topic in this project. Most of the information on these aspects have been cited from the earlier reports.

The project was initiated in the summer of 1981 by a six week field-work program in both the Camsell River and Echo Bay sectors (Fig. 1). In the Camsell River sector, the Terra (or Silver Bear) mine was the only operating mine at that time. Samples were collected from the different levels of the mine. Core samples and samples from the ore dump were collected from the Norex mine. In the Echo Bay sector, samples were collected from the Eldorado, Contact Lake and Echo Bay mines. Since the El Bonanza and Bonanza mines were abandoned, samples could not be collected from the underground levels. Core samples were collected from

the El Bonanza mines. Samples from trenches were collected from the Bonanza mine. In the following year samples were collected only from the Camsell River sector as Echo Bay Mines Limited had closed all of its operations in the Echo Bay sector. In the Camsell River sector samples were collected from the newly found vein systems at the Norex and Smallwood mines. Samples were also collected from the deeper levels of the Terra mine. Samples from the Northrim mine were made available by Dr. R.D. Morton who had earlier collected the suite of samples from different levels of the mine. Details of the investigation are presented in the following sections.

2. REGIONAL GEOLOGIC SETTING OF THE SILVER DEPOSITS OF THE NORTHWEST TERRITORIES

2.1 Introduction

The Bear Province, located in the Northwest Territories of Canada, occupies an area of about 130,000 sq.km (Fig. 2). It extends along the western margin of the Canadian Shield from the Great Slave Lake to Coronation Gulf. The Slave Province lies to the east, and in the west and northwest it is bounded by the Phanerozoic platform deposits (Fraser *et al.*, 1972). According to Fraser *et al.*, (1972), the province may be divided into two main tectonic units. They are, the Wopmay Orogen and the Amundsen Basin (Fig. 2).

2.1.1 The Wopmay Orogen

The Wopmay Orogen consists of three major tectonic units : the Epworth fold belt, the Hepburn metamorphic-plutonic belt, and the Great Bear batholith (Fraser *et al.*, 1972). Hildebrand (1982) also divided the orogen into three major zones. These are, the Asiak fold and thrust belt, Great Bear magmatic zone, and the Hottah Terrane (Fig. 2). The Asiak Fold belt lies to the east of the Orogen and it is comprised of continental derived sediments and volcanic rocks that were thrust eastward (Hildebrand, 1982). It grades into the Hepburn metamorphic-plutonic belt to the west. The Hepburn metamorphic belt is comprised of massive to foliated granitic rocks. The oldest plutons are protomylonitic, while the youngest are comparatively undeformed diorites and gabbros (Hoffman *et al.*, 1980). The plutons of this belt have been dated at 1890 ± 20 Ma (Van Schmus and Bowring, 1980).

The Great Bear batholithic complex lies to the west of the Hepburn metamorphic-plutonic belt. It comprises of high level plutons, mostly, I-types, which intrude the related volcanics. The Great Bear Batholithic Complex will be discussed in a later section.

The Hottah Terrane lies to the west of the Great Bear batholithic Complex. This belt is comprised of poly-deformed and metamorphosed sedimentary and volcanic rocks which are cut by a variety of pre-tectonic intrusions (Hildebrand, 1982). According to Hildebrand (1982), the deformation of the terrane is younger than 1.915 Ga.

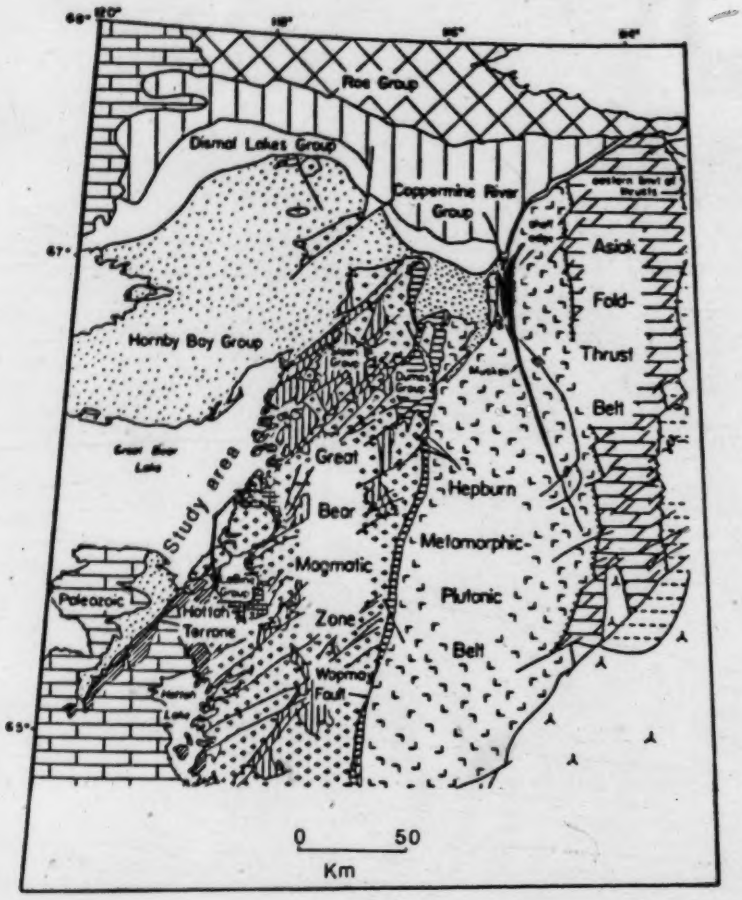

Figure 2. Regional geology of the Wopmay Orogen and adjacent areas (modified after Hildebrand, 1983).

2.1.2 The Amundsen Basin

The Amundsen Basin in the north of the Province comprises the post Aphebian sedimentary and volcanic rocks. The basin was a depositional site for shallow water sediments from Paleohelikian through Hadrynian time (Fraser *et al.*, 1972).

2.2 The Great Bear Batholith

The Great Bear batholith lies on the eastern shore of the Great Bear Lake. It is 450 km in length and 125 km in width. The batholith comprises plutonic and volcano-sedimentary rocks. Hoffman (1978) designated all the non-plutonic rocks in the region as McTavish Supergroup, while the plutonic rocks have been termed the Great Bear Batholith. Zircons from plutonic and volcanic rocks of the region have been analyzed by the U-Pb method by Van Schmus and Bowring (1980) and by Bowring and Van Schmus (1982). According to these authors, the plutons and the upper part of the volcanic section in the Great Bear suite were formed around 1860 ± 10 Ma ago, and the lower part of the volcanic sequence around 1875 Ma ago.

The McTavish Supergroup has been divided into three groups, namely, the Labine Group, the Sloan Group and the Dumas Group, which are separated by unconformities. The Labine Group is exposed in three areas, the Echo Bay-Hornby Bay area, the Conjuror Bay-Camsell River area and the Hottah Lake area (Hildebrand, 1981). The Labine Group which is structurally the lowest, is composed of tholeiitic and calc-alkaline flows, pyroclastic rocks and sedimentary rocks (Badham, 1973; Hildebrand, 1981,1982). According to Hildebrand (1981) the Labine Group in the Echo Bay region may be divided into four formations. These are:

(i) The Port Radium Formation: It is composed of thin bedded arenites and argillites with minor carbonates and tuff. It is the oldest unit in the Group.

(ii) The Echo Bay Formation: This formation overlies the Port Radium formation conformably and is comprised of mainly andesite flows with minor rhyodacite flows,

and associated clastic rocks. It is further subdivided into Mile Lake, Surprise and Sparkplug Lake members.

(iii) The Cameron Bay Formation: It is composed of volcanic and sedimentary rocks, namely, ignimbrites, conglomerates, arenites (lacustrine), etc.. It is further subdivided into Lindsley Tuff, McKenzie Tuff and Stevens Tuff members.

(iv) The Feniak Formation: It is composed of tuffs and pyroclastic rocks.

The Labine Group in the Camsell River region has been divided into the following units by Hildebrand (1983):

(i) The Conjuror Bay Formation: This forms the oldest unit and is composed of quartz arenite mudstone, ash-flow tuff and breccias.

(ii) The Bloom Basalt: It is composed of pillow basalt, breccia, tuff and dolomite.

(iii) The Moose Bay Tuff: It is composed of sandstone, mudstone, breccia, andesite, limey argillite and rhyolitic ash-flow tuff.

(iv) The Terra Formation: It is composed of mudstone, sandstone, limestone, rhyolitic flows and ashstone.

(v) The Camsell River Formation: It is composed of andesitic lavas, sandstone, mudstone and conglomerate.

(vi) The White Eagle Tuff: It is composed of lithic and crystal-rich dacite, ash-flow tuff and breccia.

(vii) The Uranium Point Formation: It is composed of sandstone, comglomerate, lapilli tuff, mudstone and ashstone.

(viii) The Animal Andesite: It is composed of andesitic lavas and breccias.

(ix) The 'Younger Ash-Flow Tuffs': These are simple cooling units of dacite rhyolite ash-flow tuffs.

The above volcano-sedimentary units have been intruded by numerous dykes, sills and plutons (e.g. the Rainy Lake Intrusive Complex). Detailed descriptions of these are given in Hildebrand (1983).

2.2.1 Intrusive Rocks of the Batholithic Complex

In the Great Bear batholith the plutons are epizonal, massive, have sharp contacts and have narrow contact metamorphic aureoles (Hoffman *et al.*, 1976). The plutonic rocks of the complex are shown in Figure 3. (Hoffman and McGlynn, 1977). The plutons may be up to 75 km in diameter, and are mainly potassic in composition. The plutons are both concordant and coeval with the volcanics, and discordant and post-volcanic. The classification of the plutons as given by Hoffman and McGlynn (1977) is as follows:

(i) hornblende monzonite suite,

(ii) biotite hornblende adamellite suite,

(iii) biotite granite suite, and

(iv) hornblende diorite tonalite suite.

(i) Hornblende monzonite suite: This suite includes the Rainy Lake and Balachey Lake plutons of the Camsell River sector, and the Contact Lake and Glacier Lake plutons of the Echo Bay sector. These plutons are lower in quartz than other plutons, and have undergone intense hydrothermal alterations. Differentiation due to gravity settling has resulted in the division of the Rainy Lake pluton into a lower syenodiorite and a upper syenite. The margin of the pluton is monzonite porphyry.

(ii) Biotite hornblende adamellite suite: The Hogarth, Gilleran, Torrie, Kamut and other plutons comprise this suite. These plutons are fine-grained, have wide contact aureoles and are locally discordant.

(iii) Biotite granite suite: This suite, which includes the Richardson, Hixon, Adam and Spence plutons has intrusions that are circular to multilobate in plan, and have chilled margins and holocrystalline interiors.

(iv) Hornblende diorite tonalite suite: These occur in the eastern part of the batholith. The dykes and stocks are 1 to 5 km in diameter and coarse-grained, and probably post-date folding

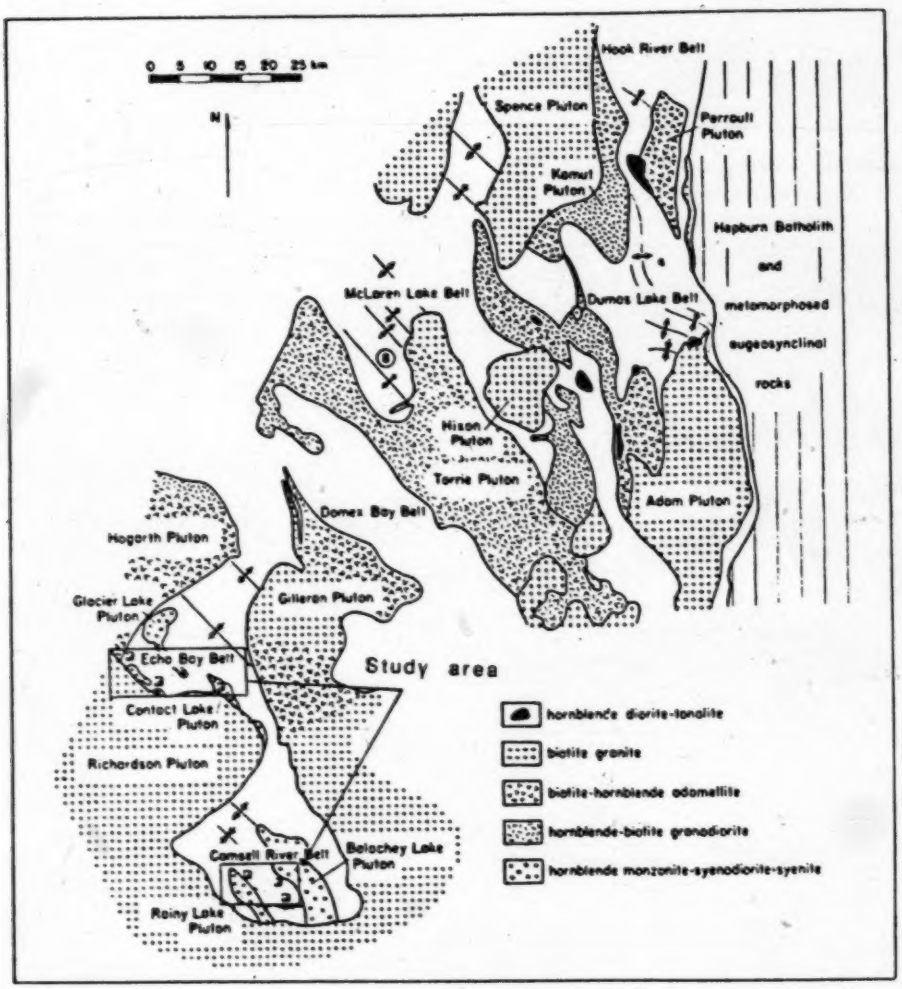

Figure 3. Intrusive rocks of the Great Bear Magmatic Zone (modified after Hoffman and McGlynn, 1977).

of the volcanic piles.

2.2.2 Structural Features of the Batholithic Complex

The volcanic and plutonic rocks of the complex have been affected by vertical northeast-trending faults which splay and coalesce, and were most active between 1700-1400 Ma ago (Badham, 1973). The north to northwest trending faults were probably active after the final period of plutonism, but before the main activity of the northeast trending faults. The northeast trending faults have right-lateral strike-slip displacements which in some cases may be up to 15 km (Hoffman and McGlynn, 1977). Dip-slip displacements occurred on these faults during subsequent tectonic activity of the region. These faults were the loci of later intrusions and mineralization.

The volcanic rocks of the complex have been broadly folded, the axes of these folds plunge gently and trend northwest (Badham, 1973; Hoffman and McGlynn, 1977). According to Hildebrand (1982), the folds are *en echelon* and were the product of oblique convergence. Near intrusive contacts, the folds increase in frequency, but decrease in amplitude.

2.2.3 Giant Quartz Veins

The 'Giant Quartz veins' were first studied by Kidd (1933) and Furnival (1935). They occur along the northeast trending fault systems of the region and have high dip. They are variable in width and length and may be up to 80 km in length and over 150 m in width. More than eighty veins have been reported from the region. These massive quartz veins have been deposited during three distinct periods which correspond to movements and brecciation of the earlier deposited quartz. Hematite, pyrite, copper sulphides, and locally pitchblende were found to be associated with the last period of quartz deposition. Chloritisation, carbonatisation and argillic alterations of the wall-rocks have been reported by Mursky (1973).

The majority of the veins are believed to be older than 1200 Ma. Miller (1982a,b), however, dated pitchblende, which post-dates the quartz, from the Rayrock vein at 511 ± 86

Ma.

2.2.4 Non-Granitic Intrusions

Diabase dykes and sheets are common in the region. The dykes preferentially occupy the east-west and north-south trending faults (Mursky, 1973). The diabase sheets outcrop mainly along the east shore of Great Bear Lake. The diabase sills at Port Radium and at Echo Bay mine belong to a swarm of sills termed the Western Channel diabase (Irving *et al.*, 1972). The sill at the Echo Bay mine has been dated at 1345 ± 48 Ma (Miller (1982a,b) revised it to 1392 ± 48 Ma) by Thorpe (1978). The sills have been found to cut across the mineralized veins at the Port Radium and Echo Bay deposits (Robinson, 1971). The dykes and sills of the area have been reported by Mursky (1973) to be identical in composition, with equal amounts of plagioclase (45%) and augite (45%), minor biotite (5%) and interstitial micrographic quartz and albite (5%).

Badham (1973) reported two sets of dykes in the Camsell River sector. These are :

(i) An altered older set of dykes. The diabase exposed on the Terra peninsula probably belongs to this category. It is cut by an east-trending diabase.

(ii) The second set comprises the northwest, northeast and east trending dykes and the Gunbarrel gabbro.

The east-west swarm of diabase dykes which postdate faulting in the Echo Bay area have been termed the Cleaver Diabase by Hoffman (1982) and Hildebrand (1983). Hildebrand (1983) considered the east-west dykes in the Camsell River sector to belong to the same suite and used the same term.

2.2.5 Metamorphism

Metamorphism in the region is varied. Robinson and Morton (1972) reported regional metamorphism of lower zeolite facies. Contact metamorphism around intrusive bodies has been reported by Campbell (1955), Robinson and Morton (1972), Badham (1973) and Hoffman and

McGlynn (1977).

3. THE SILVER DEPOSITS

3.1 Introduction

The major silver deposits of the region occur within two separate sectors, namely, the Echo Bay Sector in the north and the Camsell River Sector, about 50 km to the south. The principal deposits in the Echo Bay Sector (Fig. 4) include the following :

(i) the Eldorado mine at Long. 118°02'00" W and Lat. 66°05'00" N

(ii) the Echo Bay mine at Long. 118°01'00" W and Lat. 65°05'20" N

(iii) the Contact Lake mine at Long. 117°47'00" W and Lat. 66°00'00" N

(iv) the El Bonanza mine at Long. 118°04'25" W and Lat. 66°00'00" N

(v) the Bonanza mine at Long. 118°05'30" W and Lat. 66°00'38" N

The principal deposits in the Camsell River sector (Fig. 6) include the following :

(i) the Terra (or Silver Bear) mine at Long. 180°07'00" W and Lat. 65°35'20" N

(ii) the Northrim (or Silver Bay) mine at Long. 117°59'00" W and Lat. 65°35'20" N

(iii) the Norex mine at Long. 117°58'00" W and Lat. 65°35'10" N

(iv) the Smallwood mine at Long. 117°57'00" W and Lat. 65°35'00" N

In addition, a number of minor occurrences, including the Lypka, the Republic and the Bloom Island veins, have been reported from the region.

3.2 The Echo Bay Sector

3.2.1 The Eldorado Deposit

The Eldorado mine is located at Port Radium on the eastern shore of the Great Bear Lake (Fig. 4). The Eldorado mine, which was abandoned in 1982, was the first Canadian mine to supply uranium in the early thirties. Full-scale production from the property was not attained until 1934 by Eldorado Gold Mines Limited, which was changed to Eldorado Mining and Refining Limited, and then to Eldorado Nuclear Limited. Between the period 1934 to 1940 and 1942 to 1960, it was an important producer of uranium. The mine was reopened in 1976 as a producing silver mine under the management of the Echo Bay Mines Limited.

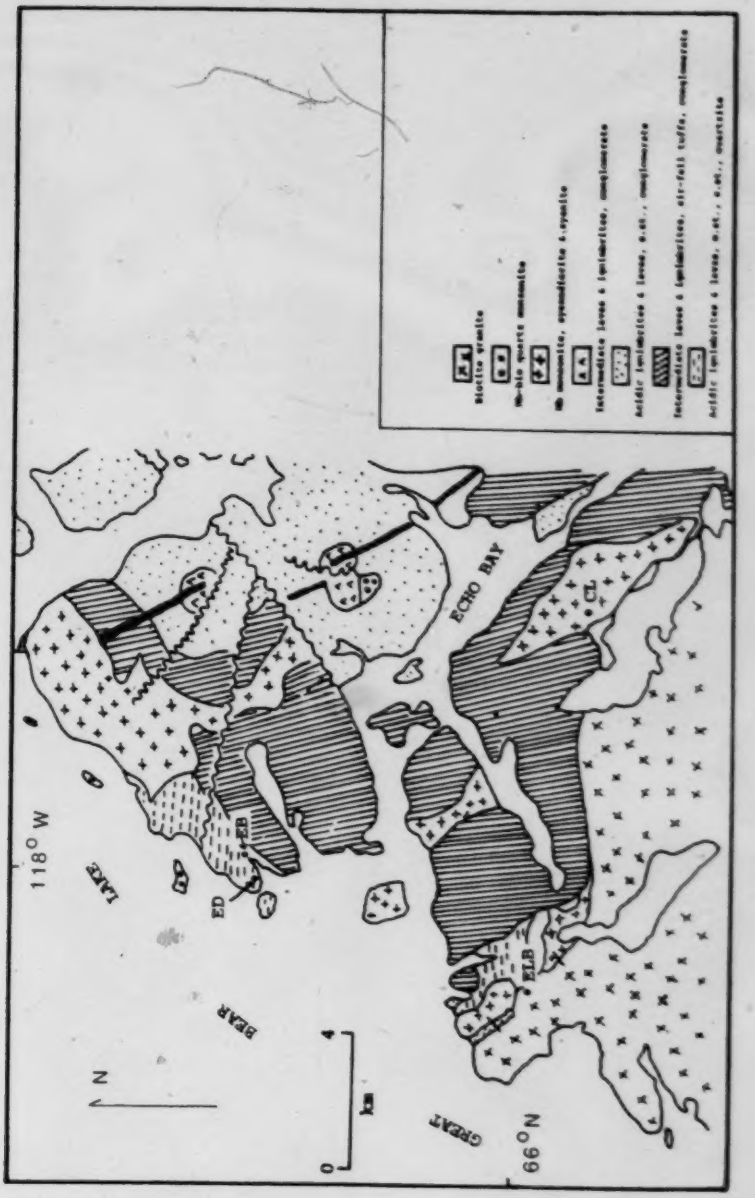

Figure 4. Location and geology of the silver deposits in the Echo Bay sector (modified after Hoffman *et al.*, 1976).

According to the old stratigraphic nomenclature, the rocks in and around the mine belong to the Echo Bay Group, which was further subdivided into the Lower and Upper Groups. Hildebrand (1981) has assigned the volcano-sedimentary rocks of the area to the Port Radium Formation, which forms the lowermost part of the Labine Group in this area. The lower part of the succession is primarily comprised of sedimentary rocks, namely, mudstone, sandstone, conglomerate and limestones. Thin intercalations of volcanic flows and sediments overly the sedimentary sequences. The predominantly sedimentary succession is overlain by thick piles of andesitic flows and air-fall tuffs belonging to the Echo Bay Formations. The volcano-sedimentary rocks have been intruded by the Cobalt porphyry and the Mystery Island intrusive suite (Hildebrand, 1981). According to Hildebrand, the Cobalt porphyry intrusions comprise of podiform to irregular-shaped intrusions of hornblende-plagioclase porphyry and microdiorite. The Mystery Island intrusive suite comprises intrusive bodies varying in composition from granodioritic to dioritic. Basic dykes and sheets constitute the youngest intrusive rocks in the area.

Shears and faults constitute the major structural features within the deposit. Small-scale folds have developed around the intrusive contacts. The fractures have been the sites of the mineralization.

The mineralized veins of the Eldorado mine are complex, as there have been repeated depositions and dilations of the veins. Within the mine the major delineating fractures are the no.1 vein and the Bear Bay shear (Fig. 5). The main veins in the mine are # 1, 2, 3, 4, 5, 5A, 6, 7, 8, 9, D and B, of which # 1, 2, 3, 4, 6, 7 and 9 are apparently devoid of any silver mineralization. The silver-bearing veins (5, 5A, 8, D and B) are typified by abundant carbonates, not common to the 'barren' vein systems. Uraninite, native silver, native bismuth, hematite, Ni-Co-Fe arsenides and sulpharsenides, sulphides and sulphosalts represent the common opaque minerals. Quartz, dolomite and calcite were found to be the common gangues, with minor amounts of siderite and rhodochrosite. Wall-rock alteration is extremely variable. The alteration halo varies from about a centimetre to a few metres in extent. Chloritization,

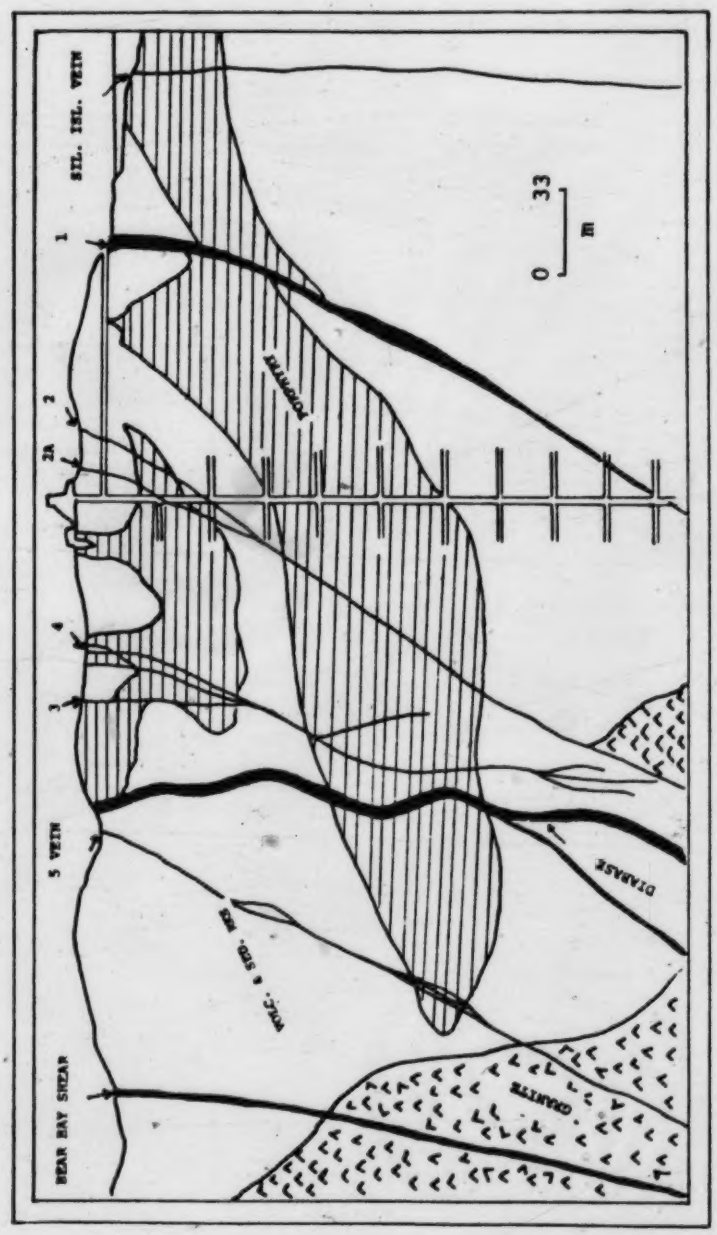

Figure 5. Cross-section through the Eldorado mine showing the different vein zones (modified after Campbell, 1957).

hematitization, carbonatization and argillization are the main types of alterations.

3.2.2 The Contact Lake Deposit

The Contact Lake mine is on the northeast of the Contact Lake, approximately 14 km southeast of Port Radium (Fig. 4). The mine was closed in August, 1982, a few days after the author had visited the site. Due to safety reasons it was not advisable to go underground. Ores were being hauled at that time from the 2nd level, and samples for this study had to be collected from the ore dump. Core samples were supplied by G. Woollett of Trigg, Woollett and Olson Consulting Ltd., Edmonton, Alberta.

The oldest rocks consist of porphyritic andesitic flows, flow breccias, fine-grained felsic pyroclastic and minor sedimentary iron formation and conglomerate. The silver-bearing veins are hosted by the granodiorite belonging to the Mystery Island intrusive suite. Diabase dykes are the youngest rocks in the area.

Twelve veins were identified by geologists of the Echo Bay Mines Limited, either by underground developments, diamond drilling, trenching or sampling. Numerous other veins were found in the property. No identification numbers were assigned to these veins.

The vein mineralogy is similar to the Eldorado deposit. Wall-rock alterations include chloritization, carbonatization, silicification and hematitization.

3.2.3 The Echo Bay Deposit

The Echo Bay deposit is located about 2 km ENE of the Eldorado deposit (Fig. 4). The Consolidated Mining and Smelting Company of Canada Limited staked claim to this property in 1930. Although initial development work started in 1932, silver production started only in 1964 under the auspices of Echo Bay Mines Limited.

The geology of the deposit is similar to that of the Eldorado deposit. The veins are hosted by tuffs and andesitic lava flows. Intrusive rocks include the hornblende plagioclase porphyry and the younger diabase sheets which are spatially and temporally related to the

mineralization.

In the summer of 1981 only the no. 3 adit level was accessible, and the ore was being hauled out from the newly discovered 316A stope. Unlike the Eldorado deposit, pitchblende was found to occur only in minor quantity. Native silver, native bismuth, Ni-arsenides (Co and Fe arsenides were not found), sulpharsenides, minor sulphosalts, sulphides and hematite were the common opaque minerals in gangues of dolomite, quartz and calcite.

3.2.4 The El Bonanza Deposit

The El Bonanza deposit is located about 9 km south of Port Radium (Fig. 4). The El Bonanza property was staked in 1931 by Eldorado Gold Mines. El Bonanza Mining Corporation Limited took over the property in 1950, and finally Echo Bay Mines Limited took over.

The veins are hosted by a narrow strip of altered volcano-sedimentary rock (cherts, siltstones and tuffs) which is intruded by granites, granodiorites, hornblende-plagioclase porphyry and diabases.

Two silver-bearing veins were reported by the geologists of the Echo Bay Mines Limited in the property. These are the Bonanza and the Spud veins. Uranium was found to be absent in the veins.

The Bonanza deposit is located about a kilometre northwest of the El Bonanza deposit, and the setting is very similar to the latter.

3.3 The Camsell River Sector

3.3.1 The Terra Deposit

The Terra deposit, also known as Silver Bear, is located about 50 km south of Port Radium, on the southern bank of the Camsell River (Fig. 6).

The veins are hosted by rocks belonging to the Terra formation of the Labine Group (Hildebrand, 1983). The veins cross-cut the calc-argillites, rhyolitic ashstones and massive

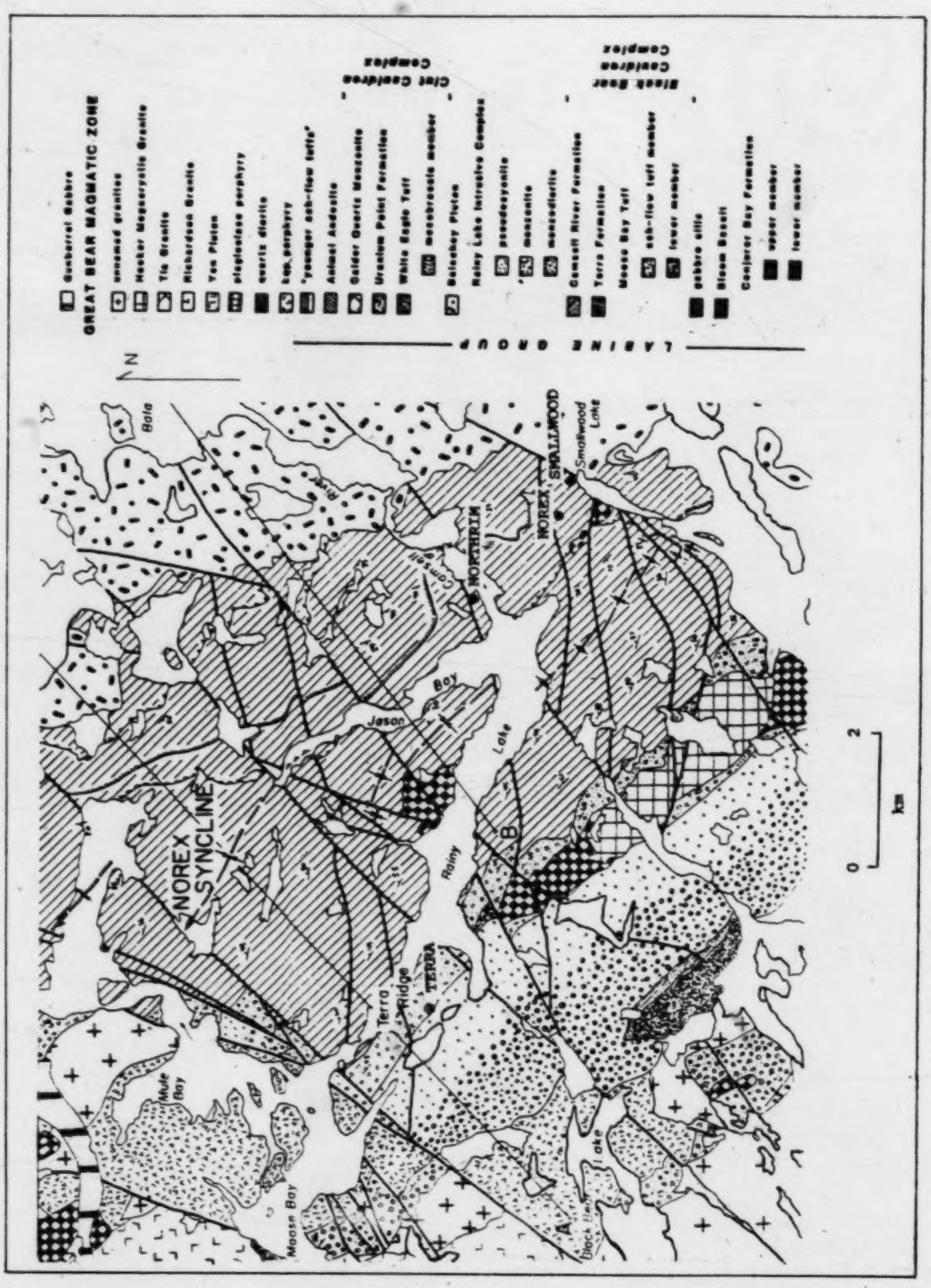

Figure 6. Location and geology of the silver deposits in the Camsell River sector (modified after Hildebrand, 1983).

sulphide bands, which were interpreted as 'skarn' by Badham (1973). The volcaniclastic sedimentary rocks have been intruded by a differentiated intrusive body, which has been termed as the Rainy Lake Intrusive Complex (Tirrul, 1976; Hildebrand, 1983). According to these workers, the Complex is compositionally and mineralogically zoned, and is about 1500 m thick and 10-11 km across. The pluton has been divided into five major lithological units (Tirrul, 1976). These are from the top to the bottom, an upper border monzonite, fine grained syenite, coarse grained syenite, monzonite, and monzodiorite. Diabase sheets represent the youngest intrusives in the area.

Mineralization occurs along northeast trending faults. The principal veins (no. 2, 3, 7, 8, 9, 10, 11, 12, 13, 14 and 15) are composite, complex and variable in thicknesses. The occurrence of economically viable mineralization is very erratic.

A large number of opaque minerals have been identified in the veins. Calcite, dolomite and quartz were the most abundant gangue minerals. Fluorite was found occasionally. Chlorite, K-feldspar and muscovite were rare. Hematitisation, chloritisation, silicification and carbonatisation are the commonly found alteration types.

3.3.2 The Norex Deposit

The Norex deposit is located about 9 km ESE of the Terra deposit (Fig. 6). The Norex vein, also called the Graham vein, was discovered in 1932, but mining commenced only in 1968. The mine was closed down in 1971, but was reopened in 1981-82 when the no. 3 vein was discovered by diamond drilling. The vein which was more than 60 m in length and 1 to 4 cm in width, produced high grade silver.

The silver-bearing veins are hosted by andesitic lava flows and tuffs which are cut by a plagioclase porphyritic granodioritic dyke that strikes to the northeast.

Native silver, native bismuth, Ni-Co arsenides and sulpharsenides, hematite, sulphides and minor sulphosalts were found in the veins, along with quartz, dolomite and calcite. Unlike the other deposits, quartz was found to be the major gangue mineral. Chloritisation is the

common wall rock alteration product.

3.3.3 The Smallwood Deposit

The Smallwood deposit is located approximately 1 km SE of the Norex mine (Fig. 6). Three veins were discovered in 1981-82. These veins, designated as no. 1, 3 and 4 were about 200 m in length with variable width. Andesite porphyry and tuffs host the veins. Vein mineralization was found to be similar to Norex, except for quartz which was not as predominant as in the Norex deposit.

3.3.4 The Northrim Deposit

The Northrim deposit, also known as Silver Bay, is located about 2 km north of the Norex mine , on the northern bank of the Camsell river (Fig. 6). Silver Bay Mines Limited mined out the high grade ore until 1970, when Federated Mining Corporation took over the property. Terra Mining and Exploration took over the property in 1981.

The veins are hosted mainly by basalts and tuffs. Mineralization occurs mainly along EW trending fractures which occur between the major NE trending faults. Vein mineralogy is very similar to the Terra deposit.

4. ORE- AND GANGUE- MINERALOGY

4.1 Introduction

In all the deposits studied, the ore bodies occur as veins in fractures and shear zones. These veins commonly trend along a northeastly direction. Locally, however, this trend may change to east-west, north and north-north west. The veins are discontinuous, and pinch and swell both along the strike and dip directions. The veins vary in thickness from less than a centimetre to more than a metre in places. The veins have obviously been reopened several times, and subjected to different pulses of mineralization. Mineralization has most commonly taken place in dilatant zones within the systems. The mineralized zones or pods or lenses are variable in length and width. The mineralized zones enclose fragments of wall rock and earlier vein minerals.

4.2 Mineralogy of the Veins

A large number of minerals have been identified in the veins of the Great Bear Lake silver deposits. These minerals have been deposited at different stages during the history of the ore deposits. The principal opaque minerals include, uraninite, hematite, Ni-Co-Fe arsenides and sulpharsenides, native silver, native bismuth, Ag-Cu-Bi-Fe-Pb-Zn sulphides and sulphosalts. The principal gangue minerals include, quartz, calcite, dolomite and fluorite. In addition, rhodochrosite, siderite, chlorite, muscovite and potassium feldspar have also been identified in variable proportions from different deposits. These minerals, however, are not ubiquitous in all the deposits.

4.3 Arsenides

Arsenide minerals are very common in the veins of these deposits. The arsenide minerals which are associated with native silver in these deposits include nickeline, maucherite, safflorite, rammelsbergite, pararammelsbergite, loellingite, skutterudite, cobaltite, gersdorffite, arsenopyrite and glaucodot. Withers (1979) reported three other types of arsenide minerals from the Northrim deposit. They are : Bi-bearing safflorite(?), a phase intermediate in

composition between rammelsbergite and gersdorffite, and a new mineral with a formula of PbAs. Langisite, alloclasite and clino-safflorite which have been identified in similar ores of Cobalt-Gowganda region (Petruk *et al.*, 1971) have not been found in these deposits.

Prior to this investigation very few quantitative electron microprobe analytical data were available. The present investigation was undertaken to determine the chemical composition of arsenide minerals in all the major deposits of the region, and to investigate the spatial variations in compositions.

Rojkovic (1971) performed some quantitative electron microprobe analyses on the arsenide minerals of the region. His investigations, however, did not include all the deposits. Withers (1979) also carried out semi-quantitative analyses of few arsenide minerals of the Northrim mine.

In the present investigation more than 250 spot analyses were carried out on the arsenides. Some of the results are presented in the following sections. The analytical techniques are presented in Appendix I.

4.3.1 Monoarsenides

4.3.1.1 Nickeline (NiAs)

Nickeline is the most common monoarsenide reported from the ores of the Great Bear Lake silver deposits. It is a common mineral in all the deposits, occurring in association with native silver, native bismuth and the other diarsenides and triarsenides. It occurs mainly in massive aggregates, but also as botryoids, rosettes and dendrites. In the Echo Bay mine it occurs as massive veins parallel to the wall rocks and in association with massive chalcopyrite. In the other deposits of the region, nickeline occurs only as thin veinlets associated with the other arsenides, native silver and native bismuth (Plate 1). It also occurs as inclusions (islands) within safflorite, and is most commonly rimmed by the other di- and sulpharsenides (Plate 2).

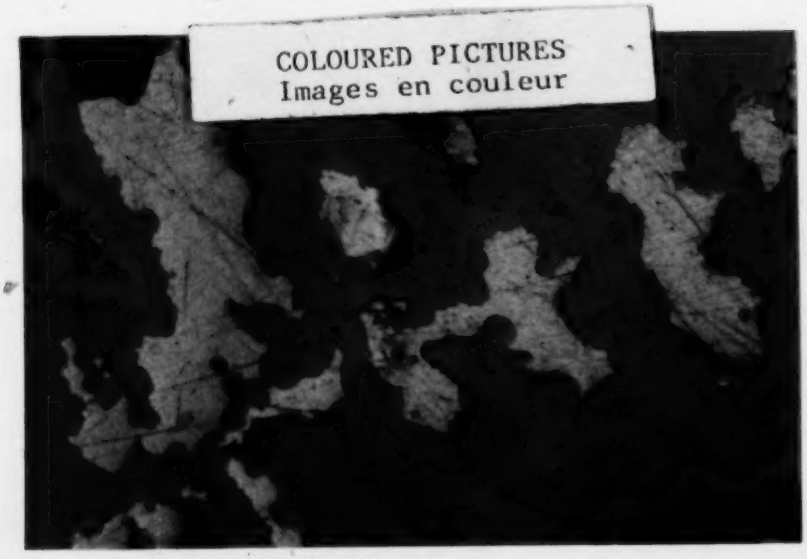

Plate 1. Dendrites of native silver rimmed by nickeline (pinkish) and rammelsbergite (bluish grey). Terra mine. P.P.L. 200X.

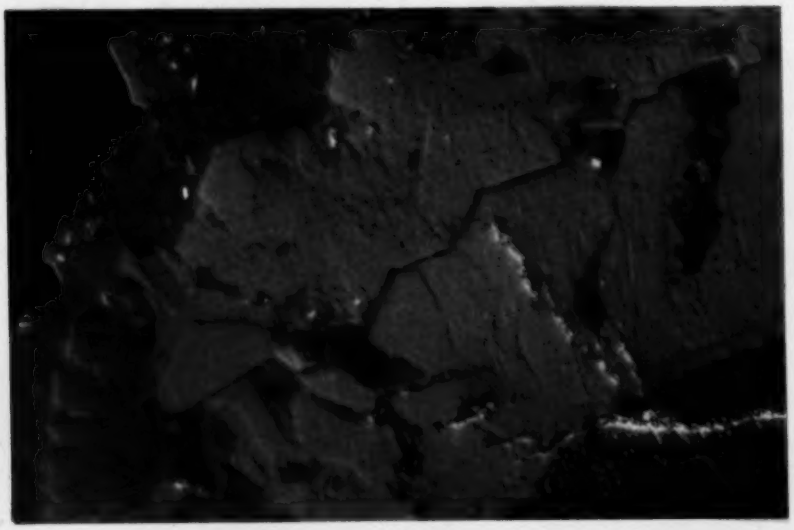

Plate 2. Nickeline (pinkish) rimmed by complex intergrowth of gersdorffite (grey), rammelsbergite (bluish grey) and cobaltite (pinkish grey). Normarsky phase interference contrast. Terra mine. 200X.

The results of the electron microprobe analyses are shown in Table 1. The results show large variations in the composition of the nickelines. A large variation in the Ni/As ratio was observed, in agreement with the experimental data of Yund (1961). There is extensive substitution of nickel by cobalt. Substitution of nickel by iron is, however, negligible. Arsenic is proxied by sulphur and antimony.

According to Yund (1962), the metal to non-metal ratio in nickelines is not restricted to 1:1. This has been found to be true in case of the Great Bear Lake nickelines. The metal to non-metal ratios are found to vary from 0.82 : 1.00 to 0.99 : 1.00. The nickelines are found to be slightly deficient in the metals. The analytical results however, agree with the experimental results of Yund (1961, 1962). The atomic percents of the metals and the non-metals are plotted in Figure 7. It is found that the samples from the Camsell River sector are more enriched in arsenic than those of the Echo Bay sector. The variations in the compositions of the nickelines from the two sectors could be attributed to minor differences in the physico-chemical conditions between the two sectors during ore depsoition.

The rims of individual nickeline grains were found to be depleted in nickel relative to the cores. The variations in composition were not only found from one sample to another, but also within the same sample. In a few analyses, a concomitant decrease in nickel content was found to accompany an increase in arsenic and cobalt contents. The variation in the composition is apparently related to the association of the nickelines with variable proportions of arsenides. Similar results were obtained by Rojkovic (1971). He found the nickelines to be more enriched in cobalt in grains which were rimmed by safflorite and by other cobalt minerals.

Table 1

Electron microprobe analyses of nickelines from the Great Bear Lake silver deposits, N.W.T.. Data plotted in Figure 7.

Sample nos.	Fe	Co	Ni	S	As	Sb	Total
9B/SB	N.D.	0.26	41.56	58.55	N.D.	N.D.	100.37
Cl/22A	N.D.	0.88	41.29	57.17	N.D.	0.41	99.75
6B/316/EB	N.D.	N.D.	42.92	56.62	N.D.	0.35	99.89
NX/22	N.D.	2.69	37.70	59.41	N.D.	N.D.	99.80
NR/2B	N.D.	0.51	39.53	58.64	N.D.	0.49	99.17
SW/1	N.D.	0.84	40.10	57.40	1.34	N.D.	99.68
2B/250/ED	N.D.	0.54	41.67	54.66	1.97	0.39	99.23
ELB/1	N.D.	1.47	42.25	55.54	N.D.	0.90	100.16

N.D. - Not detected. SB - Silver Bear (or Terra). Cl - Contact Lake. EB - Echo Bay. NX - Norex. NR - Northrim. ED - Eldorado. ELB - El Bonanza.

Table 1 (continued)

Atomic proportions of nickelines calculated on the basis of As+S+Sb=1.00

Sample nos.	Fe	Co	Ni	S	As	Sb
9B/SB	0.00	0.02	0.90	0.00	1.00	0.00
Cl/22A	0.00	0.02	0.92	0.00	0.99	0.01
6B/316/EB	0.00	0.00	0.96	0.00	0.99	0.01
NX/22	0.00	0.02	0.81	0.00	1.00	0.00
NR/2B	0.00	0.01	0.86	0.00	0.99	0.01
SW/1	0.00	0.02	0.85	0.05	0.95	0.00
2B/250/ED	0.00	0.01	0.89	0.07	0.92	0.01
ELB/1	0.00	0.03	0.96	0.00	0.99	0.01

SB - Silver Bear (or Terra). Cl - Contact Lake. EB - Echo Bay. NX - Norex. NR - Northrim. SW - Smallwood. ED - Eldorado. ELB - El Bonanza.

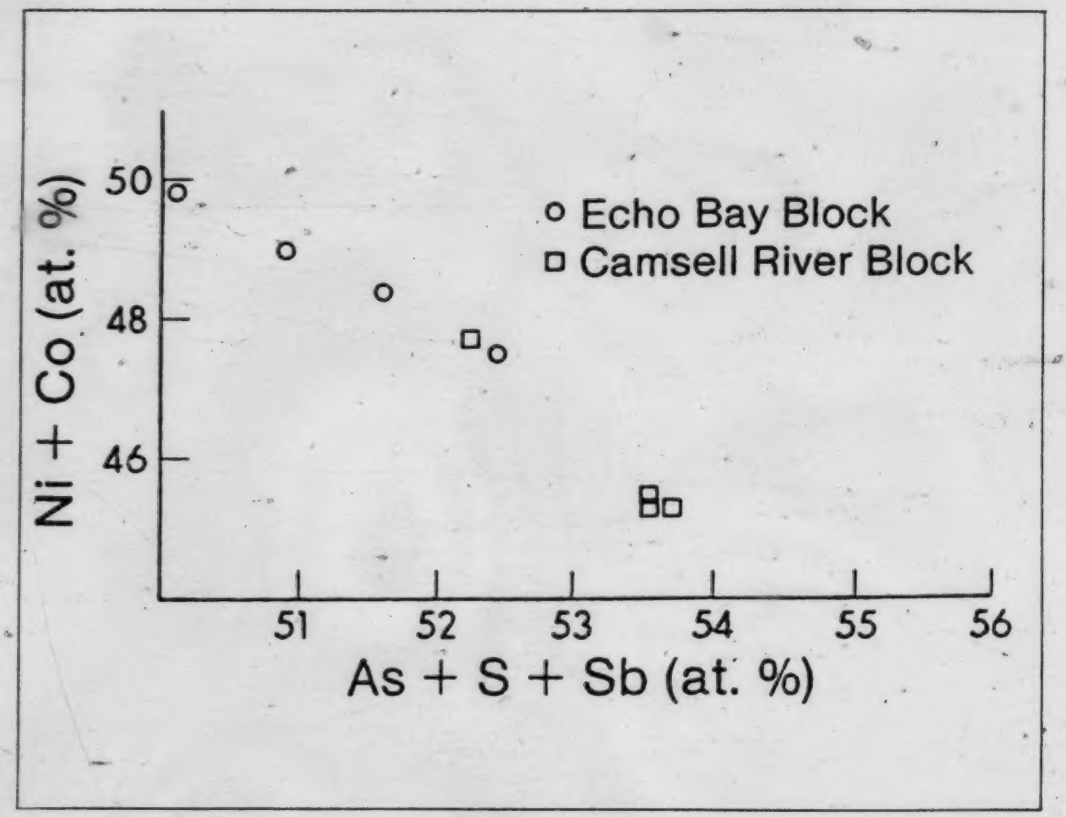

Figure 7. Variations of As + S + Sb : Ni + Co ratios of nickelines in the ores of the Great Bear Lake silver deposits. Data listed in Table 1.

4.3.2 Metal-Rich Arsenides

4.3.2.1 Maucherite ($Ni_{11}As_8$)

Maucherite is not very common in the ores of the Great Bear Lake silver deposits. It has been identified in the ores of the Contact Lake and the Terra mine. However, Rojkovic (1971) reported the occurrence of maucherite from the Echo Bay deposit. It was not identified during this investigation. In the aforesaid deposits it occurs as bands with nickeline. The results of the electron microprobe analyses of maucherite are given in Table 2. The results show that there is no noteworthy variation in the composition of the maucherites in either of the deposits.

4.3.3 Diarsenides

The diarsenide minerals include rammelsbergite, safflorite, loellingite and pararammelsbergite. The above nomenclature was first used by Holmes (1947). According to him the 'orthorhombic' diarsenides exhibit both discontinuous and limited diadochy between cobalt, nickel, and iron; those high in nickel are completely separated from the iron-bearing members by the isometric arsenide. He retained the term rammelsbergite ($NiAs_2$) for the common high nickel member, and pararammelsbergite ($NiAs_2$) for the rarer nickel-rich form. The iron rich variety was termed loellingite ($FeAs_2$). The cobalt-rich variety was termed safflorite ($CoAs_2$). He arbritrarily placed the boundary between safflorite and loellingite at 70% mole per cent $FeAs_2$.

Roseboom (1963) followed the classification proposed by Holmes (1947) in his investigations of the Co-Ni-Fe diarsenides. Roseboom also revealed that the Co-Ni-Fe diarsenides have two distinct compositional groups: the rammelsbergites (and pararammelsbergites) and the loellingite-safflorite series. He found that the synthetic diarsenides show extensive solid solution at 800°C, except for a small region in the Ni-Fe join (Fig. 8).

Table 2

Electron microprobe analyses of maucherites from the Great Bear Lake silver deposits, N.W.T..

Sample nos.	Fe	Co	Ni	S	As	Sb	Total
Cl/28	N.D.	2.90	47.20	0.80	47.90	0.90	99.70
14B/SB	0.80	1.80	47.60	N.D.	48.70	0.84	99.74

Atomic proportions of maucherites calculated on the basis of As+S+Sb=8.00

Sample nos.	Fe	Co	Ni	S	As	Sb
Cl/28	0.00	0.60	9.60	0.30	7.62	0.08
14B/SB	0.17	0.40	9.88	0.00	7.92	0.08

N.D. - Not detected. Cl - Contact Lake. SB - Silver Bear (or Terra).

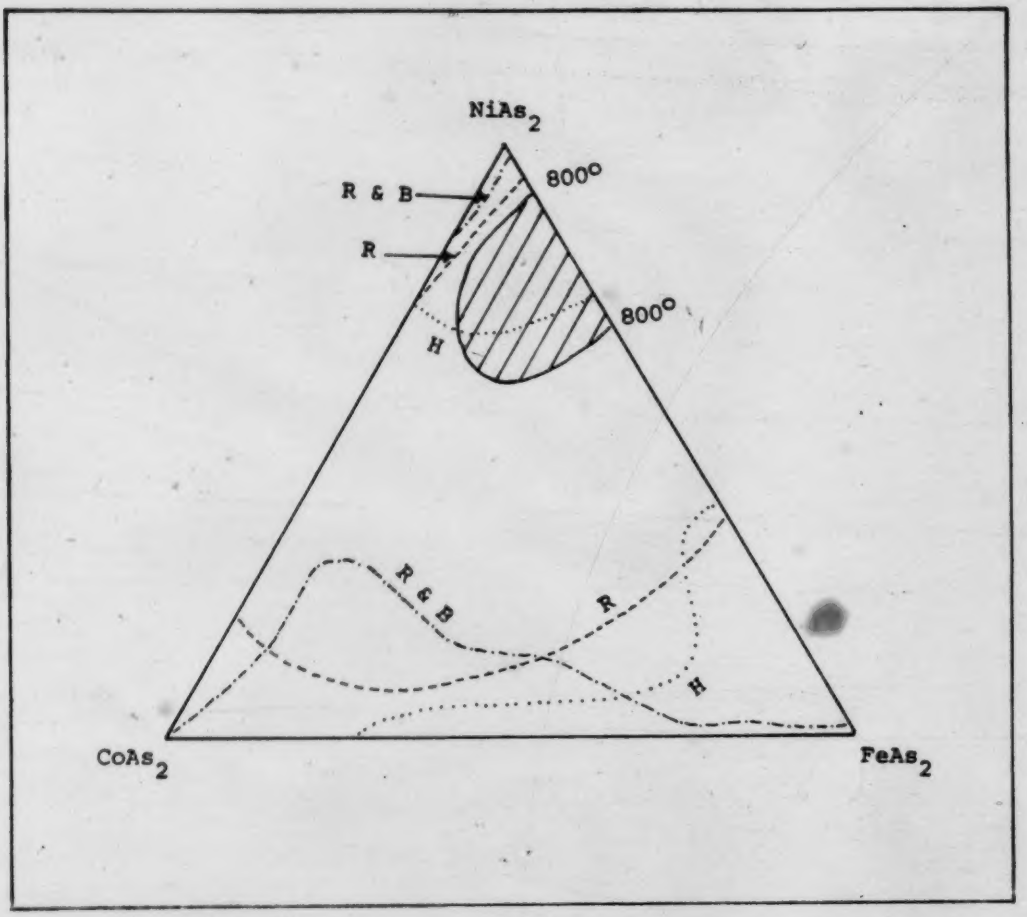

Figure 8. Compositional limits of natural diarsenides. H - Holmes (1947). R - Roseboom (1963). R & B - Radcliffe and Berry (1968).

The compositional limits of natural Ni-Co-Fe diarsenides according to Holmes (1947), Roseboom (1963), and Radcliffe and Berry (1968) are shown in Figure 8. Oen *et al.* (1971) reported nickelian loellingites which fall outside the limits of the aforesaid workers. Petruk *et al.* (1971) also reported safflorites which fall outside these limits. Rudashevskii *et al.* (1979) also reported variable compositions from the ore-bearing veins of the Khovuaksinsk Ni-Co deposit, U.S.S.R.. They found that the miscibility between Fe and Co and between Co and Ni varieties is discontinuous. They attributed the variations in chemical compositions to variations in the physico-chemical conditions of formation.

The diarsenides of nickel, cobalt and iron are abundant in the ores of the Great Bear Lake silver deposits. The nickel-rich phase is represented by rammelsbergite, whilst the cobalt- and iron-rich phases are represented by safflorite and loellingite respectively. Pararammelsbergite, the other nickel-rich phase is not very common. The diarsenides occur as complex intergrowths with the other arsenides, namely, nickeline, the sulpharsenides and the triarsenides. They occur as dendrites, as rosettes and as rims around native silver, native bismuth and nickeline cores. They also occur as tubercles and as massive aggregates. Electron microprobe analyses have shown that the diarsenides of the Great Bear Lake silver deposits fall outside the compositional limits specified by the earlier workers. Some of the analyses are plotted in Figure 9 along with the compositional limits of Holmes (1947), Roseboom (1963) and Radcliffe and Berry (1968).

4.3.3.1 Safflorite ($CoAs_2$)

Safflorite has been identified in the ores of the Eldorado, Contact Lake, Terra, Northrim, Norex and Smallwood mines. It was not identified in the ores of the Echo Bay and El Bonanza mines. Safflorite occurs as complex intergrowths with rammelsbergite and the sulpharsenides. It occurs as rosettes and as dendrites. In the rosettes it usually occurs as rims around nickelines. It also occurs as star-shaped and isolated anhedral grains with inclusions of native silver (Plate 3).

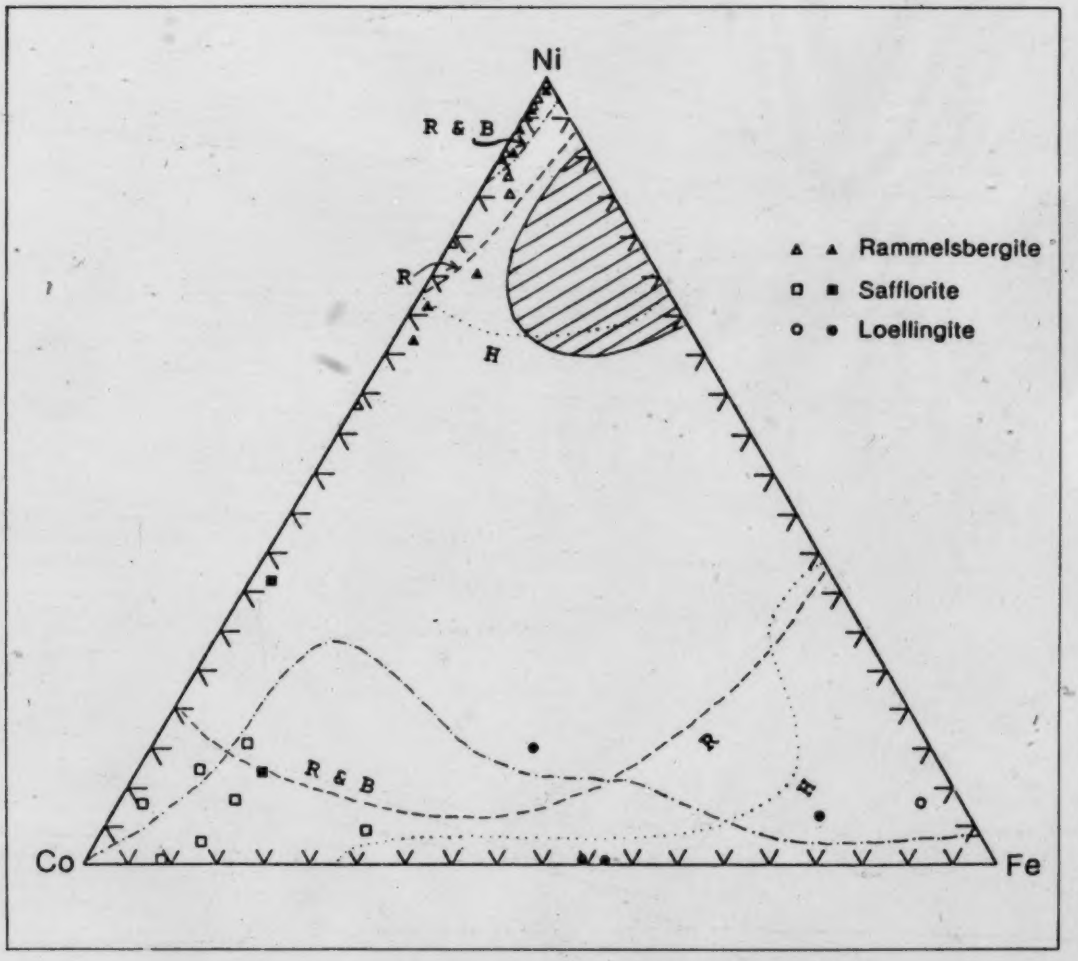

Figure 9. Compositional variations of the diarsenides in the ores of the Great Bear Lake silver deposits. H - Holmes (1947). R - Roseboom (1963). R & B - Radcliffe and Berry (1968). Closed symbol - Echo Bay sector. Open symbol - Camsell River sector. Data listed in Tables 3, 4 and 5.

COLOURED PICTURES
Images en couleur

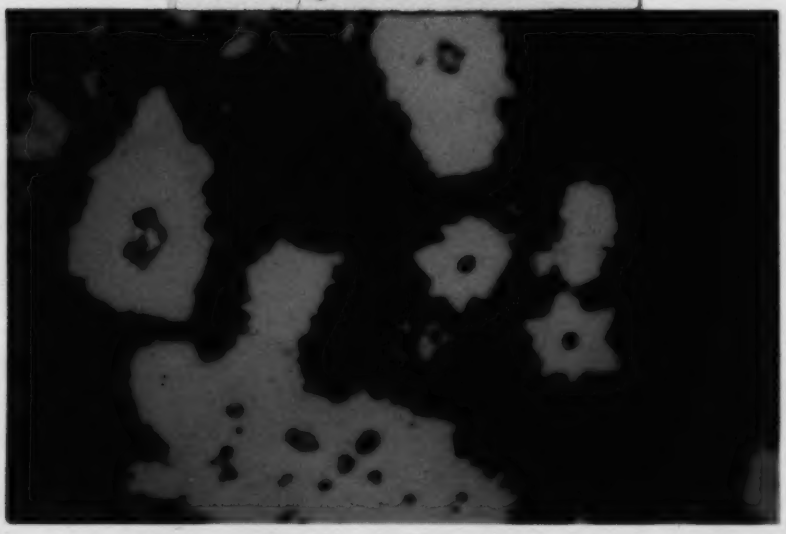

Plate 3. Inclusions of native silver in safflorite stars. Contact Lake mine. P.P.L. 200X.

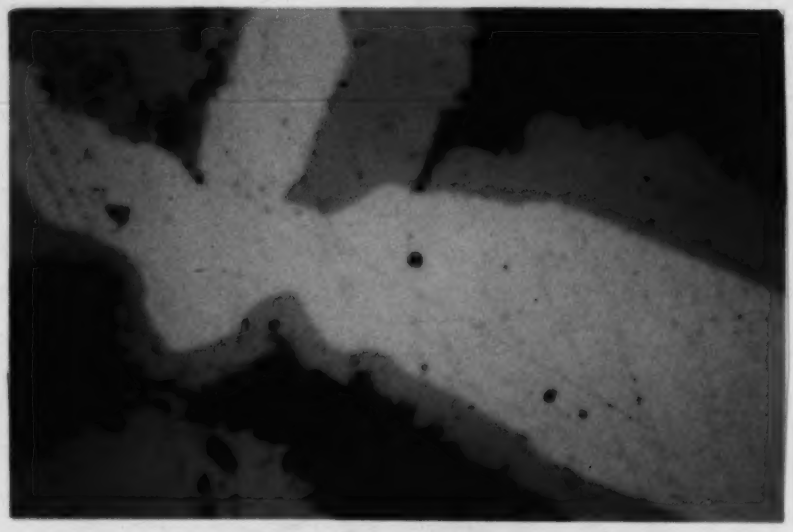

Plate 4. A dendrite of native silver being rimmed by rammelsbergite. Smallwood mine. P.P.L. 200X.

Table 3

Electron microprobe analyses of safflorites from the Great Bear Lake silver deposits, N.W.T.. Data plotted in Figure 9.

Sample nos.	Remarks	Fe	Co	Ni	S	As	Sb	Total
C1/32	--	7.82	18.37	1.14	0.78	70.41	1.11	99.59
2A/3L/7V/SB	(Core)	2.54	27.35	N.D.	7.50	59.99	2.06	99.44
2A/3L/7V/SB	(Rim)	2.04	24.20	3.60	6.42	60.80	2.19	99.25
3B/125/ED	--	3.00	16.75	2.75	0.78	75.63	0.50	99.41
2B/250/ED	--	0.57	17.79	10.64	3.81	65.93	1.44	100.18
SW/2A	(Core)	3.46	26.45	0.90	2.86	65.48	0.62	99.77
SW/2A	(Rim)	3.62	23.62	2.65	1.98	66.86	0.58	99.31
NX/22	--	2.74	20.47	4.32	1.55	69.92	0.35	99.35
NR/2B	--	0.73	24.80	2.12	1.18	70.82	N.D.	99.65

Atomic proportions of safflorites calculated on the basis of As+S+Sb=2.00

Sample nos.	Fe	Co	Ni	S	As	Sb	Fe+Co+Ni	As+S+Sb
C1/32	0.28	0.62	0.04	0.05	1.93	0.02	0.98	2.00
2A/3L/7V/SB	0.09	0.88	0.00	0.45	1.52	0.03	0.97	2.00

2A/3L/7V/SB	0.07	0.80	0.12	0.39	1.58	0.03	0.99	2.00
3B/125/ED	0.10	0.55	0.09	0.05	1.95	0.00	0.74	2.00
2B/250/ED	0.02	0.60	0.36	0.24	1.74	0.02	0.98	2.00
SW/2A	0.12	0.91	0.03	0.18	1.82	0.00	1.06	2.00
SW/2A	0.13	0.81	0.09	0.12	1.88	0.00	1.03	2.00
NX/22	0.10	0.70	0.15	0.10	1.90	0.00	0.95	2.00
NR/2B	0.03	0.84	0.07	0.08	1.92	0.00	0.94	2.00

N.D. - Not detected. Cl - Contact Lake. SB - Silver Bear (or Terra). ED - Eldorado. SW - Smallwood. NR - Northrim. NX - Norex.

The electron microprobe analytical results are presented in Table 3 and compositional variations are shown in Figure 9. The results show maximum contents of 7.82% iron, 27.35% cobalt, 10.64% nickel, 7.50% sulphur, 75.63% arsenic and 2.19% antimony. The metal to non-metal ratios were found to vary from 0.74 : 2.00 to 1.06 : 2.00. Samples C1/28 and 3B/125/ED, from Contact Lake and Eldorado deposits respectively, show high concentrations of arsenic. This is, however, within the range of maximum published arsenic content in safflorites. Safflorites containing up to 80 mole% $CoAs_2$ have been reported. The depletion in arsenic content in some samples may be attributed to substitution of arsenic by antimony and by sulphur.

Zoning in the safflorites is quite common. Analyses of two zoned crystals showed depletion of cobalt towards the rim, whilst nickel was found to increase. No significant zoning of As:S ratio was observed. The depletion in the content of cobalt may be due to its association with the nickel-bearing arsenide minerals, namely, rammelsbergite and gersdorffite.

4.3.3.2 Loellingite ($FeAs_2$)

Loellingite, the iron end-member of the $CoAs_2$-$FeAs_2$ series, is not as widespread as safflorite and rammelsbergite in the Great Bear Lake ores. It was identified only in three deposits, namely, Eldorado, Terra and Contact Lake. In the Contact Lake deposit it occurs in massive form, enclosing star-shaped native silver grains. In the Eldorado and Terra deposits, it occurs in intimate association with the other arsenides. It was differentiated from the other diarsenides by its stronger anisotropy.

The electron microprobe analytical results are shown in Table 4 and compositional variations are shown in Figure 9. There is appreciable substitution of iron by cobalt, and to lesser extent by nickel. Substitution of arsenic by sulphur and by antimony is insignificant. Metal zoning was observed in sample number C1/31. The concentration of iron is found to decrease towards the rim. This is accompanied by a concomitant increase in the nickel content towards the rim.

Table 4

Electron microprobe analyses of loellingites from the Great Bear Lake silver deposits, N.W.T.. Data plotted in Figure 9.

Sample nos.	Fe	Co	Ni	S	As	Sb	Total
Cl/31	14.75	11.28	N.D.	N.D.	73.32	0.30	99.65
Cl/31	14.58	12.36	0.09	N.D.	72.04	0.52	99.52
Cl/31	11.19	11.65	3.97	0.91	72.11	0.31	100.14
1A/250/ED	20.25	4.35	1.65	1.23	71.50	0.62	99.60
1A/912/SB	24.61	1.26	2.25	0.83	69.82	0.59	99.36

Atomic proportions of loellingites calculated on the basis of As+S+Sb=2.00

Sample nos.	Fe	Co	Ni	S	As	Sb	Fe+Co+Ni	As+S+Sb
Cl/31	0.54	0.39	0.00	0.00	1.99	0.01	0.93	2.00
Cl/31	0.54	0.43	0.00	0.00	1.99	0.01	0.97	2.00
Cl/31	0.40	0.40	0.13	0.05	1.94	0.01	0.93	2.00
1A/250/ED	0.72	0.15	0.05	0.08	1.91	0.01	0.92	2.00
1A/912/SB	0.91	0.04	0.08	0.05	1.94	0.01	1.03	2.00

N.D. - Not detected. Cl - Contact Lake. ED - Eldorado. SB - Silver Bear (or Terra).

4.3.3.3 Rammelsbergite ($NiAs_2$)

Rammelsbergite is the most common diarsenide within the ores of the Great Bear Lake silver deposits. It has been identified in all the deposits of the region in variable proportions. It occurs as dendrites, rosettes and aggregates of euhedral crystals. It is most commonly associated with nickeline, safflorite, native silver, native bismuth and sulpharsenides, such as, cobaltite and gersdorffite. It encloses native silver and carbonate cores in the dendrites and in turn is rimmed either by cobaltite or by gersdorffite (Plate 4). Wherever safflorite is associated with the rammelsbergite it occurs as alternating bands. It was identified under the microscope by its higher reflectivity and weaker anisotropy compared to the other diarsenides.

The electron microprobe analytical results are given in Table 5 and compositional variations are shown in Figure 9. The results show that there are no systematic variations in the compositions of the rammelsbergite. The metal to non-metal ratios are found to vary from 0.93 : 2.00 to 1.01 : 2.00. Metal zoning was observed in the samples from the Eldorado (sample # 3B/125/ED), the Contact Lake (sample # 22A/Cl) and in the Norex (sample # NX/22) deposits. In all these samples, the rammelsbergites are associated with nickeline cores. The cores are found to be more depleted in nickel relative to the rims. The concentrations of nickel and cobalt are found to be related to the associated mineral assemblages. Rammelsbergite is found to be enriched in nickel when in association with nickeline, and in cobalt when in association with safflorite. There seems to be no correlation between the proximity of native silver and the composition of rammelsbergite.

4.3.3.4 Pararammelsbergite ($NiAs_2$)

Pararammelsbergite is not very common in the ores of the Great Bear Lake silver deposits. It was identified only in the ores of the Terra deposit where it occurs in association with native bismuth, nickeline and rammelsbergite. It forms rims around nickeline. It is very similar to rammelsbergite in its optical properties. However, it lacks the bluish anisotropy colour of rammelsbergite.

Table 5

Electron microprobe analyses of rammelsbergites from the Great Bear Lake silver deposits, N.W.T.. Data plotted in Figure 9.

Sample nos.	Remarks	Fe	Co	Ni	S	As	Sb	Total
14B/SB	(Core)	N.D.	0.54	26.67	0.74	70.98	0.73	99.66
14B/SB	(Rim)	N.D.	0.97	26.56	0.56	71.28	0.68	100.05
NR/3	(Core)	N.D.	N.D.	27.76	2.07	69.08	0.53	99.44
NR/3	(Rim)	N.D.	N.D.	27.72	1.42	70.56	0.47	100.17
3B/125/ED	(Core)	0.32	2.27	24.36	N.D.	73.82	N.D.	100.77
3B/125/ED	(Rim)	1.28	5.32	19.88	N.D.	74.44	N.D.	100.92
Cl/22A	(Core)	0.32	7.83	20.13	1.34	69.74	0.54	99.90
Cl/22A	(Mid pt.)	0.42	8.91	18.70	1.40	70.27	0.29	99.99
Cl/22A	(Rim)	0.30	N.D.	26.99	1.39	70.34	0.32	99.47
NX/22	(Core)	N.D.	11.73	16.34	0.20	71.11	N.D.	99.38
NX/22	(Mid pt.)	N.D.	5.90	21.95	N.D.	71.15	N.D.	99.00
NX/22	(Rim)	N.D.	2.57	24.59	1.43	71.16	N.D.	99.75
EB/316/6A	(Core)	N.D.	1.00	27.60	1.20	69.60	0.30	99.90
EB/316/6A	(Rim)	N.D.	1.26	27.8	1.32	68.90	0.60	99.88
ELB/1	(Core)	N.D.	2.65	26.80	1.02	67.92	1.25	99.64
ELB/1	(Rim)	N.D.	1.89	27.6	0.98	68.60	0.96	100.03
SW/1	(Core)	0.90	3.26	24.80	0.60	69.50	0.70	99.76
SW/1	(Rim)	0.60	2.96	25.60	0.40	70.50	N.D.	100.06

Table 5 (continued)

Atomic proportions of rammelsbergites calculated on the basis of As+S+Sb=2.00

Sample nos.	Fe	Co	Ni	S	As	Sb	Fe+Co+Ni	As+S+Sb
14B/SB	0.00	0.02	0.92	0.04	1.96	0.00	0.94	2.00
14B/SB	0.00	0.03	0.90	0.04	1.96	0.00	0.93	2.00
NR/3	0.00	0.00	0.95	0.12	1.88	0.00	0.95	2.00
NR/3	0.00	0.00	0.95	0.10	1.90	0.00	0.95	2.00
3B/125/ED	0.01	0.08	0.85	0.00	2.00	0.00	0.94	2.00
3B/125/ED	0.05	0.18	0.68	0.00	2.00	0.00	0.91	2.00
CI/22A	0.01	0.27	0.69	0.08	1.92	0.00	0.97	2.00
CI/22A	0.02	0.30	0.64	0.08	1.92	0.00	0.96	2.00
CI/22A	0.01	0.00	0.93	0.08	1.92	0.00	0.94	2.00
NX/22	0.00	0.42	0.59	0.00	2.00	0.00	1.01	2.00
NX/22	0.00	0.21	0.78	0.00	2.00	0.00	0.99	2.00
NX/22	0.00	0.09	0.87	0.08	1.92	0.00	0.96	2.00
EB/316/6A	0.00	0.03	0.95	0.06	1.94	0.00	0.98	2.00
EB/316/6A	0.00	0.04	0.95	0.08	1.92	0.00	0.99	2.00
ELB/1	0.00	0.09	0.92	0.08	1.92	0.02	1.01	2.00
ELB/1	0.00	0.06	0.95	0.06	1.94	0.00	1.01	2.00
SW/1	0.03	0.11	0.85	0.04	1.96	0.00	0.99	2.00
SW/1	0.02	0.10	0.87	0.02	1.98	0.00	0.99	2.00

SB - Silver Bear, NR - Northrim, ED - Eldorado, CI - Contact Lake, NX - Nowex, EB - Echo Bay, ELB - El Bonanza, SW - Smallwood.

The electron microprobe analytical results are shown in Table 6. The metal to non-metal ratios are found to vary from 1.06 : 2.00 to 1.08 : 2.00. According to Yund (1961) the pararammelsbergite-rammelsbergite inversion occurs at 590°C for pure $NiAs_2$ in equilibrium with nickeline and under the vapour pressure of the assemblage. But substitution of arsenic by sulfur lowers the inversion to 475 ± 25°C. Since the presence of cobalt and iron further lowers the inversion temperature, the pararammelsbergites in this deposit probably formed at some temperature lower than 450°C.

4.3.4 Triarsenides

Palache *et al.* (1944) classified the isometric triarsenides with the general formula $(Co,Ni)As_{3\pm x}$ into two groups : (i) the skutterdite-Ni skutterudite series in which the value of x varies from 0.0 to 0.5, (ii) the smaltite-chloanthite series, in which the value of x varies from 0.5 to 1.0.

According to Holmes (1947) there was no real basis for the above classification, for many of the analyses were carried out on impure specimens. Holmes (1947) instead classified the higher arsenides into two groups : (a) the isometric triarsenides, namely, the skutterudite series and (b) the 'orthorhombic' diarsenide series. Holmes (1947) suggested that the names smaltite, chloanthite, chathamite, and arsenoferrite, which were formerly associated with the alleged series of isometric diarsenides, should be dropped. According to him the term 'skutterudite' should be applied to all isometric arsenides of Co, Ni, and Fe and in a restricted sense to those in which cobalt is dominant; the prefixes ***nickelian*** and ***ferrian*** would indicate the dominance of nickel and iron respectively. In this investigation the classification proposed by Holmes (1947) has been followed.

Roseboom (1962) carried out investigations on the compositions and cell dimensions of skutterudites. He synthesized skutterudites by heating mixtures of cobalt, nickel, iron and arsenic at 600°C to 800°C in sealed evacuated silica tubes. According to him the apparent deficiency of arsenic in natural skutterudites is due to the presence of other phases as

Table 6

Electron microprobe analyses of pararammelsbergites from the Great Bear Lake silver deposits, N.W.T..

Sample nos.	Fe	Co	Ni	S	As	Sb	Total
4B/111/SB	N.D.	0.80	29.26	0.60	69.82	N.D.	100.48
4B/111/SB	0.42	1.33	27.78	1.21	67.64	0.84	99.22

Atomic proportions of pararammelsbergites calculated on the basis of As+S+Sb=2.00

Sample nos.	Fe	Co	Ni	S	As	Sb	Fe+Co+Ni	As+S+Sb
4B/111/SB	0.00	0.03	1.05	0.40	1.96	0.00	1.08	2.00
4B/111/SB	0.02	0.05	0.99	0.09	1.90	0.01	1.06	2.00

N.D. - Not detected. SB - Silver Bear.

impurities. He found only very small deficiency of arsenic in the synthetic skutterudites. Like the natural skutterudites, which vary widely in cobalt, nickel and iron concentrations, but in which pure nickel- and iron- end members are unknown, the synthetic skutterudites were also found to vary in nickel, cobalt, and iron. Roseboom found that the limits of solid solution vary little with temperature between 600°C and 800°C and concluded that most natural skutterudites fall within the limits of solid solution observed for the synthetic phases.

Radcliffe (1968) investigated the composition of skutterudites with the help of the electron microprobe. The results obtained by him were similar to Holmes (1947). The maximum concentrations he obtained were 82 wt.% $CoAs_3$, 7 wt.% $NiAs_3$, and 11 wt.% $FeAs_3$. According to him, the deficiency in arsenic is due to the presence of some metal atoms in arsenic lattice sites. The deficiency of total atoms from the ideal 32 indicates that some arsenic lattice sites are vacant.

4.3.4.1 Skutterudite ($CoAs_{3\pm x}$)

Skutterudite has been identified in all the silver deposits of the Great Bear Lake region and commonly occurs as aggregates or suhedral crystals associated with native silver, native bismuth, the diarsenides and the sulpharsenides. It was easily distinguished under the microscope from the other arsenides by its idiomorphic form and lack of anisotropy (it is isotropic).

The electron microprobe analytical results for the skutterudites are given in Table 7 and the compositional variations are shown in Figure 10. Rojkovic (1971) reported higher concentrations of arsenic. He, however, did not analyse for antimony, which occurs in concentrations up to 1.5 wt.% and clearly substitutes for arsenic. The results show that the skutterudites from the Great Bear Lake silver deposits are cobaltian skutterudites with variable proportions of nickel and iron. Zoning is quite common in most of the analysed skutterudites. The cores of the grains are found to be depleted in cobalt relative to the rims in all the samples analysed, except in the one from the Echo Bay deposit (sample # 6A/316/EB) where the reverse case was observed. Investigations by Holmes (1947),

Table 7

Electron microprobe analyses of skutterudites from the Great Bear Lake silver deposits, N.W.T.. Data plotted in Figure 10.

Sample nos.	Remarks	Fe	Co	Ni	S	As	Sb	Total
Cl/28	(Core)	2.25	18.34	2.24	0.52	77.46	N.D.	100.81
Cl/28	(Rim)	1.56	19.84	1.45	1.01	76.40	N.D.	100.26
ED/3B/125	(Core)	3.00	17.75	2.44	N.D.	76.29	N.D.	99.48
ED/3B/125	(Rim)	1.26	19.26	1.72	N.D.	77.16	N.D.	99.4
NR/1	(Core)	1.58	17.34	1.81	N.D.	79.60	N.D.	100.33
NR/1	(Rim)	1.26	20.62	0.98	0.84	76.33	N.D.	100.03
NX/5A	(Core)	2.60	17.82	1.27	1.08	77.32	0.28	100.37
NX/5A	(Rim)	0.74	20.30	N.D.	1.00	78.00	0.53	100.57
SB/209/1B	(Core)	5.37	14.09	2.66	0.58	77.39	N.D.	100.09
SB/209/1B	(Rim)	2.62	18.27	1.62	0.98	76.37	N.D.	99.86
SW/6X	(Core)	0.22	11.85	9.25	1.03	76.42	0.84	99.61
SW/6X	(Rim)	0.24	14.98	6.09	0.99	77.28	0.31	99.89
EB/316/6A	(Core)	0.25	14.82	6.16	N.D.	77.95	0.28	99.46
EB/316/6A	(Rim)	0.32	12.09	8.38	N.D.	77.41	0.74	98.94
ELB/8X	(Core)	4.06	15.82	1.70	0.88	77.71	0.30	100.47
ELB/8X	(Rim)	1.73	18.86	0.11	0.81	78.05	N.D.	99.56

N.D. - Not detected. Cl - Contact Lake. ED - Eldorado. NR - Northrim. NX - Norex. SB - Silver Bear (or Terra). SW - Smallwood. EB - Echo Bay. ELB - El Bonanza.

Table 7 (continued)

Atomic proportions of skutterudites calculated on the basis of Fe+Ni+Co=1.00

Sample nos.	Fe	Co	Ni	S	As	Sb	Fe+Co+Ni	As+S+SB
Cl/28	0.10	0.80	0.10	0.04	2.66	0.00	1.00	2.70
Cl/28	0.07	0.86	0.07	0.08	2.62	0.00	1.00	2.70
ED/3B/125	0.14	0.76	0.10	0.00	2.56	0.00	1.00	2.56
ED/3B/125	0.06	0.86	0.08	0.00	2.72	0.00	1.00	2.72
NR/1	0.08	0.84	0.08	0.00	3.01	0.00	1.00	3.01
NR/1	0.06	0.90	0.04	0.07	2.60	0.00	1.00	2.67
NX/5A	0.12	0.82	0.06	0.09	2.79	0.00	1.00	2.88
NX/5A	0.04	0.96	0.00	0.08	2.91	0.00	1.00	2.99
SB/209/1B	0.25	0.63	0.12	0.05	2.71	0.00	1.00	2.76
SB/209/1B	0.12	0.81	0.07	0.08	2.65	0.00	1.00	2.73
SW/6X	0.01	0.56	0.43	0.09	2.81	0.02	1.00	2.92
SW/6X	0.01	0.70	0.29	0.08	2.84	0.00	1.00	2.92
EB/316/6A	0.02	0.70	0.28	0.00	2.86	0.00	1.00	2.86
EB/316/6A	0.02	0.58	0.40	0.00	2.87	0.02	1.00	2.91
ELB/8X	0.20	0.72	0.08	0.07	2.80	0.00	1.00	2.87
ELB/8X	0.08	0.87	0.05	0.07	2.82	0.00	1.00	2.89

Cl - Contact Lake. ED - Eldorado. NR - Northrim. NX - Norex. SB - Silver Bear (or Terra). SW - Smallwood. EB - Echo Bay. ELB - El Bonanza.

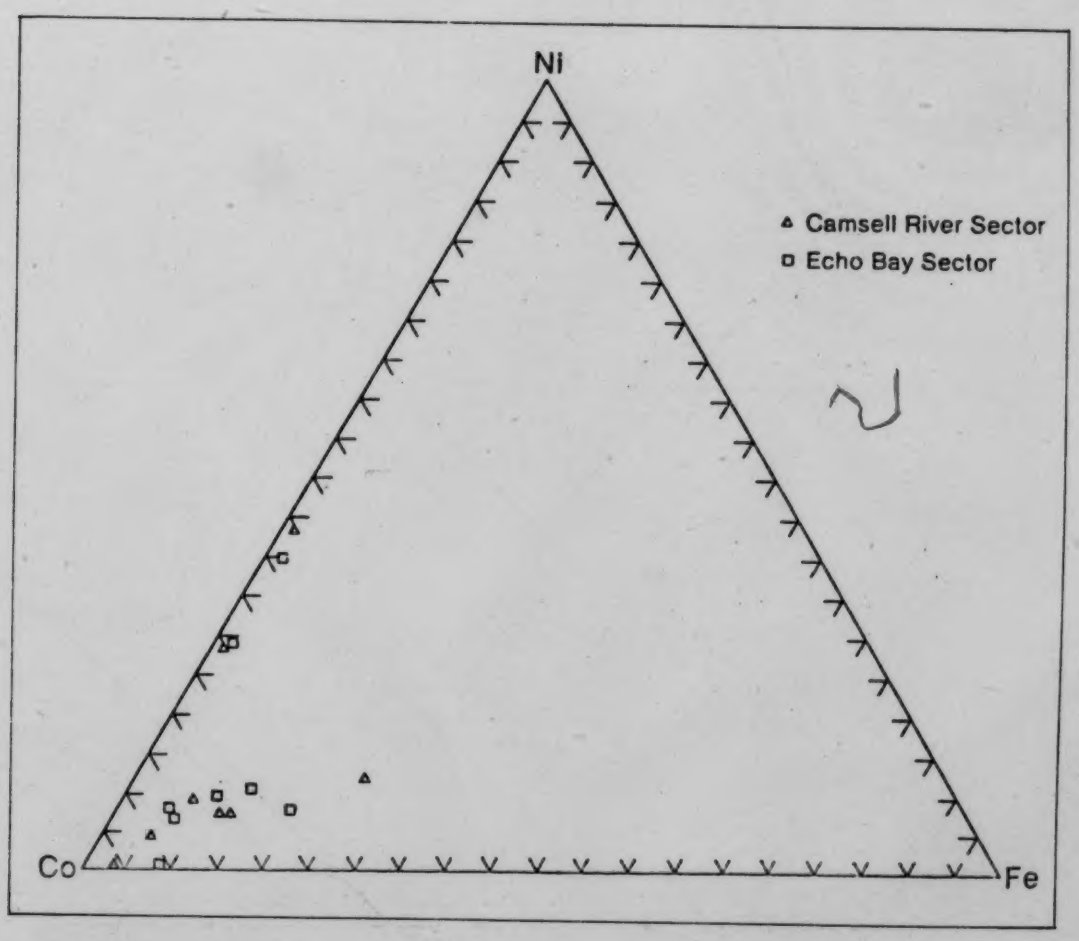

Figure 10. Compositional variations of skutterudites in the ores of the Great Bear Lake silver deposits. Data listed in Table 7.

Roseboom (1962) and Radcliffe (1968) had revealed arsenic deficiency in skutterudites. However, in this study some of the analysed skutterudites were found to be enriched in arsenic.

4.3.5 Sulpharsenides

Cobaltite, gersdorffite, arsenopyrite and glaucodot are the only sulpharsenides which have been identified in the ores of the Great Bear Lake silver deposits. Cobaltite and gersdorffite are more widespread than arsenopyrite and glaucodot. Quantitative electron microprobe analysis of glaucodot was not carried out.

4.3.5.1 Cobaltite (CoAsS)

The cobaltite commonly occurs as intergrowths with, and rims around, the other arsenides.

The results of the electron microprobe analyses of the cobaltites are given in Table 8 and the compositional variations are shown in Figure 11. Although the ideal composition of cobaltite is CoAsS, Bayliss (1969, 1982) and Klemm (1965) have shown that nickel and iron may substitute for cobalt, and sulphur and arsenic may substitute for each other. The cobaltites from the Great Bear Lake silver deposits show variable composition. Iron and nickel are found to substitute for cobalt in varying amounts. The degree of substitution of nickel for cobalt was found to be related to the associated minerals. The cobaltites which are associated with gersdorffite are found to be more enriched in nickel. The rims near gersdorffite were found to be more enriched in nickel relative to the cores. This may be the cobaltian gersdorffite reported by Petruk *et al.* (1971). There is no correlation between cobalt and iron.

The metal to non-metal ratios and the variations in the As:S ratios are shown in Table 8. The atomic percents of sulfur and arsenic of the analysed cobaltites are plotted in Figure 12. It is found that the cobaltites clearly fall into two groups. The cobaltites from the Echo Bay sector are found to be more enriched in sulfur and depleted in arsenic. The

Table 8

Electron microprobe analyses of cobaltites from the Great Bear Lake silver deposits, N.W.T.. Data plotted in Figures 11 and 12.

Sample nos.	Fe	Co	Ni	S	As	Sb	Total
SB/14B	1.04	19.61	12.17	15.80	50.51	0.40	99.53
Cl/32	N.D.	21.20	12.42	17.83	46.84	1.25	99.54
NR/3	3.60	29.34	0.64	17.66	48.45	0.33	100.02
NX/6A	2.14	22.64	8.57	15.37	50.55	N.D.	99.27
1/500/ED	0.44	28.45	4.90	18.49	47.34	0.36	99.98
6A/316/EB	1.00	24.30	6.68	21.90	46.70	N.D.	100.58
SW/6X	1.9	21.62	5.26	17.67	52.67	0.82	99.94

N.D. - Not detected. SB - Silver Bear (or Terra). Cl - Contact Lake. NR - Northrim. ED - Eldorado. EB - Echo Bay. SW - Smallwood.

Table 8 (continued)

Atomic proportions of cobaltites calculated on the basis of As+S+Sb=2.00

Sample nos.	Fe	Co	Ni	S	As	Sb
SB/14B	0.03	0.57	0.36	0.85	1.15	0.00
Cl/32	0.00	0.60	0.36	0.93	1.05	0.00
NR/3	0.10	0.83	0.02	0.92	1.08	0.00
NX/6A	0.07	0.66	0.25	0.83	1.17	0.00
1/500/ED	0.01	0.80	0.14	0.95	1.05	0.00
6A/316/EB	0.03	0.63	0.17	1.05	0.95	0.00
SW/6X	0.05	0.58	0.14	0.88	1.11	0.01

SB - Silver Bear (or Terra). Cl - Contact Lake. NR - Northrim. NX - Norex. ED - Eldorado. EB - Echo Bay. SW - Smallwood.

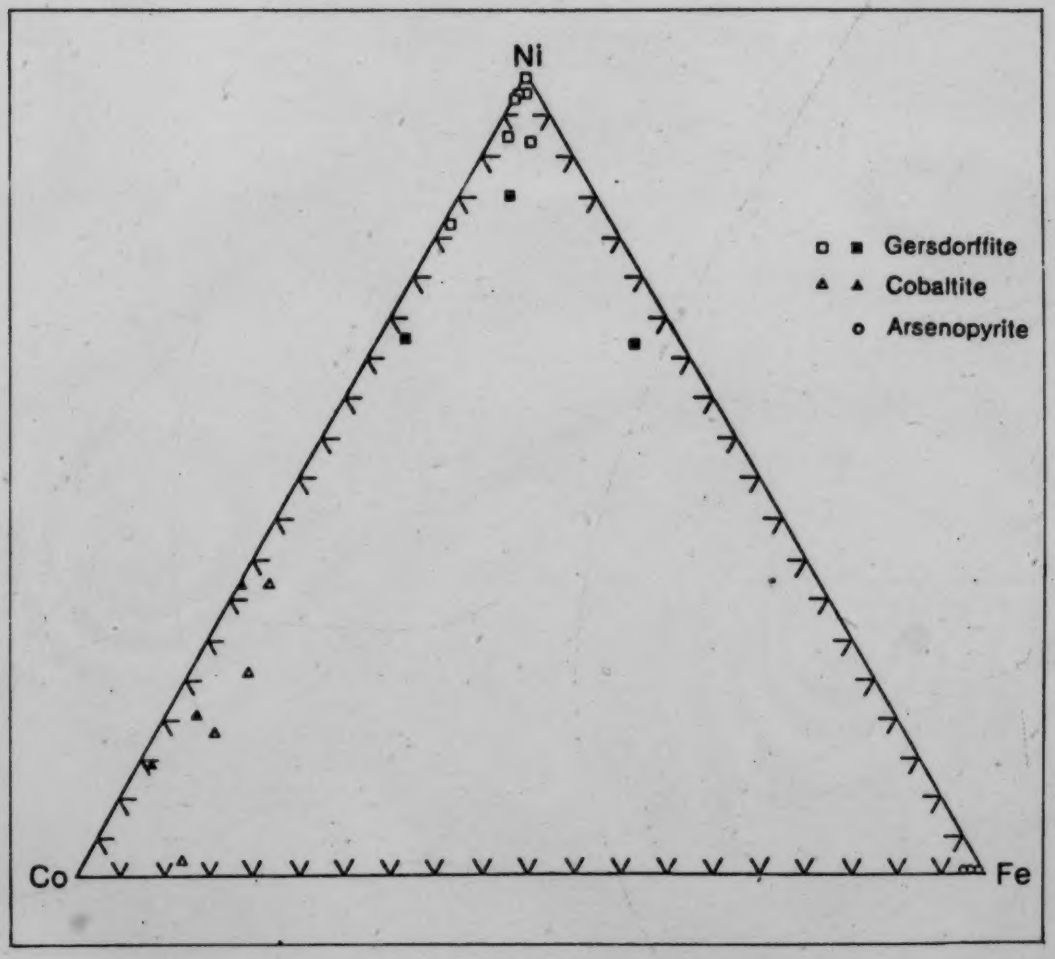

Figure 11. Compositional variations of the sulpharsenides in the ores of the Great Bear Lake silver deposits. Closed symbol - Camsell River sector. Open symbol - Echo Bay sector. Data listed in Tables 8, 9 and 10.

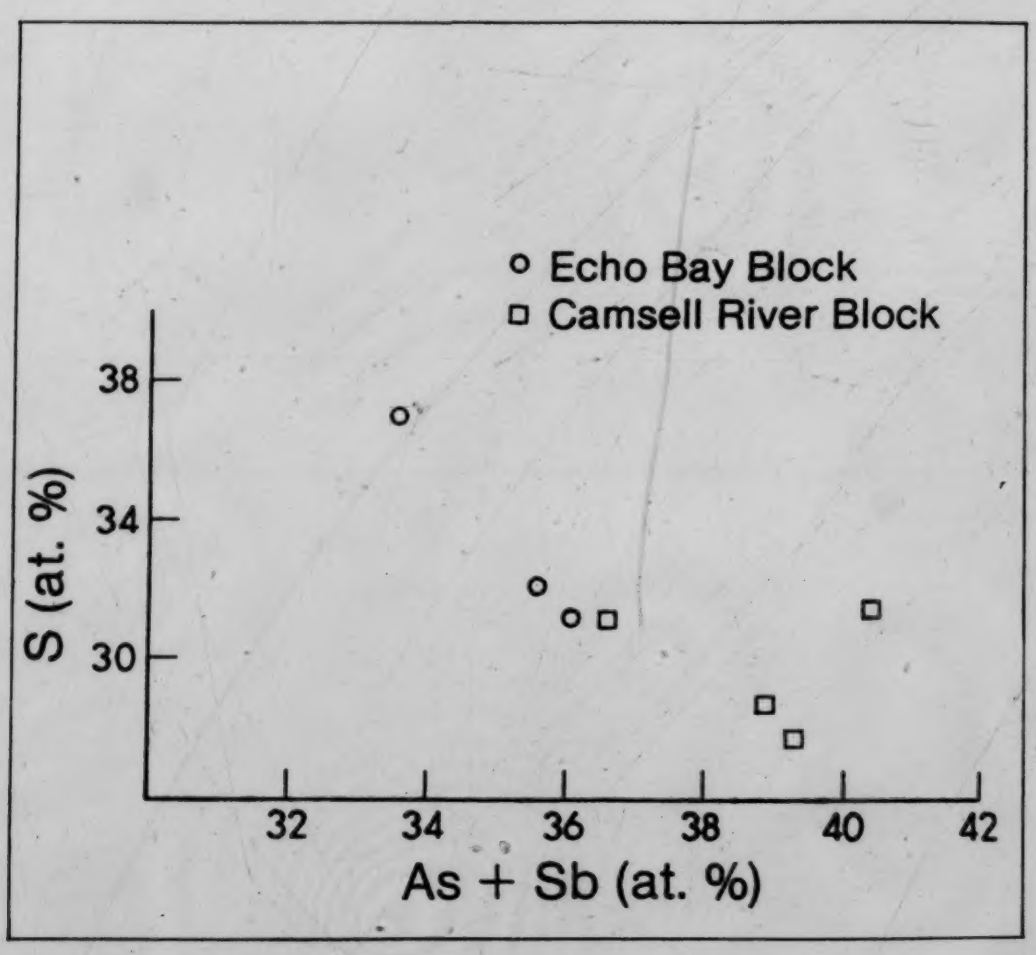

Figure 12. Variations of As + Sb : S ratios of cobaltites in the ores of the Great Bear Lake silver deposits. Data listed in Table 8.

variations in the compositions of the cobaltites from the two sectors may be attributed to one of the following reasons :

(i) the cobaltites in the two sectors were formed at different times under different conditions;

(ii) the cobaltites formed at the same time but under different physico-chemical conditions.

4.3.5.2 Gersdorffite (NiAsS)

Gersdorffite, like cobaltite, occurs as rims around the other arsenides. It is most commonly associated with skutterudite, nickeline and cobaltite.

Two varieties of gersdorffite have been recognised in the ores of the Great Bear Lake silver deposits. Optically, the first variety is light grey in colour, while the second variety is dark grey in colour (Plate 5). The difference in optical properties was found to be correlated with the chemical composition. The first variety is enriched in arsenic. This may be the arsenian gersdorffite reported by Petruk *et al.* (1971) from the Cobalt-Gowganda ores. The second variety is the normal gersdorffite.

The electron microprobe results of the gersdorffites are shown in Table 9 and Figure 11 shows the compositional variations of gersdorffites in the region. Although gersdorffite has an ideal composition of NiAsS, there may be significant deviations from the ideal. According to Klemm (1965) nickel is substituted by cobalt and iron, and according to Yund (1962) arsenic and sulphur can substitute for each other in the range of $NiAs_{1.77}S_{0.23}$ to $NiAs_{0.77}S_{1.23}$. Antimony can substitute for both sulphur and arsenic. According to Yund (1962) synthetic gersdorffite is homogeneous over a large compositional interval. According to him the variation in the maximum arsenic of gersdorffite from 450°C to 660°C is only about 3.00 weight percent $NiAs_2$. Thus the solvus at this temperature range cannot be used as a potential geothermometer for natural gersdorffites.

Zoning was not observed in all the samples analysed. In two specimens the cores were found to be more enriched in nickel relative to the rims. A wide variation in the As:S

COLOURED PICTURES
Images en couleur

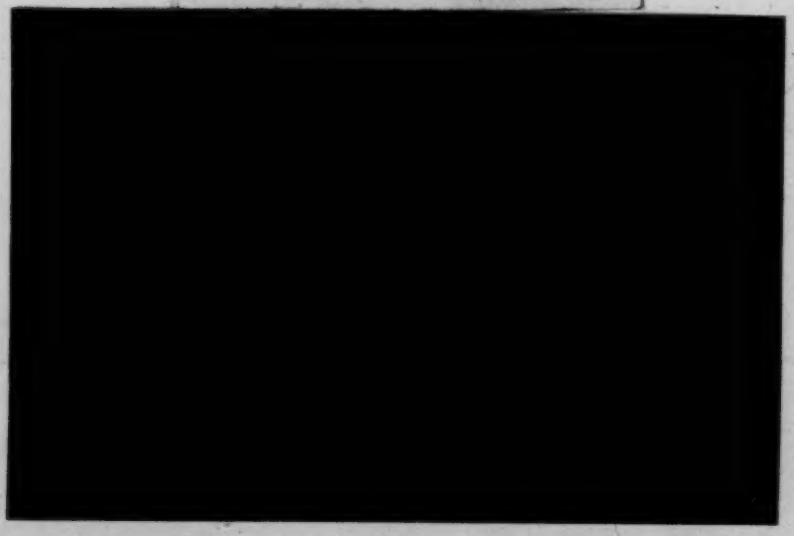

Plate 5. Intergrowths of gersdorffite (grey), arsenian gersdorffite (bluish grey) and nickeline (pinkish)being replaced by native bismuth (pale brownish). Norex mine. P.P.L. 200X.

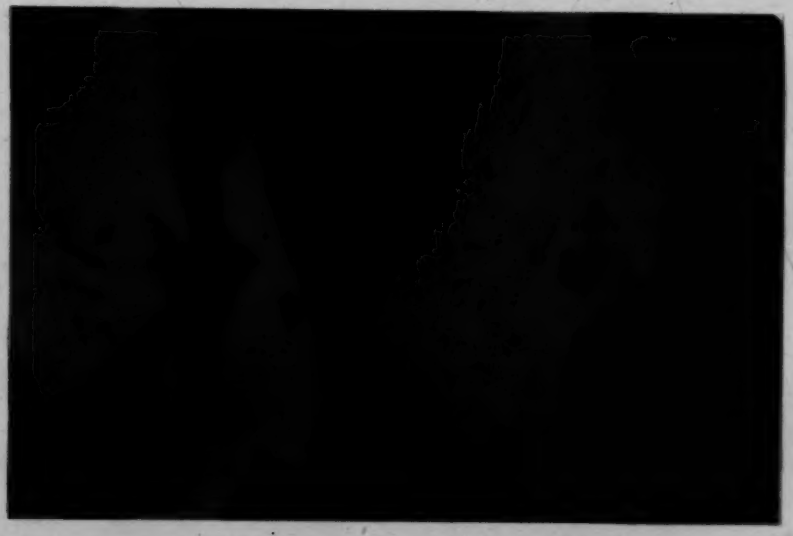

Plate 6. Idiomorphic (diamond-shaped) and sub-idiomorphic grains of arsenopyrite within gangue (black). Terra mine. P.P.L. 200X.

Table 9

Electron microprobe analyses of gersdorffites from the Great Bear Lake silver deposits, N.W.T.. Data plotted in Figures 11 and 13.

Sample nos.	Remarks		Co	Ni	S	As	Sb	Total
SB/14B	(Core)	N.D.	.96	32.19	16.06	49.63	0.97	99.81
SB/14B	(Rim)	0.50	2.04	30.46	17.78	48.12	1.02	99.92
NR/1	..	0.18	5.18	23.80	7.06	62.81	0.14	99.17
NX/22	..	1.58	1.32	30.35	17.05	48.31	0.20	99.81
NX/24	..	N.D.	0.45	30.38	9.48	58.91	0.20	99.42
NX/24	(Core)	N.D.	0.74	32.94	16.53	49.03	0.58	99.82
NX/24	(Rim)	N.D.	N.D.	30.26	18.12	51.20	0.62	100.20
3B/125/ED	..	9.44	0.99	21.56	19.01	48.98	0.40	100.38
6A/316/EB	..	1.96	3.2	28.90	16.60	49.10	N.D.	99.76
CI/31	..	8.62	1.63	20.29	18.64	49.95	0.28	99.41

N.D. - Not detected. SB - Silver Bear. NR - Northrim. NX - Nexus. ED - Eldorado. EB - Echo Bay. CI - Contact Lake.

Table 9 (continued)

Atomic proportions of gersdorffites calculated on the basis of As+S+Sb=2.00

Sample nos.	Fe	Co	Ni	S	As	Sb
SB/14B	0.00	0.03	0.92	0.87	1.11	0.01
SB/14B	0.02	0.06	0.86	0.92	1.07	0.01
NR/1.	0.00	0.16	0.76	0.42	1.58	0.00
NX/22	0.05	0.04	0.88	0.91	1.09	0.00
NX/24	0.00	0.01	0.95	0.55	1.45	0.00
NX/24	0.00	0.02	0.96	0.88	1.12	0.00
NX/24	0.00	0.00	0.82	0.91	1.09	0.00
SB/12A/ED	0.27	0.03	0.59	0.95	1.05	0.00
6A/316/EB	0.05	0.09	0.84	0.88	1.12	0.00
CI/32	0.25	0.04	0.55	0.93	1.07	0.00

SB - Silver Bear, NR - Northrim, NX - Norex, ED - Eldorado, EB - Echo Bay, CI - Contact Lake.

ratio was observed. The variations were observed in the same sample as well as from different samples from the same deposit.

The arsenian gersdorffites was found only in the Camsell River sector (Fig. 13). The normal gersdorffite was found in both the sectors. According to Withers (1979) the arsenian gersdorffite may be the product of reaction between rammelsbergite and gersdorffite during a minor thermal pulse. He, however, did not specify the source of heat. It is more likely that the arsenian gersdorffite was formed by changes in the As:S ratio of the ore-fluid.

4.3.5.3 Arsenopyrite (FeAsS)

Arsenopyrite is not widespread in the ores of the Great Bear Lake silver deposits. Two generations of arsenopyrites were identified. The earlier generation occurs in association with the arsenides and sulpharsenides. The later generation occurs in association with the sulphides. They commonly occur as idiomorphic grains and in massive form (Plate 6). The massive variety was found to be only associated with the arsenides and sulpharsenides. The idiomorphic variety was found to be associated with both the arsenides and the sulpharsenides.

The electron microprobe results of the arsenopyrites are shown in Table 10 the compositional variations are shown in Figure 11. The results show that the arsenopyrites have compositions which deviate from the ideal FeAsS. According to Clark (1960), cobalt can substitute for iron, and sulfur and arsenic can substitute for each other. Substitution of iron by cobalt was observed in the analysed arsenopyrites.

According to Kretschmar and Scott (1976) and Scott (1983) arsenopyrite can be used as geothermometer if it was formed in a sulfur buffered assemblage. Since arsenopyrite does not re-equilibrate on cooling because of its refractory nature, the temperature of formation can be determined from its composition if the sulfur activity can be estimated. Lowell and Gasparrini (1982) and Kalogeropoulos (1984) determined the temperature of crystallization from unbuffered arsenopyrites. According to Lowell and

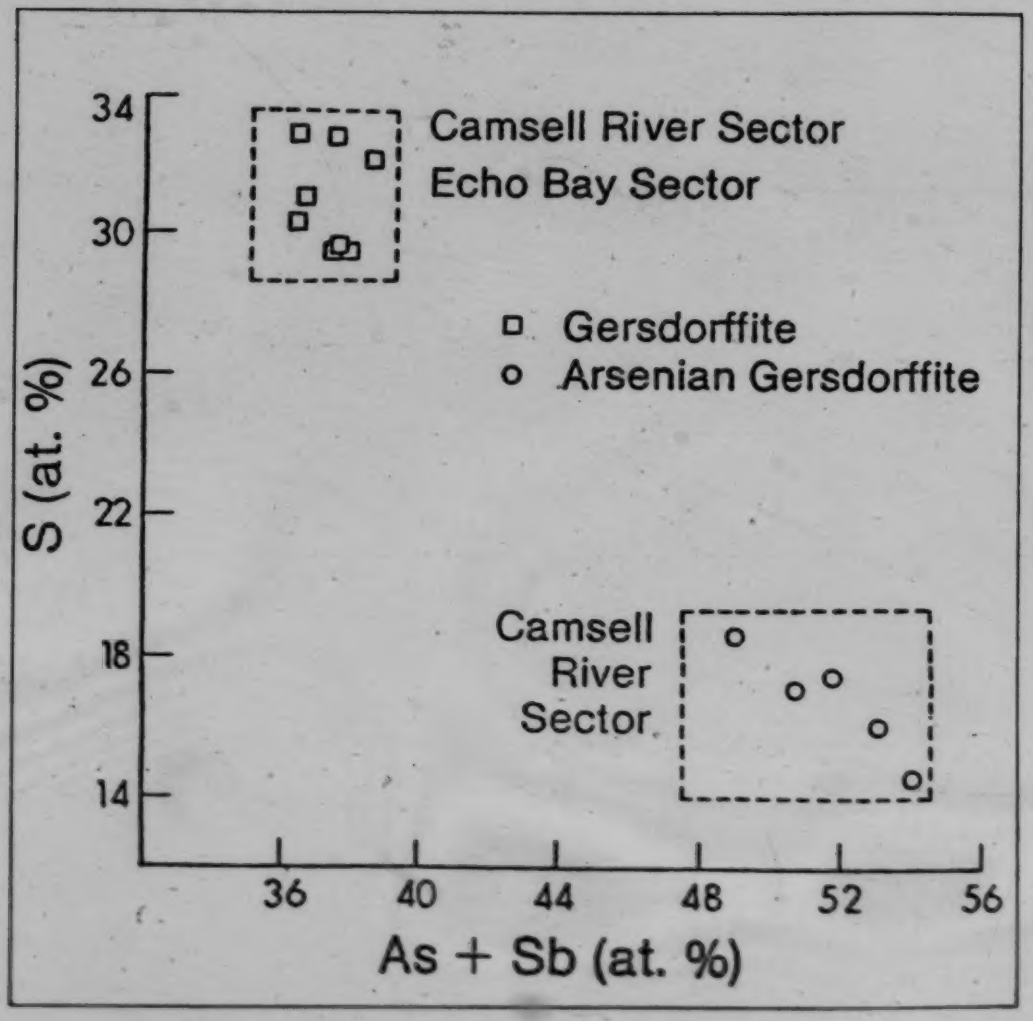

Figure 13. Variations of As+Sb : S ratios of gersdorffites in the ores of the Great Bear Lake silver deposits. Data listed in Table 9.

Table 10

Electron microprobe analyses of arsenopyrites from the Great Bear Lake silver deposits, N.W.T.. Data plotted in Figure 11.

Sample nos.	Fe	Co	Ni	S	As	Sb	Total
7B/SB	33.26	0.86	N.D.	21.62	43.95	N.D.	99.69
912/1B/SB	32.87	0.63	N.D.	22.12	44.64	N.D.	100.26
1A/125/ED	34.10	N.D.	N.D.	20.82	45.26	N.D.	100.18

Atomic proportions of arsenopyrites calculated on the basis of As+S+Sb=2.00

Sample nos.	Fe	Co	Ni	S	As	Sb
7B/SB	0.94	0.02	0.00	1.07	0.93	0.00
912/1B/SB	0.91	0.01	0.00	1.07	0.93	0.00
1A/125/ED	0.97	0.00	0.00	1.04	0.96	0.00

N.D. - Not detected. SB - Silver Bear. ED - Eldorado.

Gasparrini (1982) the compositions of arsenopyrites from unbuffered assemblages may be utilised to determine the crystallization temperature if they are unzoned, and the arsenic content is greater than 32 at.%. The absence of the asp - po - py association in the ores of the Great Bear Lake deposits clearly indicates that the fugacity of sulfur was unbuffered. Furthermore, the approach of Lowell and Gasparrini (1982) and Kalogeropoulos (1984) could not be applied because in none of the sections studied, was arsenopyrite found to coexist with pyrite, although the latter was found to occur in a few instances as isolated crystals within the gangue.

4.4 Native Silver

Native silver, the principal source of silver in the Great Bear Lake deposits, occurs in a wide variety of forms. It occurs in the form of wires, leaves, dendrites, and as interstitial grains within quartz, in massive form, and as inclusions in arsenides and other minerals (Plates 7 and 8). The different forms were found to be correlated with the associated gangue minerals, namely, the carbonates and quartz. The dendritic variety was found to be associated with the carbonates, whilst the wires and leaves were found mainly associated with quartz. In some cases, the interstitial silver grains were found to be rimmed by thin layers of gangue and safflorite. At least three generations of native silver were observed. The earlier generation occurs as inclusions in arsenides which replace it (Plate 9). This variety of native silver was also found to replace dendrites of pitchblende and carbonates. The later generations of native silver were found to be replaced by sulphides and sulphosalts (Plate 10). Replacement by acanthite was found to be very common. Both partial and complete replacement leading to pseudomorphs of acanthite after silver were observed (Plate 10).

4.4.1 Composition of Native Silver

Chemical compositions of native silvers from the Great Bear Lake region have neither been previously compared, nor thoroughly investigated for the complete spectrum of elements

COLOURED PICTURES
Images en couleur

Plate 7. Interstitial grains of native silver within quartz. Norex mine. P.P.L. 200X.

Plate 8. Native silver replacing nickeline along fractures. Eldorado mine. P.P.L. 100X.

COLOURED PICTURES
Images en couleur

Plate 9. Nickeline replacing earlier generation of native silver. Terra mine. P.P.L. 200X.

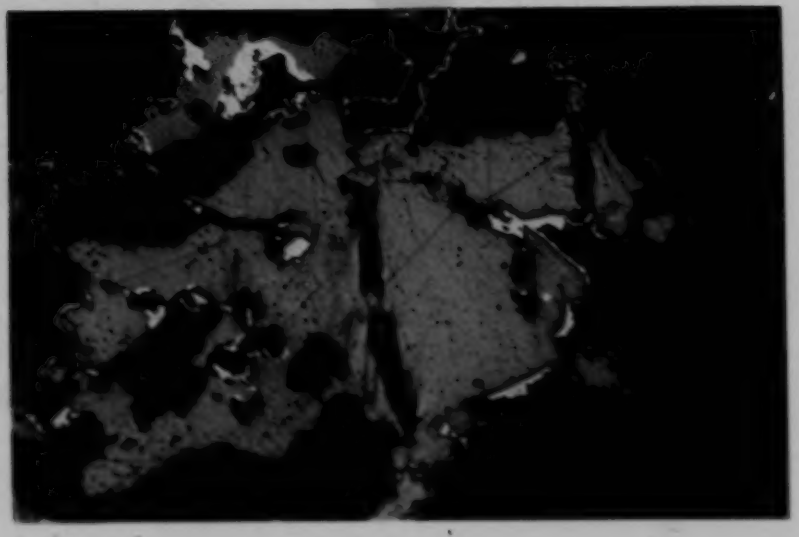

Plate 10. Pseudomorph of acanthite (bluish) after native silver. The pinkish mineral is chalcopyrite. Contact Lake mine. P.P.L. 100X.

likely to proxy in solid solution for the silver. Boyle (1968) reported a semi-quantitative spectrographic analysis of silver from the Eldorado mine. Robinson (1971) presented electron microprobe-derived analyses for Cu, Au, Ni, Hg, As and Co in four samples of silver from the Echo Bay mine. Badham (1973, 1975) reported significant amounts of Hg and traces of As in silver samples from the Terra, Northrim and Norex mines. Rojkovic (1973) stated that silver from the Echo Bay area contained very minor amounts of Hg and Sb. Shegelski (1973) and Withers (1979) also reported the presence of Hg and Sb in silvers from the Terra and Northrim mines.

4.4.2 Classification of Native Silver

Palache *et al.* (1944) forwarded the following chemical classification of native silvers on the basis of the dominant element in solid solution with the silver.

4.4.2.1 Aurian Silver

Since the atomic radii of Ag and Au are identical, continuous atomic substitution exists between Ag, auriferous Ag, electrum (Au with greater than 20 wt.%) and Au. Robinson (1971) reported 108 ppm Au in one sample from the Echo Bay deposit and Withers (1979) observed that native silver from the Northrim mine contained about 100 ppm Au.

4.4.2.2 Mercurian Silver

As the atomic radii of Ag and Hg differ by only 0.16 angstrom, there is little wonder that the natural amalgamation of the two metals is common. Native silver containing high concentrations (up to 30 wt.%) of Hg have been reported from different parts of the world. A solid mineral phase Ag_2Hg_3, moschellandsbergite is known from a wide range of deposits. According to Palache *et al.* (1944) Hg may substitute for Ag up to at least a ratio of 1.0 Hg : 4.2 Ag. Rayson and Calvert (1958) reported solubility limits of Hg-Ag to be 37.2 wt.% at 270°C, 36.5 wt.% at 100°C and 37.1 wt.% at 45°C. The silvers

from the Cobalt-Gowganda ores of Ontario have been found to contain up to 4.2 wt.% Hg (Petruk *et al.*, 1970,1971). They showed that the earlier generations of silver in the Cobalt-Gowganda area are richer in Hg and Sb than the later generations, which are devoid of both mercury and antimony. Shegelski (1973) reported a maximum of 7.23 wt.% Hg from the Terra mine. Withers (1979) reported silver up to 14 wt.% Hg in the Northrim mine.

4.4.2.3 Cuprian Silver

Cuprian silver is not as common as mercurian silver. It has been found to occur in trace quantities (Boyle, 1968). Robinson (1971) reported 143-320 ppm Cu in native silver from the Echo Bay mine.

4.4.2.4 Arsenian Silver

Since the atomic radii of As and Ag differ by 0.23 angstrom (16%), the range of solid solution might be anticipated to be much more limited. Palache *et al.* (1944) claims that silver should contain a maximum of 7 wt.% As. In addition, Broderick and Ehret (1931) claimed that compounds such as Ag_6As and Ag_3As may exist. However, according to Boyle (1968) the arsenic content of silvers is usually less than 0.5 wt.%. Clark (1972) reported 3.1 wt.% (4.4 at.%) arsenic in native silver associated with hexagonal arsenic and arsenolamprite in the Alacran deposit, Pampa Larga, Chile. All the previously cited researchers on the Great Bear Lake silvers reported traces of As from the Echo Bay and Terra mines.

4.4.2.5 Antimonian Silver

According to Palache *et al.* (1944) Sb may substitute up to 5.0 at.% in Ag. To date, the highest concentrations of Sb were found in silvers from the Cobalt-Gowganda district by Petruk *et al.* (1970,1971). These had up to 8.4 wt.% Sb. The Sb content of silver from the no.1 vein of the Eldorado mine was found to be between 1.3 and 1.6 wt.% by Boyle (1968). Withers (1979) found between 0.3 and 0.5 wt.% Sb in silvers from the Northrim

mine.

4.4.3 Electron Microprobe Analyses of Native Silver

The analytical techniques are presented in Appendix I and the results are presented in Table 11. Only Hg, Bi and Sb were found to be significant components in the Great Bear Lake region silvers. Thus Figure 14, the ternary plot of Ag-Hg-Sb, constitutes a reasonable summary of the principal variations in the samples. Hg contents were high in all the samples of this study; a sample of silver from the Northrim mine having the highest concentration, namely 4.31 wt.%. Sb was common and ranged from 0.25 to a maximum 1.16 wt.% in a silver from the Norex mine. No Sb was detected in silver from the Contact Lake locality. Te too was present in all the samples, reaching a maximum of 0.23 wt.% in a sample from the Terra mine. The highest Au concentration (0.03 wt.%) was found in the silver sample from the Northrim mine. No gold was present in the samples from the Norex and Contact Lake localities. The concentrations of Fe, Co, Ni, Zn, Pb and As were in all cases less than 0.06 wt.%. Regional variations in the distribution of mercury was found. The silver samples from the deposits of the Camsell River sector were generally found to be enriched in mercury, compared with those of the Echo Bay sector. Shegelski (1973) and Withers (1979) also reported high concentration of mercury from the Terra (7.23 wt.%) and Northrim (14 wt.%) deposits respectively, both of which occur in the Camsell River sector. The variations in mercury content do not appear to be related to the nature of the host-rocks of the veins. Instead there seems to be a possible spatial relation to the proximity of high level, felsic pluton of the Great Bear batholithic suite.

4.5 Native Bismuth

Native bismuth is very common in the ores of the Great Bear Lake deposits. It occurs in the later stages of mineralization, after the main stage silver mineralization. It occurs as skeletal grains within the arsenides, in massive form associated with coarse-grained crystalline quartz, as veinlets replacing arsenides and as exsolved blebs in sulphosalts.

Table 11

Electron microprobe analyses of native silvers from the Camsell River and Echo Bay sectors.

	Northrim NR/1A	Northrim NR/1B	Terra 1A/915/SB	Terra 1B/915/SB	Norex NX/2B/A	Norex NX/2B/B	Smallwood SW/1	Smallwood SW/2
Fe	0.03	N.D.	0.02	N.D.	N.D.	N.D.	N.A.	N.A.
Co	N.D.	N.D.	N.D.	N.D.	0.03	N.D.	N.A.	N.A.
Ni	0.03	N.D.	0.03	0.04	0.02	N.D.	N.A.	N.A.
Cu	N.D.	N.D.	N.D.	N.D.	N.D.	N.D.	N.A.	N.A.
Zn	0.04	0.04	0.06	0.02	0.03	0.04	N.A.	N.A.
As	N.D.	N.D.	N.D.	N.D.	N.D.	N.D.	N.A.	N.A.
Ag	94.89	94.75	96.03	96.56	95.82	95.81	97.32	97.23
Sb	0.36	0.25	0.58	0.69	1.16	1.16	0.90	0.91
Te	0.06	0.09	0.12	0.07	0.09	0.09	N.A.	N.A.
Au	0.03	0.02	N.D.	N.D.	N.D.	N.D.	N.A.	N.A.
Hg	4.31	4.30	2.69	2.60	2.33	2.28	1.46	1.46
Pb	0.02	0.03	0.02	N.D.	N.D.	N.D.	N.A.	N.A.
Bi	0.21	0.23	0.14	0.11	0.17	0.18	N.D.	N.D.
Total	99.97	99.70	99.69	100.09	99.65	99.52	99.68	99.60

Table 11 (continued)

	Echo Bay EB/1	Echo Bay EB/2	El Bonanza ELB/1	El Bonanza ELB/2	Cont. Lake CL/1A	Cont. Lake CL/1B	Eldorado 1/A/250/ED	Eldorado 1/B/250/ED
Fe	N.A.	N.A.	N.A.	N.A.	0.04	0.04	0.03	0.02
Co	N.A.	N.A.	N.A.	N.A.	N.D.	0.04	0.02	0.02
Ni	N.A.	N.A.	N.A.	N.A.	N.D.	N.D.	0.06	0.06
Cu	N.A.	N.A.	N.A.	N.A.	N.D.	N.D.	N.D.	N.D.
Zn	N.A.	N.A.	N.A.	N.A.	N.D.	N.D.	0.02	0.05
As	N.A.	N.A.	N.A.	N.A.	N.D.	0.02	N.D.	N.D.
Ag	99.25	99.09	99.11	99.10	97.60	97.52	96.50	96.70
Sb	0.36	0.11	N.D.	N.D.	N.D.	N.D.	1.04	0.99
Te	N.A.	N.A.	N.A.	N.A.	0.10	0.08	0.07	0.07
Au	N.A.	N.A.	N.A.	N.A.	N.D.	N.D.	N.D.	N.D.
Hg	0.29	0.23	0.34	0.38	1.82	1.77	1.62	1.60
Pb	N.A.	N.A.	N.A.	N.A.	N.D.	0.03	N.D.	N.D.
Bi	N.D.	N.D.	N.D.	0.02	0.06	0.06	0.07	0.06
Total	99.90	99.43	99.45	99.50	99.62	99.56	99.43	99.57

N.A. - Not analysed. N.D. - Not detected.

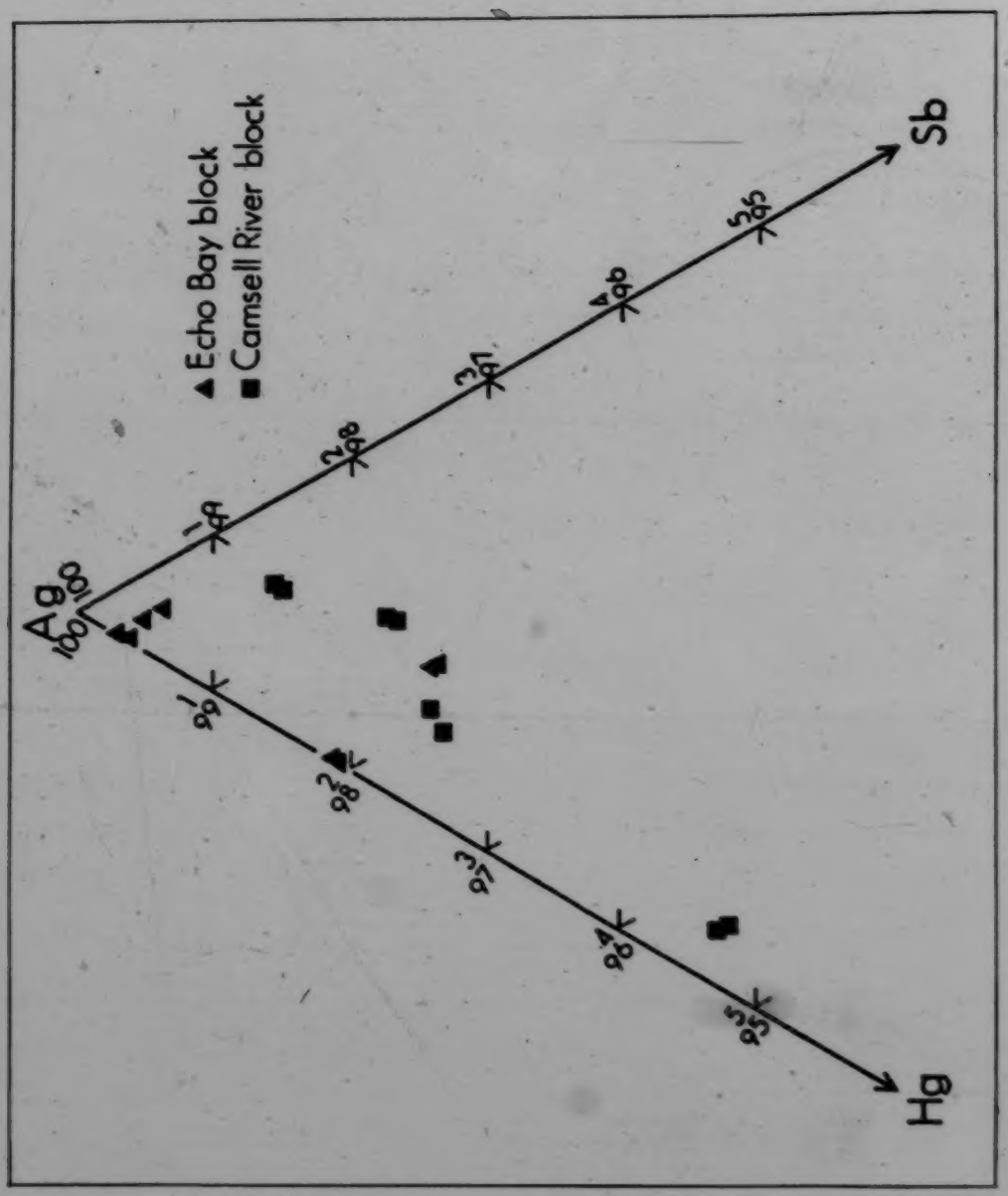

Figure 14. Ternary plot of Ag-Hg-Sb showing the variations of native silver in the ores of the Great Bear Lake silver deposits. Data listed in Table 9.

In earlier investigations, native bismuth was placed after the arsenide stage in the paragenetic sequence. However, it was found in this study that it was deposited both before and after the arsenide mineralizations. However, the main bismuth mineralization took place after the arsenide stage. The earlier generation was found to be replaced by the Ni, Co arsenides. The later generation was found to replace the arsenides and sulpharsenides along fractures (Plate 11). This variety of native bismuth occurs mainly in association with the carbonates. In some cases, however, it was found to be intergrown with quartz. This variety was found to be common in all the deposits.

The second variety, like native silver, was found to occur as interstitial grains in quartz, and as dendrites enclosed by safflorites. These dendrites have been found to be replaced by bismuthinite. The third variety was found to occur in massive form, and occurs in vugs within crystalline, colourless to white quartz. It was also found to be intergrown with quartz.

4.6 Sulphosalts

Although a number of sulphosalts have been reported by the earlier workers, not all of these minerals could be found in this investigation. This may be attributed to the restricted occurrence of some of these minerals. The sulphosalts minerals were deposited after native silver and native bismuth. They occur as isolated irregular grains and stringers which replace the earlier formed minerals.

The sulphosalts which were identified in this investigation include, pyrargyrite, polybasite, miargyrite, proustite, tetrahedrite, matildite and stromeyerite. These minerals were identified by standard ore microscopic techniques, followed by qualitative microprobe analyses. Emplectite, pavonite and stephanite were reported by Badham (1973) and rathkeite was reported by Robinson (1971) from the Echo Bay deposit. Furnival (1939) reported the occurrence of famatinite from the Contact Lake deposit.

Pyrargyrite, miargyrite, polybasite and proustite occur mainly in association with native silver and acanthite. In the Norex deposit polybasite and miargyrite were found to consist

COLOURED PICTURES
Images en couleur

Plate 11. Native bismuth replacing skutterudite along fractures. Norex mine. P.P.L. 100X.

Plate 12. Bismuthinite (grey) selectively replacing native bismuth (creamy). The enclosing mineral is safflorite. Terra mine. P.P.L. 200X.

together and replace native silver. Pyrargyrite and proustite were not found to occur together, but were found in the same polished section. They were found to occur as irregular grains replacing native silver. Stromeyerite was identified only in one sample from the Contact Lake deposit where it was found to occur as inclusions in bornite and chalcocite. Matildite occurs as irregular grains and veinlets which replace native silver and the arsenides. Tetrahedrite was found to be quite common in comparison with the other sulphosalts.

4.7 Oxides

Hematite and uraninite were the principal oxides found in the veins. Magnetite was very rare. No other oxide minerals were found in this study.

4.7.1 Uraninite

Uraninite was identified in the Eldorado, Echo Bay, Terra and Northrim deposits. It was not identified in the Norex, Smallwood, El Bonanza and Contact Lake deposits. It is not known if this mineral was not deposited in these deposits, or not present in the samples studied. Furnival (1939) reported pitchblende from the Contact Lake deposit.

Uraninite occurs in a wide variety of forms. It occurs as euhedral to anhedral grains in quartz gangue associated with hematite and pyrite. It also occurs as dendrites, rosettes and spherules. The dendrites were found to be replaced by native silver which has selectively replaced the cores. Uraninite also occurs as brecciated fragments in the hematitised wall rocks.

4.7.2 Hematite

Hematite is a very common mineral in the veins and wall rocks of these deposits. It was identified in all the deposits studied. It occurs in association with uraninite and pyrite, and as red coatings over quartz, the carbonates and arsenides. It also occurs as anhedral to subhedral grains associated with quartz and pyrite.

4.7.3 Magnetite

Magnetite is very rare in the ores of these deposits. It was identified in the Terra deposit, where it was found to occur as inclusions in cobaltite and as isolated idiomorphic grains in carbonate gangue. It was probably deposited earlier than the arsenides.

4.8 Sulphides

Sulphide minerals are common in the veins of the Great Bear Lake silver deposits. Chalcopyrite and pyrite are the most abundant and widepread, followed by galena, sphalerite, acanthite and bismuthinite. Pyrrhotite, bornite, chalcocite are not very common. Pyrrhotite was identified in two samples from the Terra deposit where it was found to be associated with the other sulphides. Chalcocite was identified only in the Contact Lake deposit where it occurs in association with bornite, chalcopyrite and tetrahedrite. Bornite was identified in the Eldorado, Echo Bay, Contact Lake and Terra deposits.

Pyrite appears early in the paragenetic sequence. It occurs in association with hematite in Stage I mineralization. It was not found to occur with the arsenides or the native metals. The later generation of pyrites were deposited along with the other sulphide minerals. Crystallization of pyrite and chalcopyrite continued until the waning stages of mineralization in the region, as they are found to coexist in vugs in calcites and quartz. The earlier generation of pyrite was found to be fractured and filled with later chalcopyrite (Plate 13). The later generation of pyrite occurs as massive aggregates as well as idiomorphic crystals.

Chalcopyrite appears in the paragenetic sequence after arsenide mineralization. However, in one sample from the Terra deposit, inclusions of chalcopyrite were found within cobaltite. It may represent an earlier pulse of chalcopyrite mineralization which probably was erratic. Textural relationships suggest that chalcopyrite crystallized over a wide range of time. It crystallized both before and after the crystallization of galena and sphalerite. It also occurs as exsolution blebs within sphalerite. It replaces native silver, the arsenides and pyrite.

COLOURED PICTURES
Images en couleur

Plate 13. Chalcopyrite replacing earlier generation pyrite along fractures. Northrim mine. P.P.L. 200X.

Plate 14. Native bismuth (creamy) which fills cleavage planes of calcite is being replaced by bismuthinite (light grey). Terra mine. P.P.L. 100X.

Galena and sphalerite were found to coexist in all the deposits. In some cases, galena was found to be replaced by sphalerite. However, in the majority of the cases, they precipitated simultaneously.

Acanthite is the next important silver bearing mineral. It occurs as subhedral grains, as reaction rims, and as thin veinlets. It replaces native silver along grain boundaries to form reaction rims around it.

Bismuthinite was found in the Terra, Eldorado, Contact Lake, Norex and Northrim deposits. It was not found in the other deposits. It most commonly occurs as anhedral grains and as thin veinlets replacing native silver and native bismuth. Pseudomorphs of bismuthinite after native bismuth were found to be common (Plate 12).

4.9 Gangue Minerals

Quartz, calcite and dolomite are the most abundant gangue minerals in the veins. Other minerals include, fluorite, siderite, rhodochrosite, K-feldspar, chlorite and muscovite.

Quartz was found to occur in variable proportions in all the stages of mineralization. Several different types of quartz were found in these veins. These varieties were :

(i) white to greyish, massive to crystalline, associated with pitchblende and hematite,

(ii) medium-grained, colourless to greyish, associated with the arsenides,

(iii) medium- to coarse-grained, grey, associated with native silver,

(iv) granular, white to colourless, associated mainly with wire silver and native bismuth,

(v) colourless to white, coarse, crystalline, associated with native bismuth,

(vi) colourless, crystalline, associated with fluorite,

(vii) white to greyish, massive, associated with arsenides and native bismuth,

(viii) crystalline, colourless to white, in vugs, and

(ix) milky white, massive, mostly unmineralized, but occasionally associated with chalcopyrite and pyrite.

Like quartz, calcite and dolomite also occur in variable form and colour. The following types of calcites were recognized :

(i) fine- to medium-grained, white to pinkish, associated with both native silver and the arsenides,

(ii) coarse-grained, colourless, associated with coarsely crystalline dolomite, and

(iii) crystalline (scalenohedrons), colourless, occur in vugs and as thin encrustations over the earlier mineralizations.

The following types of dolomites were recognized :

(i) white to greyish white, crystalline, pre-arsenide stage,

(ii) fine-grained, pinkish, associated with native silver and arsenides,

(iii) coarse, crystalline, pinkish white, associated with the arsenides, and

(iv) coarse, crystalline, white, associated with the sulphides.

Fluorite was found only in the Terra deposit. Jory (1964) reported fluorite from the Eldorado deposit. It was not found in this study. In the Terra deposit, fluorite, which is green to purple in colour, occurs as coarse and crystalline aggregates, associated with pink crystalline dolomite and colourless crystalline quartz.

Siderite and rhodochrosite were found in the Eldorado deposit. Siderite occurs in crystalline form in vugs within quartz. Rhodochrosite, which is pinkish red in colour and fine-grained, occurs in association with fine-grained dolomite.

K-feldspar, K-mica, and chlorite were not found to be as widespread as quartz or carbonates. They were commonly found to occur as thin veinlets and stringers within quartz and carbonates.

4.10 Secondary Minerals

Erythrite, annabergite, malachite, azurite and unidentified secondary uranium minerals were the common secondary minerals found in these deposits.

4.11 Interpretations of Ore Textures

Textures of ore minerals and associated gangue minerals not only provides information about relationships among individual grains, but also provides information about the nature of processes, such as, initial ore deposition, post-depositional re-equilibration or metamorphism, deformation, etc. (Craig and Vaughan, 1981). Hence correct interpretation of ore textures is very important in understanding the origin of ore deposits. Edwards (1947), Bastin (1950a), Ramdohr (1980), Park and MacDiarmid (1970) have described the various textures observed in ore minerals and their interpretations. The following types of textures were observed in the ores of the Great Bear Lake deposits.

4.11.1 Replacement Texture

Replacement textures are very common in the ores of the Great Bear Lake deposits. Replacement of the earlier formed minerals by the later minerals was found to be common among the ore and gangue minerals (Plates 8 to 15). Replacement was found to take place along fractures and grain boundaries. Selective replacement of zoned skutterudite by native bismuth and gangues, of native silver by acanthite, and of native bismuth by bismuthinite was observed. Native bismuth and nickeline have also been replaced by chalcopyrite.

4.11.2 Dendrites and Rosettes

The arsenides, native silver, uraninite, and carbonates exhibit dendritic textures. The dendrites were observed both under the microscope and in hand specimens. The arsenide dendrites enclose rhombs of native silver and carbonates. Native silver dendrites were found to be rimmed by carbonate gangue and arsenides, and dendrites of carbonates were found to be rimmed by a thin layer of arsenides (Plates 17 and 18).

Although formation of dendrites is highly favoured by sublimation, dendrites may also form by precipitation from solution and solidification from a melt (Stanton, 1972). Jory (1964), Robinson (1971) and Badham (1973) have discussed the mode of formation of the

COLOURED PICTURES
Images en couleur

Plate 15. Native bismuth replacing massive skutterudite. Norex mine. P.P.L. 200X.

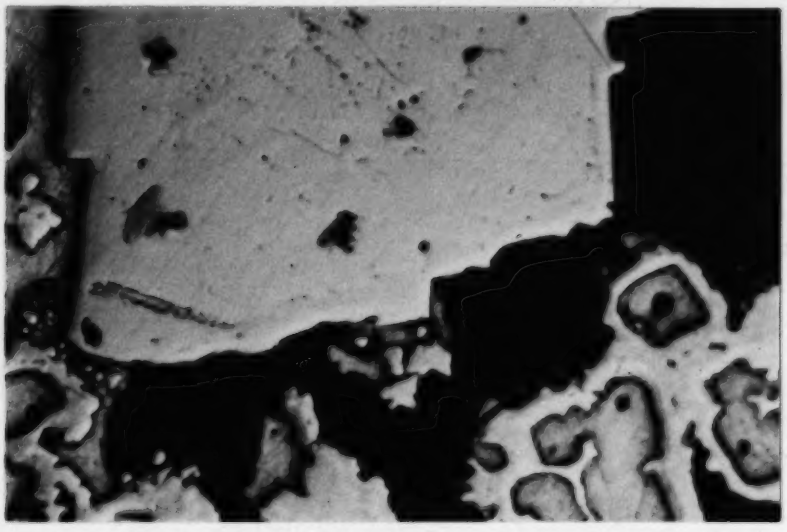

Plate 16. Inclusions of native bismuth (pale brownish) within gersdorffite. The sub-idiomorphic grain is skutterudite. Norex mine. P.P.L. 100X.

COLOURED PICTURES
Images en couleur

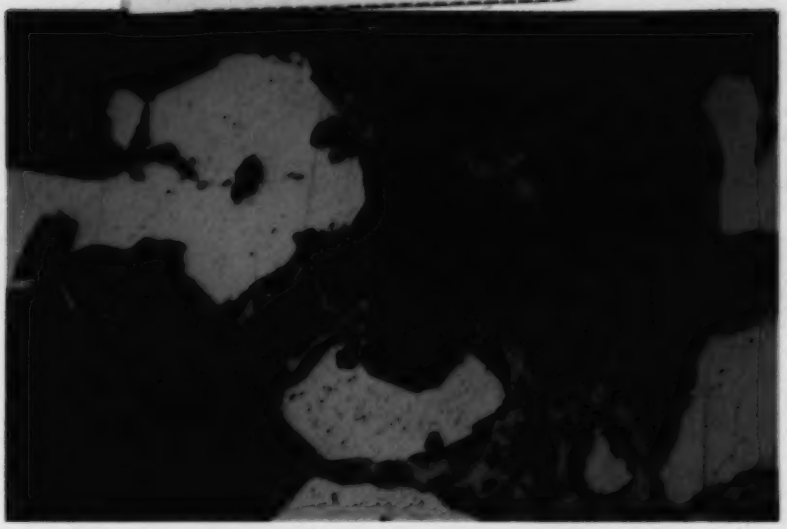

Plate 17. Native silver rimmed by carbonates and arsenides. Terra mine.P.P.L. 100X.

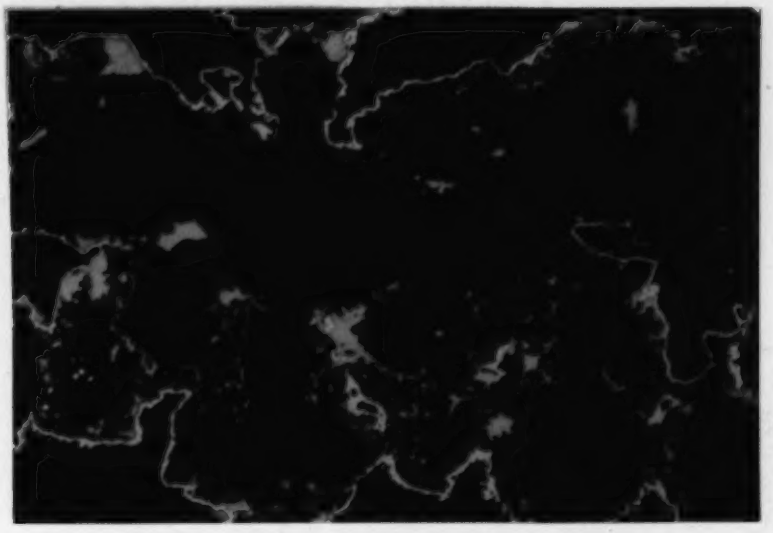

Plate 18. Dendrites of carbonates rimmed by arsenides. Eldorado mine. P.P.L. 100X.

dendrites in the ores of Great Bear Lake deposits. Similar dendritic patterns have also been found in the ores of the Cobalt-Gowganda region of Ontario. Bastin (1949, 1950b) suggested that silver in the veins precipitated first in the dendritic form, followed by the arsenides around it.

In the Great Bear Lake ores, textural evidences indicate that the earlier generation of native silver was first deposited as dendrites and followed by precipitation of carbonates and arsenides around it (Plate 17). In a second type, carbonate cores were selectively replaced by later silver along healed fractures.

The arsenides were most commonly found to occur as rosettes, which consist of cores and outer layers. The cores were usually native silver, native bismuth or nickel-rich arsenides, commonly, nickeline (Plates 1, 2 and 19). The outer layers were usually found to be cobalt-rich but occasionally, thin layers of gersdorffite and arsenopyrite were found to rim such rosettes. The rosettes were found to be intricately zoned, thereby suggesting changes in the fluid composition with time. Misra and Fleet (1975) investigated a Ni-Co-As assemblage from Cobalt, Ontario, and suggested that gross chemical zoning may be a primary feature, but other variations in composition may be the result of later chemical readjustments through solid state diffusion at lower temperatures. In the case of the Great Bear Lake ores, solid state diffusion may have taken place locally, but the overall texture suggests open space filling, with fluctuations in the compositions of the fluids.

4.11.3 Other Textures

Exsolution textures were found only with the sulphides. Exsolution blebs of chalcopyrite were found within sphalerites. Cataclastic textures were exhibited by pyrite and the arsenides. Fractures which resulted from cataclastic deformation were later in-filled by sulphides, native silver, native bismuth and by other gangue minerals.

COLOURED PICTURES
Images en couleur

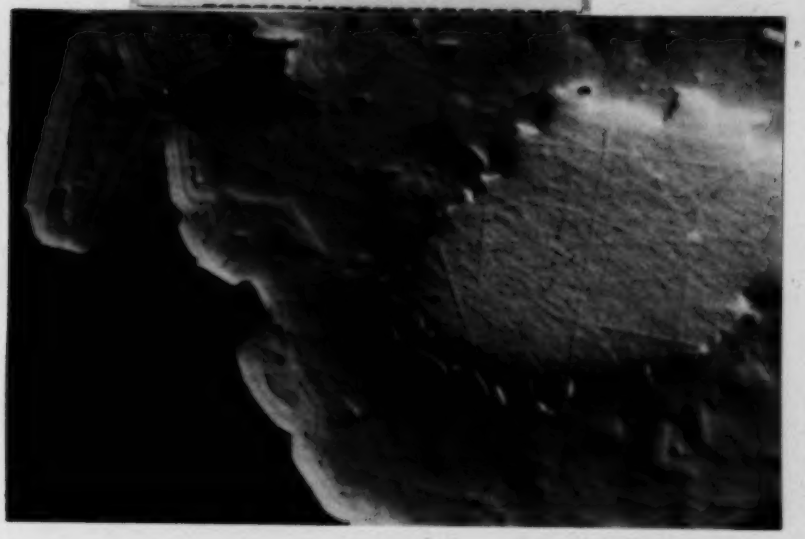

Plate 19. Native silver rimmed by complex intergrowth of arsenides. Note the differences in relief of the arsenide phases. Normarsky phase interference contrast. Terra mine. 200X.

Plate 20. Inclusions of arsenopyrites in a groundmass of bismuthinite, safflorite and native bismuth. Terra mine. P.P.L. 50X.

4.12 Parageneses

The sequence of mineralization was determined by microscopic and hand specimen studies. The large number of minerals present in the veins made it difficult to determine the parageneses. However, every effort was made to determine the paragenetic sequence of each deposit, and then to synthesize a generalised pattern for the whole region.

The parageneses of different deposits are given in Figures 15 to 21 and a generalised pattern of paragenetic sequence is given below. On the basis of structural and textural evidence, five major stages of mineralization have been recognized. These are, from oldest to youngest :

Stage I : quartz - pitchblende - hematite ± sulphides

Stage II : arsenides - Ag - carbonates - quartz ± fluorite

Stage III : Ag - Bi - carbonates - quartz

Stage IV : sulphosalts - sulphides - carbonates - quartz

Stage V : sulphides - carbonates - quartz

The above paragenetic sequence is a general one for the deposits of the region. Locally there may be differences, for many of the minerals found in the larger deposits, like Eldorado and Terra, were not found in the veins investigated in this study. The absence of some of the minerals may be attributed to the following reasons :

(i) the physico-chemical conditions were not suitable for the deposition of the minerals;

(ii) the occurrence of these minerals was restricted in space, that is, the minerals might have been deposited in one vein and not in the other.

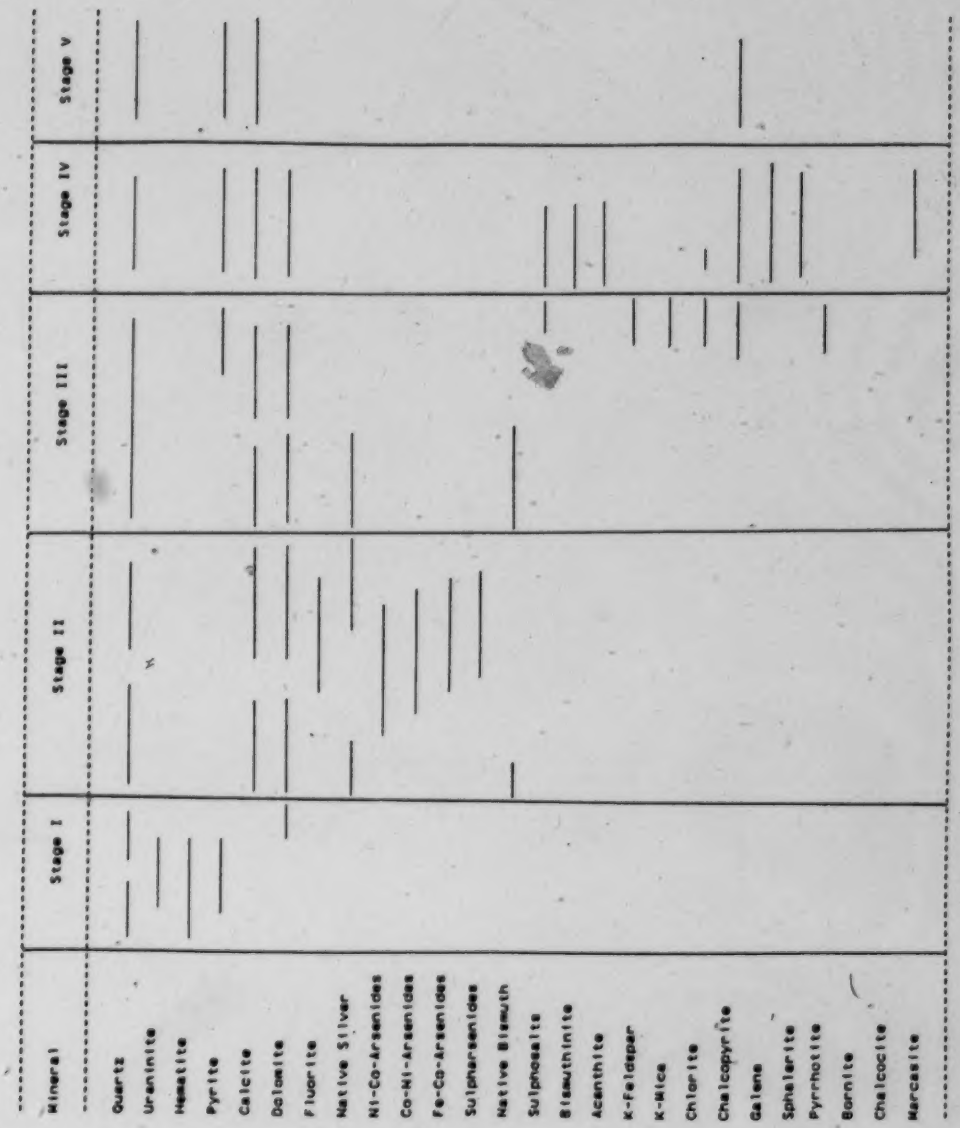

Figure 15. Paragenesis of the Terra deposit.

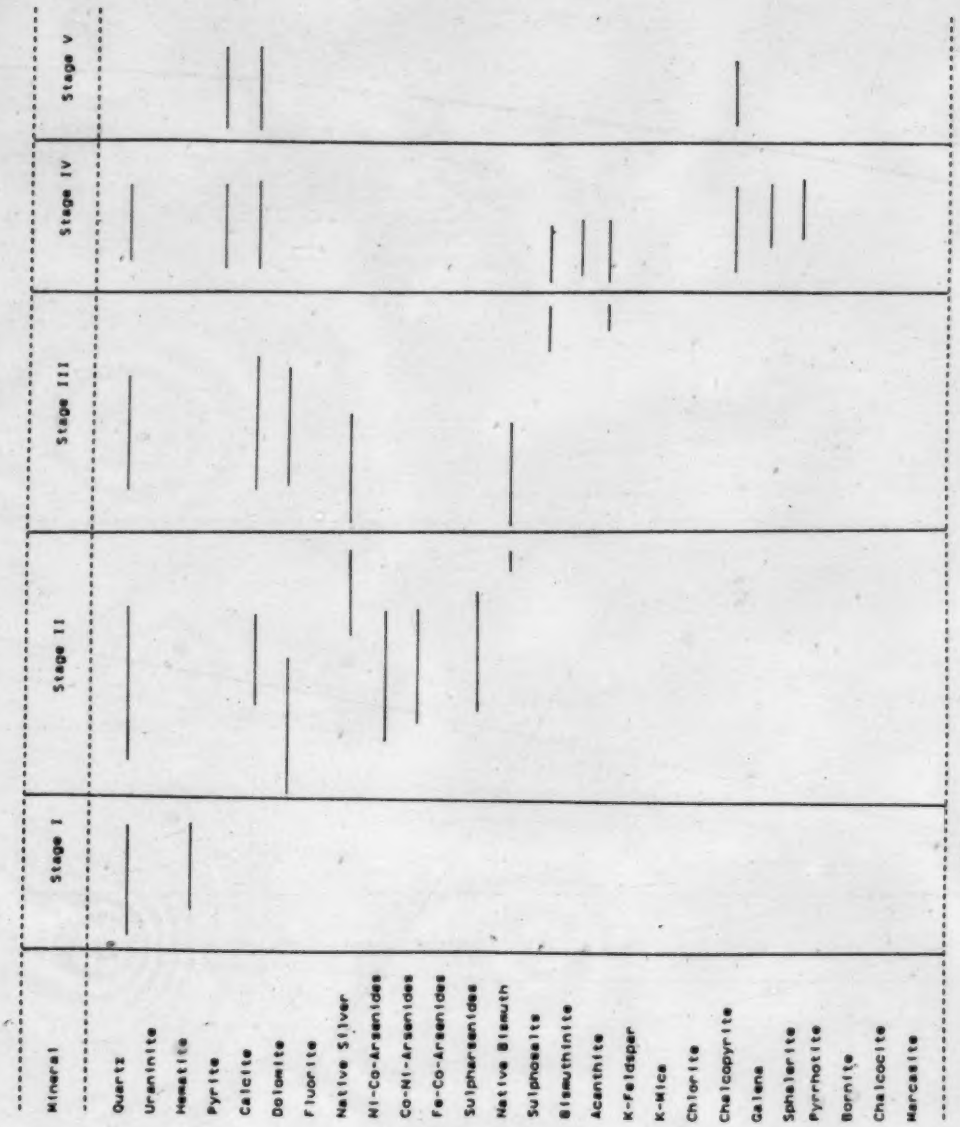

Figure 16. Paragenesis of the Norex deposit.

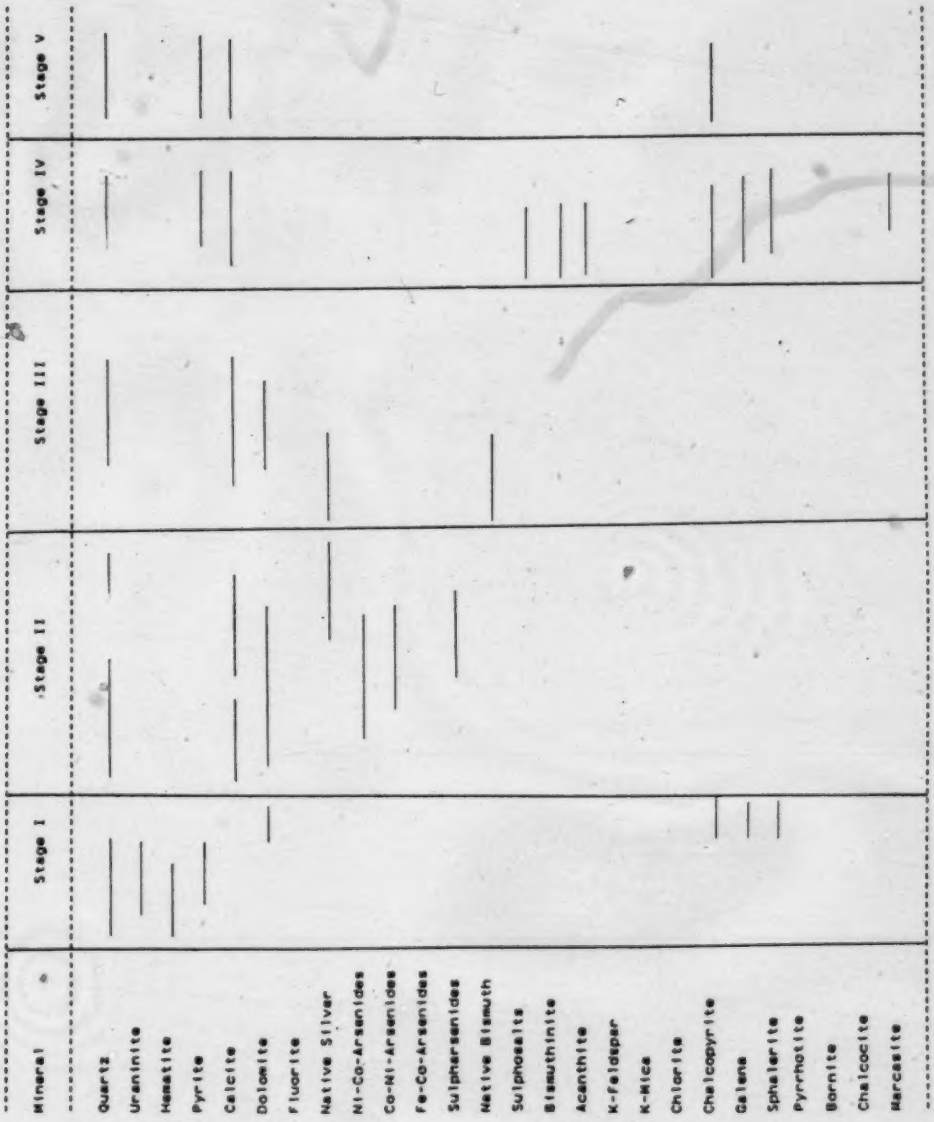

Figure 17. Paragenesis of the Northrim deposit.

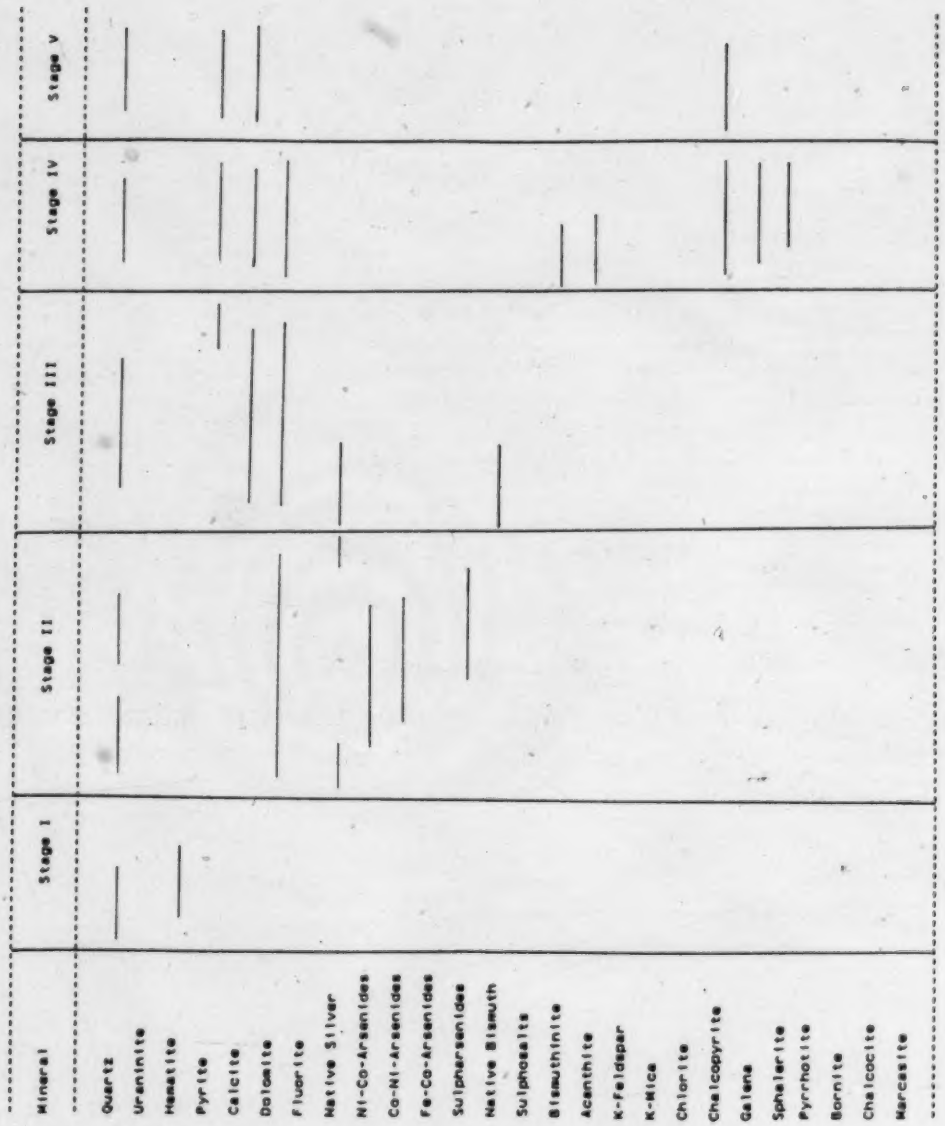

Figure 18. Paragenesis of the Smallwood deposit.

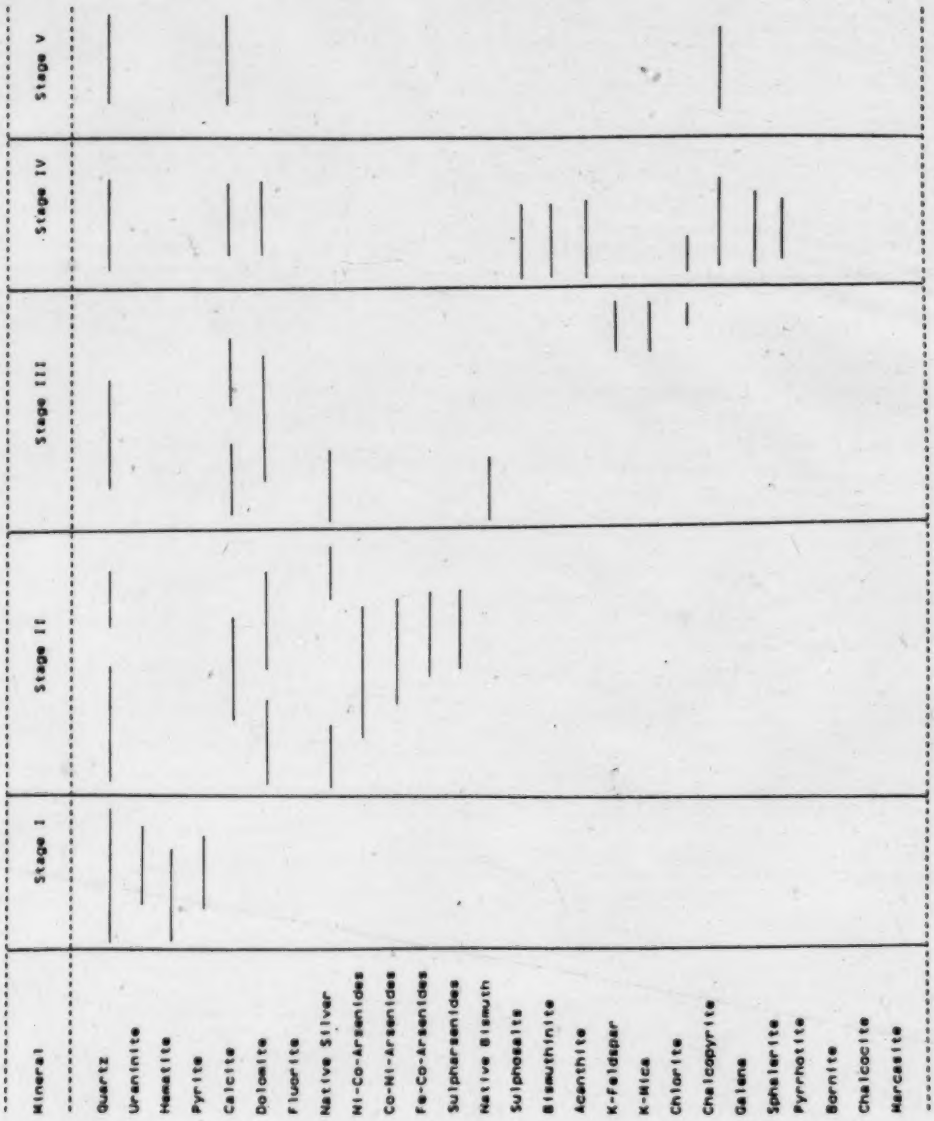

Figure 19. Paragenesis of the Eldorado deposit.

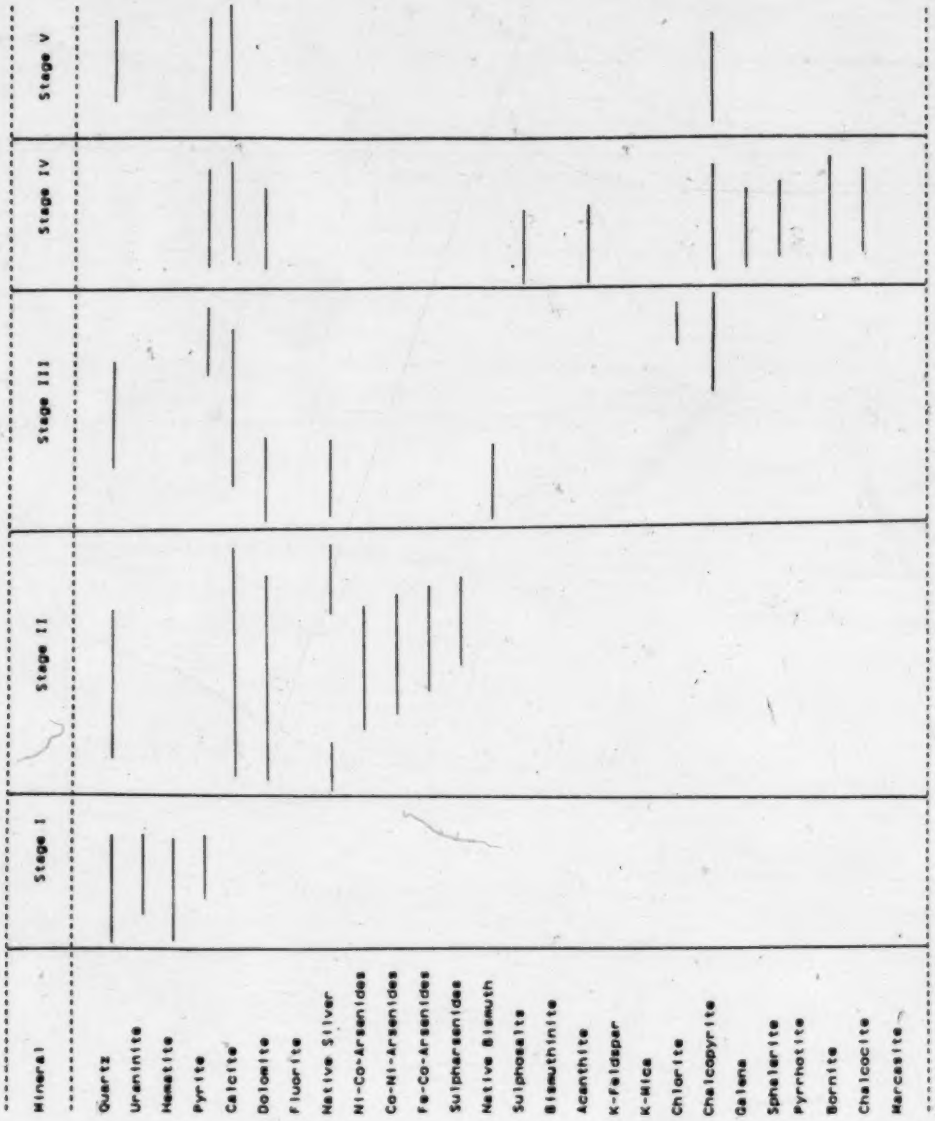

Figure 20. Paragenesis of the Contact Lake deposit.

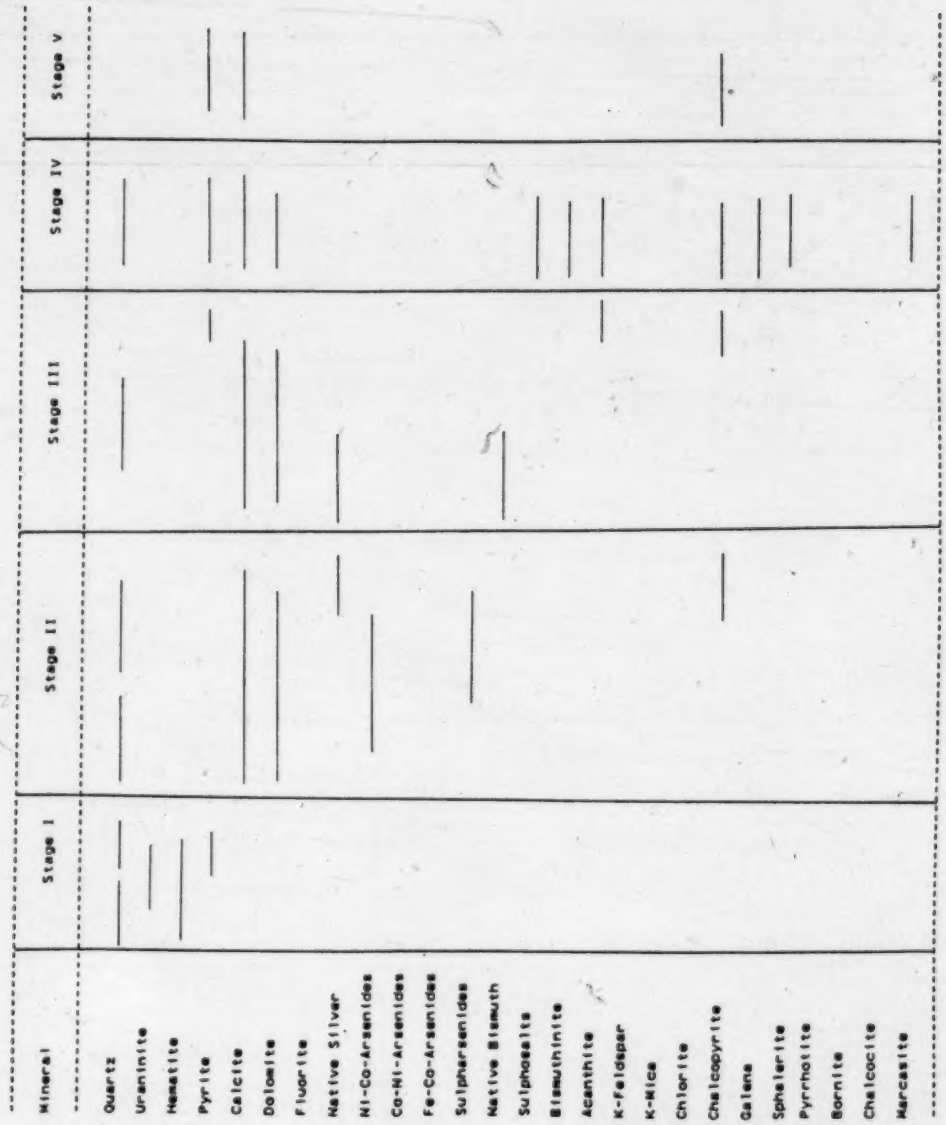

Figure 21. Paragenesis of the Echo Bay deposit.

5. FLUID INCLUSION STUDY

5.1 Introduction

Fluid inclusions are samples of fluids trapped in the crystal during crystallization or recrystallization. Fluid inclusions have proved to be a powerful tool in the study of the genesis of ore deposits. Workers on fluid inclusions have greatly benefitted by the extensive research carried out by Edwin Roedder on fluid inclusions since the late 1950s. Fluid inclusion studies have helped in understanding the pressure-temperature regimes of mineralization, and also the actual composition of the ore-bearing fluids. In recent years the field of fluid inclusion studies has been extended to petrological problems, and to studies involving the upper mantle and extraterrestrial materials (Hollister and Crawford, 1981; Roedder, 1984). The basic principles governing fluid inclusion microthermometry and the definitions of the commonly used terms are given in Roedder (1984).

5.2 Fluid Inclusion Studies in the Great Bear Lake Silver Deposits

Very few data from fluid inclusions are available from the Great Bear Lake argentiferous deposits. Robinson (1971), Robinson and Ohmoto (1973), Shegelski (1973), and Shegelski and Scott (1975) carried out fluid inclusion studies on select phases from some of the deposits. Robinson (1971) and Robinson and Ohmoto (1973) reported homogenization temperatures of 150 ± 10°C and 130 ± 10°C in dolomite and quartz belonging to later stages of the Echo Bay deposit respectively. They found the salinity of the fluids to be about 30 wt.% NaCl equivalent. Shegelski (1973) carried out fluid inclusion studies on quartz and carbonates from the Terra deposit, and reported salinities of the fluids to be between 30 and 35 wt.% NaCl equivalent, and pressure-corrected homogenization temperatures of 180° to 370°C. Shegelski and Scott (1975) reported salinities between 30 and 35 wt.% NaCl equivalent and a wide range of pressure-corrected homogenization temperatures from 180° to 510°C, in carbonates intimately associated with nickel diarsenides.

The present investigation constitutes a more detailed study of these and the other deposits of the region and thus augments the existing data. It is noteworthy that in the earlier

investigations, not all the paragenetic stages of mineralization were investigated. Moreover, salinities of the fluids were determined only by the dissolution of halite daughter crystals. During the present study every effort was made to determine the composition, temperature and pressure of inclusions in minerals of all stages and from all the deposits sampled. However, this was not possible for the following reasons:

(i) representative samples of each stage from all the major stages could not be collected, as some of the deposits were already abandoned or on the verge of closure, and

(ii) many of the gangue minerals in veins were not suitable for such microthermometric studies.

Suitable samples from different paragenetic stages were selected for heating and freezing experiments. The methods of investigations are presented in detail in Appendix I.

5.3 Petrographic Descriptions of the Inclusions

5.3.1 Classification of Inclusions

The classification of inclusions followed in this study is the same as that given by Roedder (1981, 1984), which is based upon the origin of the inclusions. Following this scheme the inclusions in quartz, fluorite, calcite and dolomite have been classified as primary, secondary and pseudosecondary. The criteria for distinguishing the origin of such inclusions were those given by Roedder (1981).

All three types of inclusions were identified in the quartz samples. The primary inclusions were identified on the basis of their random orientation, isolated occurrence, and by their larger dimensions. The last criterion was not always valid, as in some cases secondary inclusions were also found to be quite large. The secondary inclusions were identified on the basis of their oriented pattern along extensive healed fractures. The pseudosecondary inclusions were also found to occur along fractures which terminated over short distances and before the margins of grains were reached. Pseudosecondary inclusions, however, were rare. In the

calcites, dolomites, and fluorites, the primary inclusions were identified in the same manner as in quartz. The secondary inclusions in calcites and dolomites were found to be arranged along cleavage planes, while in fluorites they were found to occur along both cleavages and random fractures. Pseudosecondary inclusions were not identified in the calcites, dolomites and fluorites.

5.3.2 Types of Inclusions

The fluid inclusions (both primary and secondary) in the quartz, calcite, dolomite and fluorite exhibited variable shapes and sizes. The sizes of the inclusions varied from less than 5 microns to more than 150 microns along the longest axis. The inclusions were on the average around 15 to 30 microns in diameter. Larger inclusions were found to occur in calcites and fluorites. Inclusions in quartz were generally smaller than 15 microns, with occasional isolated inclusions of about 30 to 40 microns in diameter. The inclusions were commonly irregular in shape, but equant, subequant and negative crystals were also found.

Several types of inclusions were distinguished in the minerals of these deposits (Plates 21 to 30). They are as follows:

Type A : Type A inclusions contained a liquid phase, and a vapour phase, the volume of which was about 50% of the total volume of the inclusions . This type of inclusion was found in quartz which was intimately intergrown with the arsenides, and was found only in samples from the Camsell River sector. They homogenized in the liquid phase.

Type B : Type B inclusions contained a liquid phase and a very high proportion of vapour phase (more than 50%).

Type C: Type C inclusions contained a vapour-rich phase, halite daughter crystal and a liquid phase.

Type D: Type D inclusions contained a liquid phase, and a vapour phase, the volume of which was between 30 and 40% of the total volume of the inclusions. Type D inclusions were found in calcites and fluorites.

POOR COPY
COPIE DE

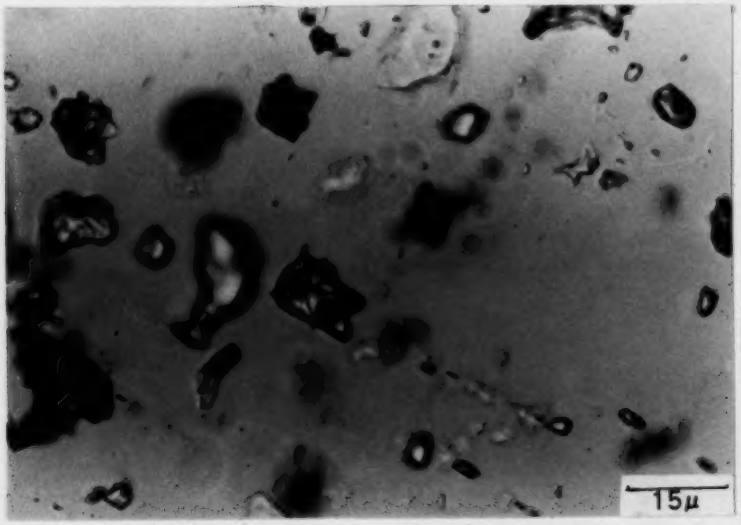

Plate 21. A primary inclusion in quartz containing a liquid phase, a vapour phase and unidentified radiating daughter crystals. Terra mine.

Plate 22. Primary two phase (vapour-rich) inclusions in quartz intimately associated with the arsenides. Norex mine.

QUALITEE INFERIEURE

Plate 23. A primary three phase (liquid, vapour and halite crystal) inclusion in quartz. Terra mine.

Plate 24. A primary two phase (liquid and vapour)inclusion in dolomite. Terra mine.

POOR COP
COPIE DE

Plate 25. A primary two phase (liquid and vapour) inclusion in dolomite. Eldorado mine.

Plate 26. A primary two phase (liquid and vapour) inclusion in quartz. Contact Lake mine.

QUALITEE INFERIEURE

Plate 27. A primary two phase (liquid and vapour) inclusion in dolomite. Terra mine.

Plate 28. A primary two phase (liquid and vapour)inclusion in calcite. Terra mine.

POOR COPY
COPIE DE QUALITEE INFERIEURE

Plate 29. A primary three phase (liquid, vapour and halite crystal) inclusion in dolomite. Terra mine.

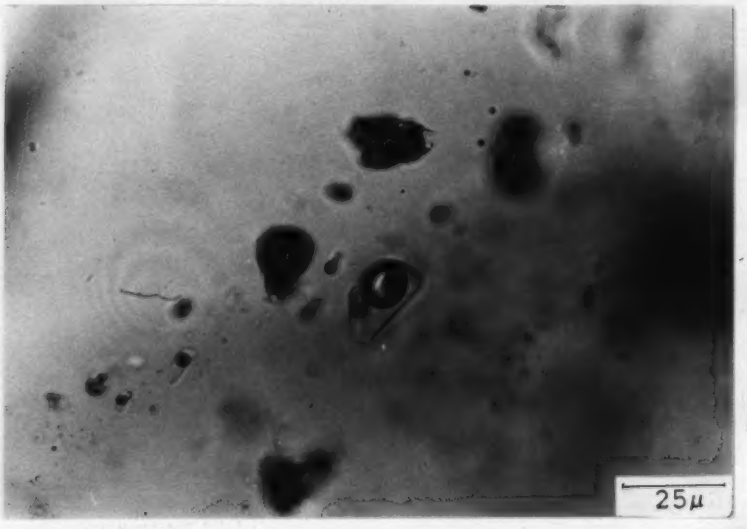

Plate 30. A primary inclusion in fluorite containing a liquid phase, CO_2 and a halite daughter crystal. Terra mine.

Type E: Type E inclusions contained a liquid phase, and a vapour phase, the volume of which was less than 30% of the total volume. Type E inclusions were common in all the deposits, and were mostly secondary, but primary inclusions belonging to this category were also found.

Type F: Type F inclusions consisted of liquid, vapour and halite daughter crystals. Type F inclusions were found in variable proportions in many of the samples. Halite daughter crystals were rare in inclusions which homogenized at temperatures above 350°C.

Other Types: In one sample of calcite from the Terra deposit, a hematite daughter crystal was identified by its hexagonal habit and red colour. A fluorite sample from the Terra deposit was found to contain liquid CO_2 upon freezing. CO_2 was not detected in other samples. A quartz sample, also from the Terra deposit, associated with native bismuth was found to contain a liquid phase, a vapour phase and unidentified radiating daughter crystals. Robinson (1971) reported a solid inclusion in quartz from the Echo Bay deposit. He assumed it to be a sulphate. Shegelski (1973) also reported hematite crystals in inclusions from the Terra deposit.

The distribution of the different types of inclusions was found to be informative. The coexistence of vapour-rich and liquid-rich inclusions in the same sample is obviously the result of trapping of a boiling or effervescing fluid. The coexistence of saturated and undersaturated inclusions, however, is rather puzzling. Rye and Sawkins (1974), Landis and Rye (1974), Ahmad and Rose (1980) and Shelton (1983) also reported coexistence of these two types of inclusions. A plausible explanation of this phenomenon is discussed in section 5.7.

5.4 Salinities of the Hydrothermal Fluids

Different techniques may be applied in fluid inclusion studies to determine the salinities of hydrothermal fluids. In undersaturated solutions, that is, solutions which do not contain any halide daughter crystals, the salinity is determined by the freezing point depression technique (Roedder, 1962, 1963). In the destructive method the host mineral is crushed and the leachate is analyzed by conventional chemical techniques, namely, the atomic absorption spectrophotometry, flame photometry, etc.. In recent years, Raman spectroscopy

(Guilhaumou *et al.*, 1978; Rosasco and Roedder, 1979; Dhamelincourt *et al.*, 1979), neutron activation (Touray, 1976; Grappin *et al.*, 1979; Luckscheiter and Parekh, 1979), laser, ion and electron microprobes (Tsui and Holland, 1979; Bennett and Grant, 1980; Nambu *et al.*, 1977; Nambu, 1980; Metzger *et al.*, 1977; Dolomonova *et al.*, 1974, Murck *et al.*, 1978; Ypma and Fuzikama, 1980), and ICP spectroscopy (Thompson *et al.*, 1980) have been used in determining the composition of fluid inclusions.

The salinity of saturated solutions, that is, inclusions with daughter crystals, may be determined by dissolution of the crystal upon heating or from phase volumes (Kelly and Turneaure, 1970; Roedder, 1981, 1984). In the former method it must be assumed that the inclusion fluid is pure NaCl-H_2O. The composition can then be determined from the Tm[1] of NaCl combined with the data on the system NaCl-H_2O (Keevil, 1942; Sourirajan and Kennedy, 1962; Khaibullin *et al.*, 1980). The second method involves careful estimation of the volume of each phase.

In the present investigation the salinities of the inclusion fluids were determined by the freezing-point depression technique and from the dissolution temperatures of the halite daughter crystals upon heating. In the latter case it was assumed that the hydrothermal fluids were very close to the pure NaCl-H_2O system. The validity of this assumption was checked during the freezing runs. In inclusions whose first melting (Te) temperature was observed, the temperature (-19.8 to -22°C) was found to be close to the first melting temperature at -21.1°C (-20.8°C) of pure NaCl brines. The presence of other salts, namely KCl and $CaCl_2$ depresses the first melting temperature (Crawford, 1981).

It was mentioned earlier that the inclusions in the vein minerals have variable sizes, ranging from a few microns to more than 150 microns. For freezing experiments, inclusions which were usually larger than 15 microns were chosen. For smaller inclusions it was not possible to detect the actual freezing temperature. Freezing experiments were carried out on type A, B, and D inclusions. Since the presence of halite daughter crystals indicates the salinity

---

[1]Temperature of melting of the daughter crystal

to be more than 26.3 wt.% NaCl equivalent, freezing was not done on this type of inclusion. In the majority of the cases the inclusions were frozen down to about -90°C. The vapour bubble was found to contract or deform below about -40°C. The salinities of the saturated solutions in over-saturated inclusions were determined by heating experiments. The temperatures at which the halite daughter crystals dissolved were recorded and the corresponding salinities were determined from the NaCl solubility curves of Keevil (1942) and of Sourirajan and Kennedy (1962).

The salinities determined by both methods are presented in Table 12. The salinities determined by the freezing-point depression technique were in the range of 15 to 23 wt.% NaCl equivalent. The salinities determined by heating of the saturated inclusions were in the range of 30 to 35 wt.% NaCl equivalent. Since it was not possible to determine the sequence of entrapment of the inclusions, it was not possible to determine the temporal variations in salinity of the hydrothermal fluids.

5.5 Temperatures of the Hydrothermal Fluids

Homogenization temperatures of primary and secondary inclusions were measured. Homogenization temperatures were measured on the same inclusions, either after each freezing experiment, or at a later time. In many cases the inclusions were found to decrepitate before the homogenization temperature was reached. In other cases the vapour bubble was found to disappear into dark recesses of the inclusions just before the homogenization temperature was reached, thus leading to slight errors. Similar problems have been reported by Taylor *et al.* (1983). In these cases an estimate of the homogenization temperature was made. The temperature was estimated to be not more than 10 or 15°C from the temperature of disappearance of the vapour bubble into dark recesses of the inclusion.

The results of the heating experiments are given in Table 12. The results given are those for homogenization temperatures which have not been corrected for pressure effects. The results show clearly that the minerals of different paragenetic stages formed under distinct

Table 12

Temperature and Salinity Data for Hydrothermal Fluids in the Great Bear Lake Silver Deposits, N.W.T.. Temperature data plotted in Figure 22.

Sample nos.	Mineral	Stage[1]	Origin[2]	Th(°C)[3]	Tf(°C)[4]	Salinity[5]
5A/125/ED	Dolomite	IV	P(5)	215-220	---	31.0 - 32.0
2/1/SUR/ED	Quartz	V	P(10)	220-256	-2.5 to -1.9	4.1 - 3.2
D/SB	Dolomite	II	P(5)	230-265	-18.1 to -19.6	21.9 - 22.2
			S(4)	155-160	---	--
3V/2L/SB	Calcite	IV	P(4)	196-205	---	31.0 - 31.8
1/1112/SB	Dolomite	III	P(4)	295-310	-15.1 to -17.1	18.7 - 20.3
			P(2)	312-315(*)	-17.6 to -18.1	20.9 - 21.2
8/5/S00/ED	Dolomite	IV	P(2)	202,203	---	30.1
			S(5)	130-135	---	--
#1/SUR/ED	Quartz	V	S(7)	102-125	---	--
711/SB	Fluorite	II	P(14)	320-460	-17.0 to -19.8	20.4 - 22.5
8V/1L/SB	Dolomite	III	P(1)	295(*)	-19.0	21.9
			P(1)	297	-18.7	21.7
513/82(B)/SB	Quartz	III	S(5)	120-140	---	28.0 - 29.0
711/SB	Fluorite	II	S(4)	220-250	---	33.0
4V/2L/SW	Quartz	II	P(1)	300	---	30.0
CL/10	Quartz	IV	P(6)	180-220	---	30.8 - 31.2
7V/3L/SB	Dolomite	II	P(4)	180-210	-13.9 to -14.6	17.8 - 18.4
912/3V/SB	Quartz	IV	P(6)	185-213	-15.8 to -16.4	19.4 - 19.9

7I1/SB	Dolomite	IV	P(1)	185	---	31.0
NX/Z	Quartz	I	P(3)	160-210	-10.8 to -11.3	14.8 - 15.3
NX/Z11	Quartz	II	P(6)	350-480	-16.1 to -17.6	19.7 - 20.9
NX/Z	Quartz	II	P(5)	460-480	-15.6 to -16.3	19.3 - 19.8
3/3V/3L/NX	Quartz	III	P(3)	283-323	-16.2 to -17.3	19.7 - 20.6
			P(1)	410	---	--
1/7V/3L/SB	Dolomite	II	P(5)	364-460	-15.2 to -18.8	18.9 - 21.8
			S(2)	245-263.8	---	--
513/82(B)/SB	Quartz	III	P(4)	282-350	-14.3 to -15.7	18.1 - 19.4
			S(6)	130-240	---	--
711/SB	Quartz	III	P(4)	210-266	-13.6 to -13.8	17.5 - 17.7
			S(3)	178-209	---	31.5
711/SB**	Quartz	III	P(3)	255,266	-18.6 to -20.1	21.6 - 22.7
			S(1)	180	---	--
1/3V/3L/NX	Quartz	III	P(8)	260-280	-18.2 to -19.6	21.2 - 22.4
			P(8)	328-375	-19.3 to 20.0	22.1 - 22.6
			S(2)	180,224.9	---	--
2/3V/3L/NX	Quartz	I	P(4)	223-265	-13.9 to -14.3	17.8 - 18.1
CL/10	Quartz	IV	S(4)	105-110	---	--
NR/Z	Quartz	?	S(2)	105,106	---	--
4/2V/SUR/ED	Quartz	?	P(3)	220-270	---	--
			P(3)	360-380	---	--
			S(2)	110,115	---	--
6/914/SB	Dolomite	II	P(7)	408-426	-19.3 to -20.0	22.1 - 22.6

1/3L/8V/SB	Calcite	III	P(1)	276	---	35.0
1/4V/2L/SB	Calcite	IV	P(2)	182,196	---	30.8 - 31.4
1/3L/3V/SB	Calcite	II	P(6)	235-243	---	--
CL/28	Quartz	IV	P(8)	208-228	---	31.2 - 32.0
4/3V/3L/NX	Quartz	I	P(8)	213-223	-12.6 to -13.3	16.6 - 17.2
3/4V/2L/SW	Quartz	II	P(6)	265-276	---	--
L/45/NR	Quartz	V	P(1)	175	---	--
1/4L/NR	Dolomite	II	P(5)	253-281	---	--
1/9V/2L/SB	Calcite	III	P(7)	256-278	---	--
1/514/SB	Calcite	III	P(6)	316-324	---	--
NX/3	Quartz	II	P(10)	308-343	-19.8 to -20.2	22.5 - 22.8
4/9V/3L/SB	Dolomite	II	P(7)	360-381	---	--
82/DUMP/SB	Calcite	II	P(6)	361-372	-16.1 to -16.9	19.7 - 20.3
3/1L/8V/SB	Dolomite	II	P(2)	382,394	-18.2 to -18.6	21.3 - 21.6

[1]Stages of mineralization (Figures 15 to 21). [2]P=Primary; S=Secondary; the numbers in parentheses represent number of inclusions. [3]Th=Temperature of Homogenization. [4]Tf=Temperature of Freezing. [5]Salinity is expressed as weight percent NaCl equivalent. The salinities in which Tf is not given has been determined by dissolution of halite daughter crystals. ED - Eldorado. SB - Silver Bear (or Terra). SW - Smallwood. CL - Contact Lake. NX - Norex. NR - Northrim.

temperature regimes. Homogenization temperatures in stage I quartz (primary inclusions) was found to be in the range of 150° to 250°C. The carbonates, mainly dolomite, of the pre-arsenide stage of mineralization show a temperature range of 220° to 350°C. The highest temperature range (350° to 480°C) was recorded in quartz intimately intergrown with the Ni-Co arsenides. The carbonates associated with the arsenides show slightly lower homogenization temperatures than those in quartz. Fluorite associated with late arsenides and sulpharsenides was found to contain CO_2-bearing inclusions which homogenized at temperatures as high as 460°C. Dolomites, calcites and the quartz of mid- to late- stage III mineralizations show homogenization temperatures in the range of 250° to 350°C. Evidence of boiling or of effervescence was observed in two dolomite samples of stage III. In the dolomites, the liquid-rich and vapour-rich phases were found to homogenize between 285° and 315°C. Inclusions with wide variations in filling ratios were found in quartz intergrown with the arsenides of stage II from the Norex deposit. In some of the inclusions, the vapour phase constitutes more than 75% of the total inclusion volume. Since these were very small inclusions, homogenization temperatures could not be obtained on them. However, the size of the vapour bubble suggests temperatures above 350°C. This visual estimation seems to be quite valid as other inclusions from the same section and with the same filling ratios showed homogenization temperatures around 400°C. These inclusions were probably trapped from a boiling system or one very close to the boiling point. Dolomites, calcites and the quartz from stages IV and V contained inclusions which homogenized below 300°C.

Since the homogenization temperature signifies the minimum temperature of trapping, pressure corrections must be made and added to the homogenization temperatures to obtain the true trapping temperatures of the fluid inclusions. Various methods have been utilised to determine the pressure of trapping of fluid inclusions. The pressure may be estimated by geologic reconstruction of the depth of cover, and by assuming that the formation pressure was either equal to lithostatic or hydrostatic load (Roedder, 1967). The pressure obtained may thus be used to calculate the pressure correction for the homogenization temperature.

Various other methods have been applied to make pressure corrections for homogenization temperatures. Until 1977, the method of Lemmlein and Klevtsov (1961) was extensively used for pressure corrections. The inconsistency of their method was pointed out by Potter (1977). He presented a new set of pressure correction graphs from 20° to 400°C and for 1, 5, 10, 15, 20, and 25 wt.% NaCl solutions to 2000 bars. However, the corrections are valid only if, (i) the solution is pure NaCl solution; (ii) the salinity has been correctly determined; (iii) the pressure of formation has been estimated correctly; (iv) homogenization of the inclusion is in the liquid phase. In case of (iii), the pressure must be estimated either by reconstruction of the geologic cover or by other methods. The pressure of formation can be directly determined from fluid inclusions. These methods have been discussed by Roedder and Bodnar (1980) and Roedder (1984).

The fractures in the Great Bear Lake region were both open and tight (Robinson, 1971; Robinson and Ohmoto, 1973), which suggests that the pressures fluctuated between hydrostatic and lithostatic. No evidence of boiling was found in the samples from the Echo Bay sector during this study, nor was it found in the samples during the investigation carried out by Robinson (1971) and Robinson and Ohmoto (1973). This suggests that the total pressure in this sector was greater than the vapour pressure of the hydrothermal fluids, preventing boiling. In Camsell River sector, however, evidence of boiling was found in inclusions in quartz and dolomites of stage II and III, as mentioned earlier. The coexistence of vapour-rich and liquid-rich fluid inclusions in these samples, which homogenized at similar temperatures, indicates that the hydrothermal fluids were boiling periodically. The coexistence of these inclusions obviates the need for pressure corrections, and the temperatures and pressures determined from these inclusions were the true trapping temperatures and pressures of the inclusions. Pressures determined from coexisting liquid-rich and vapour-rich inclusions were found to be between approximately 70 and 200 bars, using the data of Haas (1971) and of Sourirajan and Kennedy (1962). Since no evidence of boiling was found in the samples of the other stages, pressure corrections must be made to the homogenization temperatures. Assuming

a hydrostatic pressure of 70 to 200 bars, a pressure correction of 25°C or less must be made to the homogenization temperatures (Potter, 1977).

5.6 Density of the Hydrothermal Fluids

The density of hydrothermal fluids can be estimated from fluid inclusions quite accurately if the relative volumes of the liquid and gas phases can be determined at room temperature from geometrically regular inclusions, and if the salinity is determined by the freezing point depression technique (Roedder, 1984). Bodnar (1983) proposed a method for determining the volumes and densities of irregular inclusions from bubble diameter, Tm of ice, Th(l-v), and volumetric properties of the fluids. The density of the fluids can also be estimated from the theoretical or experimental data for H_2O-NaCl system given in the literature (Lemmlein and Klevtsov, 1961; Ellis and Golding, 1963; Haas, 1971; Urusova, 1974, 1975; Potter and Brown, 1975; Rogers and Pitzer, 1982).

The densities of the Great Bear Lake hydrothermal fluids were estimated from the salinities, filling temperatures and the P-V-T-X data of the NaCl-H_2O system. The densities of the fluids were found to be between 0.75 to 1.12 g/cm^3. The values fall within the expected range of densities for hydrothermal fluids, which according to Roedder (1967) vary from 0.5 to slightly over 1.0 g/cm^3.

5.7 Conclusions

The experimental results obtained in this study suggest considerable fluctuations in both temperature and salinity of the hydrothermal fluids responsible for the deposition of the argentiferous veins. The possible range of homogenization temperatures for the different paragenetic sequences are shown in Figure 22. The variations in temperatures were probably not continuous, as each stage represents a distinct period of mineralization separated in time. The temperature variations are therefore, more likely to reflect hydrothermal fluid pulses of various temperatures being flushed into the veins at different times. The variations in salinity are

difficult to explain. Boiling or effervescence of moderate salinity fluids may give rise to high salinity fluids. Boiling or effervescence might have been responsible for increasing the salinities of the stage II and III fluids, but evidence of boiling or effervescence was not found in the minerals of other stages. Ahmad and Rose (1980) and Shelton (1983) suggested an alternation of lithostatic and hydrostatic pressure conditions during ore deposition as the likely reason for the close spatial association of the moderate and high salinity inclusions. According to Shelton (1983), changes in pressure from lithostatic to hydrostatic may result in fluids intersecting the two phase field, leading to the separation of a high salinity liquid and low salinity vapour. The vapour phase may not be trapped in the inclusions. This mechanism could be a possible explanation for the salinity trend of the Great Bear Lake fluids if the pressure alternated between lithostatic and hydrostatic. Another possible explanation is a mixing of a highly saline magmatic fluid with a less saline fluid which could have been either of meteoric or marine origin. A possible mixing model is also discussed in the chapter on Isotope Geochemistry.

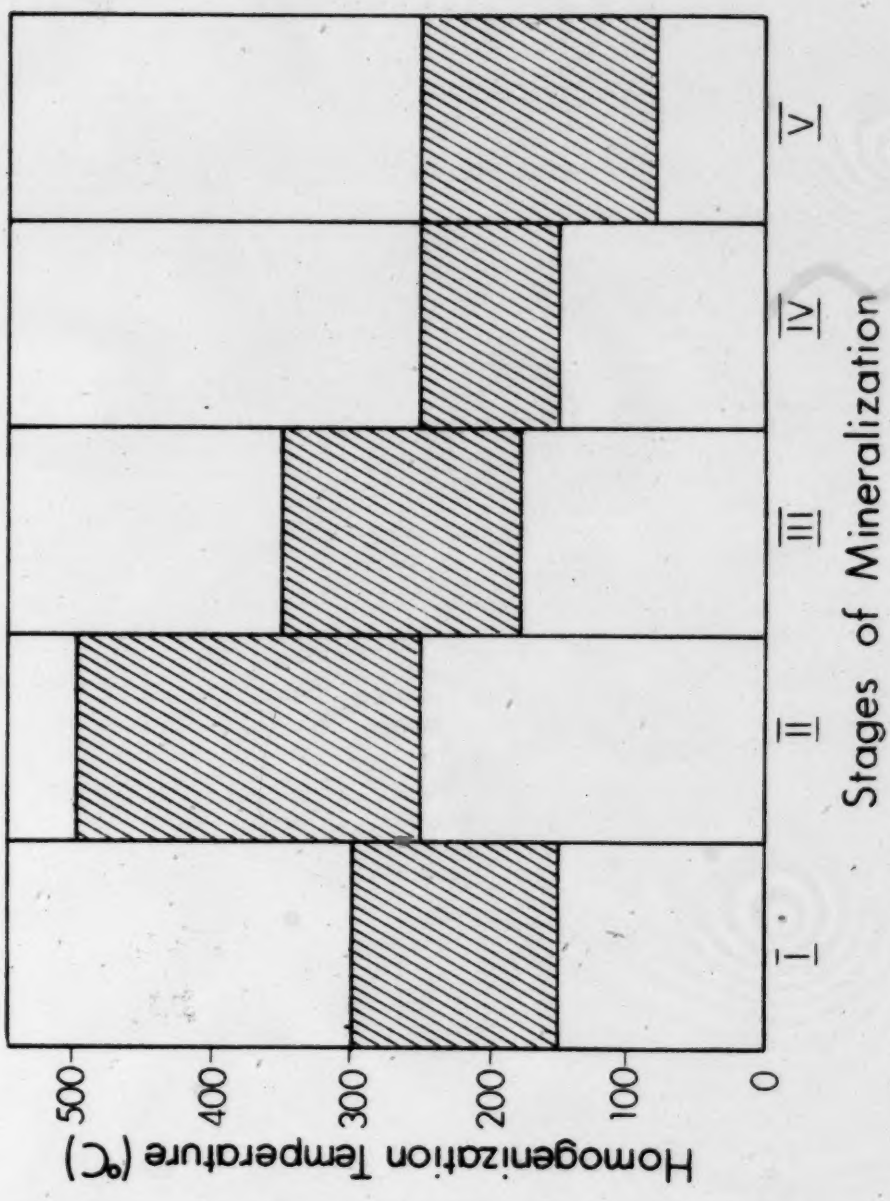

Figure 22. Relationship between homogenization temperature and different stages of mineralization in the Great Bear Lake silver deposits. Data listed in Table 12.

6. OXYGEN-, HYDROGEN- AND CARBON- ISOTOPE GEOCHEMISTRY

6.1 Introduction

Over the years various methods have been applied to determine the origin of ore deposits. Since water is a dominant constituent of ore-forming fluids, it is obvious that its origin will reflect the origin of the deposit under investigation. The advent of stable isotope analysis has greatly aided in deciphering the origin of ore-bearing fluids. Besides furnishing information about the origin, nature, and amount of hydrothermal fluid from which an assemblage of oxygen-bearing minerals was formed, oxygen isotopic studies may also help to determine the temperatures of formation of oxygen-bearing minerals, and to test equilibrium or nonequilibrium among the coeval oxygen-bearing mineral assemblages (Taylor, 1967).

The principles of stable isotope geochemistry can be found in Urey (1947), Bigeleisen and Mayer (1947), Bigeleisen (1965), and Broecker and Oversby (1970). Hoefs (1980) has summarized the application of stable isotopes to geological problems. The application of stable isotopes, mainly, oxygen and sulphur, to problems of ore deposits is extensively documented in the literature. Taylor (1967, 1974, 1979), Ohmoto and Rye (1979), and Rye and Ohmoto (1974) have reviewed the application of stable isotopes in problems of ore deposits. Sheppard (1981) has summarized the stable isotope geochemistry of systems containing gaseous mixtures, silicate melts, and hydrothermal fluids.

The experimental techniques for oxygen, carbon and hydrogen are presented in Appendix I and the results are expressed as

$$\delta = (R_1/R_2 - 1) \times 1000$$

where δ is the permil deviation of the isotopic ratios of the samples from the standards; R_1 and R_2 are the $^{18}O/^{16}O$, $^{13}C/^{12}C$ and D/H ratios of the samples and standards respectively. The $\delta^{18}O$ and δD values are expressed with respect to V-SMOW (Gonfiantini, 1978) and $\delta^{13}C$ is expressed with respect to PDB. A correction factor of + 0.82 per mil was added to the dolomite data for kinetic fractionation (Sharma and Clayton, 1965). Analytical reproducibilities for oxygen and carbon were $\pm$ 0.1 per mil and $\pm$ 0.2 per mil respectively, and for hydrogen were $\pm$ 2.0 per mil.

6.2 Results

6.2.1 $^{18}O/^{16}O$ ratios of the carbonates and quartz

The $\delta^{18}O$ values of the carbonate and quartz samples from the veins are given in Table 13 and plotted in Figures 23 and 24. Calcites show a range of $\delta^{18}O$ values of about per mil. This wide range in $\delta^{18}O$ values may be attributed to one of the following reasons : (i) variations in the temperatures of crystallization; (ii) fluctuations in the isotopic composition of the hydrothermal fluid; or (iii) post-depositional modifications of the calcites.

In contrast, the dolomite and quartz samples show a narrow range in $\delta^{18}O$, except for sample no. 8/5/SUR/ED which has a value 6.63 per mil. Dolomites are more resistant to re-equilibration, and hence retain their original isotopic signatures. In general, uniformity in $\delta^{18}O$ would reflect a uniform oxygen isotopic composition and temperature of the hydrothermal fluid during deposition of the minerals concerned. However, minerals precipitating at different times, from fluids of variable isotopic composition and temperature, may also exhibit a narrow range of $\delta^{18}O$ values. A mineral precipitating from a fluid having high $\delta^{18}O$ value and at low temperature may have a $\delta^{18}O$ value similar to a mineral precipitating from a low $\delta^{18}O$ value at high temperature. Such a mechanism was probably operative in the Great Bear Lake deposits, for the narrow range of $\delta^{18}O$ values of quartz and dolomite in these veins cannot be simply explained by uniformity of the isotopic composition and temperature of the fluids from which the minerals precipitated, because the analyzed samples actually represent quite different stages of mineralization. Each stage represent a new pulse of mineralizing fluids introduced into the veins at different times. The wide range of homogenization temperature encountered in these samples was discussed in the previous chapter on fluid inclusions. The present isotopic signature, may therefore, be attributed to variations in the isotopic compositions and temperatures of the hydrothermal fluids during the different stages of mineralization.

Table 13

Isotopic Data for Hydrothermal Minerals and Fluids in the Great Bear Lake Silver Deposits, Northwest Territories. Data plotted in Figures 23, 24 and 25.

Sample nos.	Description	$\delta^{18}O$	$\delta^{13}C$	δD	T(°C)[1]	$\delta^{18}O(H_2O)$
NX/Z	Quartz-white, earlier than arsenides.	16.5	---	-73.5	250	6.38
3/5A/125/ED	Dolomite-white to pale pinkish, coarse-grained, associated with sulfides.	14.5	-3.5	---	200	4.07
4/5V/800/ED	Dolomite-white, fine-grained, associated with native bismuth.	15.7	-4.6	---	200	5.27
8-D-8(A)/ED	Dolomite-pinkish white, later than Ni-Co arsenides.	19.4	-11.8	---	---	---
1112/SB	Dolomite-pinkish white, associated with arsenides.	14.5	-4.1	---	300	8.42
9V/2L/SB	Calcite-pinkish white, fine-grained, associated with late sulfides, encloses quartz crystals in vugs.	15.6	-6.6	---	---	---
713A/SB	Calcite-colourless, prismatic crystals.	8.7	-10.0	---	---	---
713B/SB	Calcite-colourless to white, rhombohedral crystals.	12.3	-13.3	---	---	---
513/82/SB	Calcite-white, associated with native bismuth.	11.6	-13.0	---	---	---
513/82/SB	Calcite-colourless, associated with chalcopyrite.	11.0	-11.5	---	---	---
513/82/SB	Calcite-white, earlier than arsenides; veinlets of arsenides cross-cut it.	14.0	-3.9	---	325	9.12
513/82(B)/SB	Dolomite-pinkish white, fine-grained.	14.9	-4.0	---	---	---
513/82(B)/SB	Calcite-pink, fine-grained.	19.6	-5.0	---	---	---
8V/1L/SB	Calcite-pinkish white, crystalline, associated with native silver.	14.3	-4.2	-62.9	295	8.57
1/7V/3L/SB	Calcite-white, crystalline, earlier than the arsenides.	16.3	-4.2	---	---	---

1112A/SB	Dolomite-white, associated with arsenides.	11.3	-4.2	---	400	7.78
2V/1L/SB	Calcite-white, very fine-grained, associated with arsenides and sulfides.	6.8	-6.4	---	---	---
3V/2L/SB	Calcite-pink, coarse-grained.	14.4	-4.5	---	200	4.87
711/SB	Dolomite-pink, encloses fluorite and quartz.	15.0	-4.3	---	185	3.66
711/SB	Calcite-colourless, coarse-grained, associated with sulfides.	10.0	-9.0	---	200	0.47
711/SB	Calcite-white, associated with native silver.	20.1	-3.7	---	---	---
82/DUMP/SB	Calcite-colourless, occurs in vugs within quartz, later than quartz and arsenides.	14.4	-4.2	---	---	---
514/SB	Calcite-pinkish white, fine-grained.	17.0	-4.8	-81.6	200	7.47
10/4V/2L/SW	Calcite-white, fine to medium grained.	8.3	-4.5	---	---	---
1L/CAL/SW	Calcite-white, asociated with sulfides.	13.8	-2.7	---	180	3.15
BON/5	Calcite-white, very coarse-grained.	16.0	-4.5	---	---	---
BON/9	Calcite-white, very coarse-grained.	15.9	-4.7	---	---	---
BON/9A	Calcite-colourless, coarse-grained.	10.5	-6.9	---	---	---
NR/1	Dolomite-white, fine-grained.	13.9	-5.7	---	---	---
ELB/1	Calcite-colourless, coarse-grained.	15.2	-4.8	---	---	---
ELB/5	Calcite-pinkish white, medium-grained.	9.7	-4.3	---	---	---
2/3V/3L/NX	Calcite-colourless to white, occurs as thin layers over quartz. Not related to mineralization.	12.7	-5.5	---	---	---
2/3V/3L/NX	Calcite-white, associated with native silver.	17.0	-4.6	---	---	---
3/3L/3V/NX	Calcite-pink, associated with native silver and quartz.	19.6	-4.4	---	---	---
Z7/NX	Calcite-white, fine-grained, crystalline.	15.3	-4.9	---	---	---

Z10/NX	Calcite-white, fine-grained, crystalline.	18.2	-4.8	-62.2	200	8.67
Z11/NX	Calcite-white, associated with sulfides.	23.7	-5.3	---	---	---
9/316/EB	Calcite-white, fine to medium grained, associated with sulfides.	19.3	-6.0	---	---	---
10/316/EB	Calcite-pinkish white, fine-grained.	22.5	-3.8	---	---	---
31/CL	Calcite-colourless to white, occurs as thin layers over quartz.	21.9	-10.5	---	---	---
9/CL	Dolomite-white, associated with native silver.	22.2	-3.9	---	---	---
1/CL	Dolomite-white, associated with native silver.	15.5	-3.7	-98.5	260	7.97
1/ED	Calcite-white, associated with native silver.	15.8	-4.8	-78.5	250	8.53
6/5V/500/ED	Rhodochrosite-red, occurs as aggregates, associated with native silver.	15.7	-3.3	---	---	---
5/1V/SUR/ED	Siderite-brown, occurs in vugs, not related to any mineralization.	19.5	-4.3	---	---	---
1/1/SUR/ED	Siderite-brown, occurs in vugs.	18.6	-4.4	---	---	---
L45/NR	Quartz-colourless to white, later than arsenides and native silver (Stage V).	14.32	---	---	175	-0.72
513/82(B)/SB	Quartz-colourless to white (Stage III).	14.84	---	-67.8	325	7.6
2/3V/3L/NX	Quartz-coarse-grained, white to colourless (Stage I).	16.45	---	---	240	5.6
514/SB	Quartz-white, encloses brecciated wall rocks (Stage I).	16.50	---	---	---	---
914/SB	Quartz-colourless to greyish white (Stage I).	16.33	---	---	---	---
CL/10	Quartz-colourless to white, massive; intimately intergrown with native bismuth and dolomite (Stage IV).	14.92	---	---	210	2.3

8/5/SUR/ED	Quartz-white, massive, associated with late sulfides (Stage V).	6.63	---	---	---	---
3/3V/3L/NX	Quartz-colourless, intimately intergrown with native Ag (Stage III).	14.11	---	---	300	6.0
1/SUR/ED	Quartz-colourless to white, coarse-grained, crystalline (Stage V).	15.12	---	---	238	4.2
912/SB	Quartz-white, massive (Stage II).	14.88	---	---	---	---
82/SB	Quartz-white, associated with native Ag (Stage III).	15.98	---	-87.5	250	5.6
912/3V/SB	Quartz-white to colourless, crystalline, associated with massive native bismuth (Stage IV)	14.51	---	---	200	1.3
711/SB	Quartz-colourless, crystalline, associated with fluorite and dolomite (Stage III).	15.26	---	---	270	5.9
1/SB	Quartz-white, granular, intergrown with wire silver (Stage IV).	17.25	---	---	---	---
9/4V/2L/SW	Quartz-colourless, crystalline, associated with chalcopyrite (Stage V).	16.06	---	---	150	-1.1
4V/2L/SW	Quartz-colourless to white, granular, associated with Ag and arsenides (Stage II).	15.18	---	---	300	7.0
Z11/NX	Quartz-grey to colourless, intimately intergrown with arsenides (Stage II).	14.63	---	---	425	10.0
2/7V/3L/SB	Dolomite-pinkish white, coarse-grained, crystalline, associated with arsenides (Stage II).	13.2	-4.5	-51.6	350	8.5
9/4V/2l/SW	Dolomite-white, crystalline (Stage IV or V).	12.5	-8.1	-74.2	150	-1.5

1112/SB	Dolomite-pinkish white, crystalline, associated with arsenides (Stage II).	13.8	-4.3	-48.6	300	7.7
CAR/5/SB	Calcareous siltstone---dolomite	10.6	-8.7	---	---	---
CAR/3/SB	Calcareous siltstone---dolomite	12.6	-11.6	---	---	---
1/5/125/ED	Wall rock	13.9	-3.5	---	---	---
2/5/500/ED	Wall rock	14.0	-3.8	---	---	---
3/HR/514/SB	Wall rock	15.3	-4.8	---	---	---
316/EB	Nickeline	---	---	-135.6	---	---
NX/4L	Mine water	---	---	-165.2	---	---
SB/4L	Mine water	---	---	-163.5	---	---
SB/1L	Mine water	---	---	-154.4	---	---
GB	Great Bear Lake water	---	---	-147.7	---	---
CR	Camsell River water	---	---	-146.5	---	---
SB/9L	Mine water	---	---	-163.1	---	---

[1]Temperatures obtained from fluid inclusions. NX - Norex. ED - Eldorado. SB - Silver Bear (or Terra). EB - Echo Bay. CL - Contact Lake. BON - Bonanza. ELB - El Bonanza. NR - Northrim. SW - Smallwood.

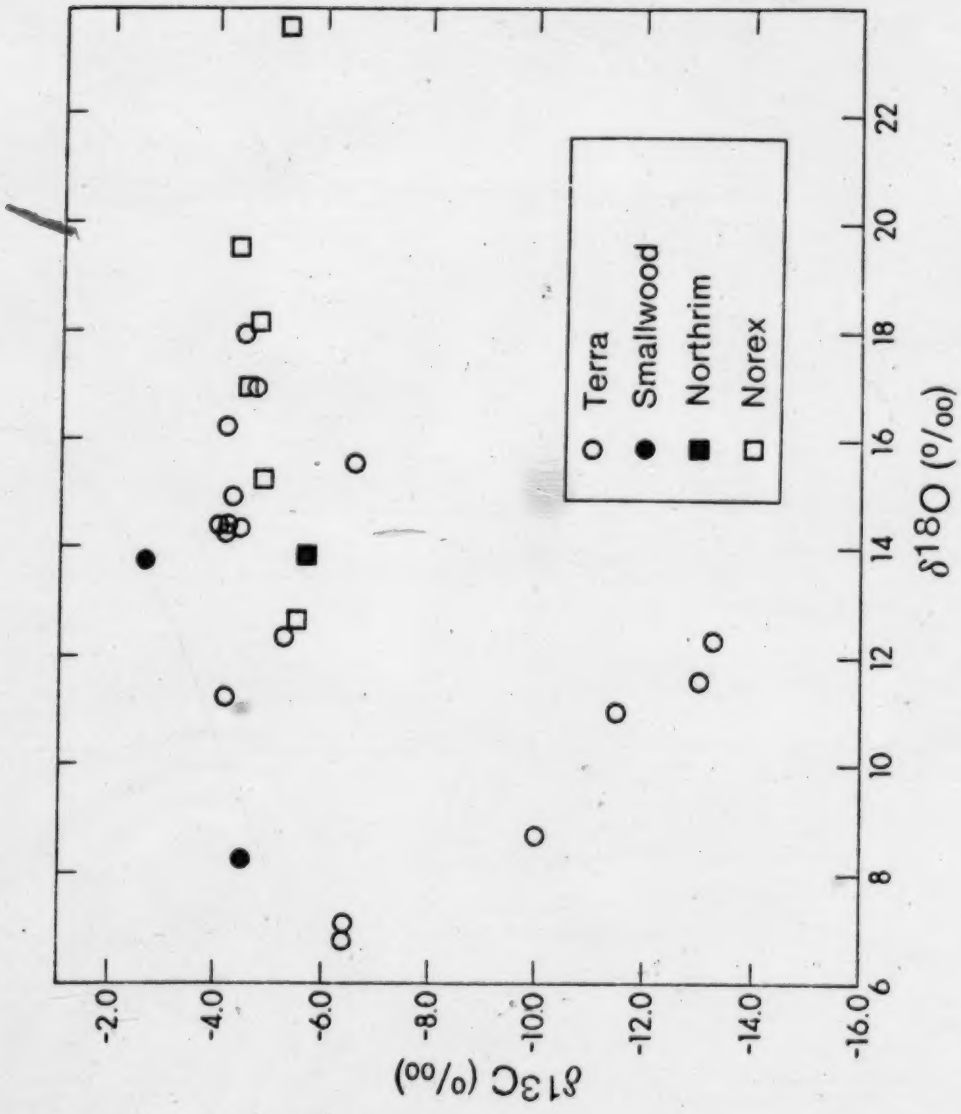

Figure 23. Carbon and oxygen isotopic composition of carbonates from the veins of the Camsell River sector deposits. Data listed in Table 13.

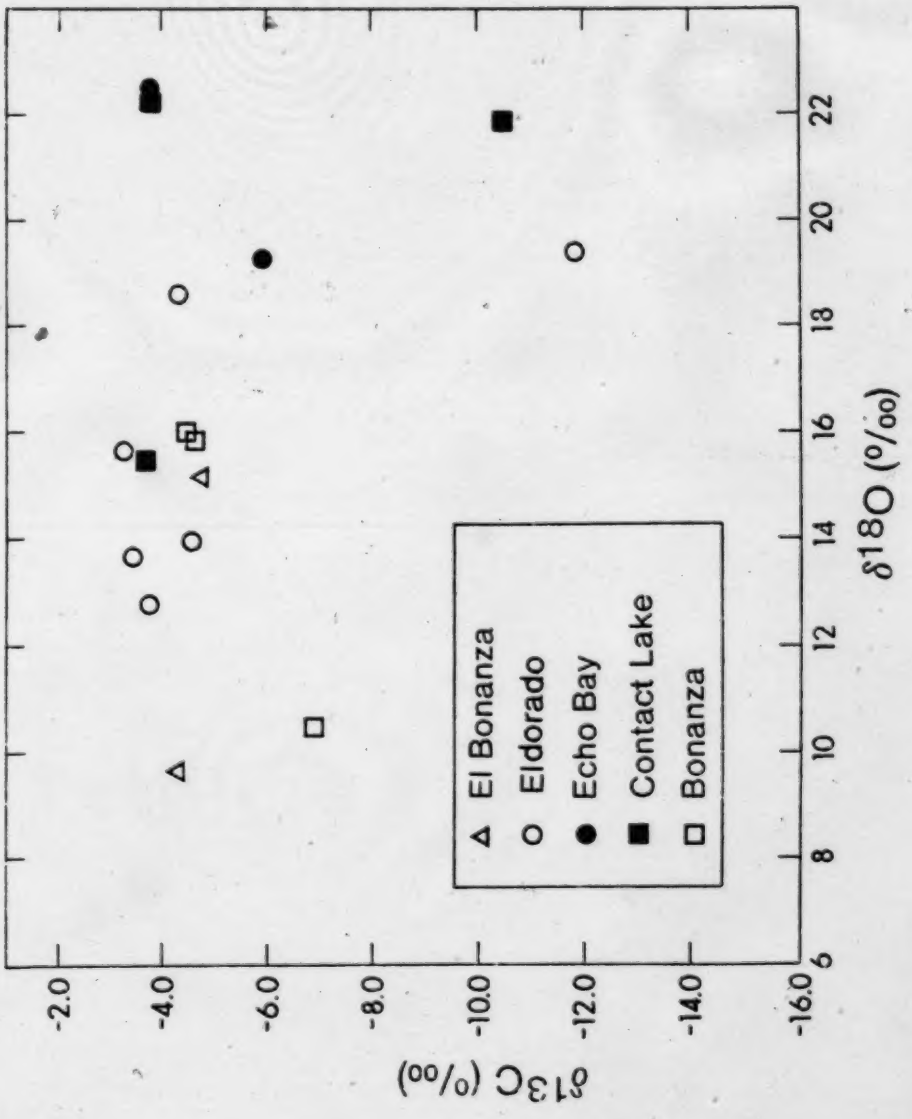

Figure 24. Carbon and oxygen isotopic composition of carbonates from the veins of the Echo Bay sector deposits. Data listed in Table 13.

6.2.2 D/H ratios of the hydrothermal fluids and present day waters

The δD values of waters from fluid inclusions are given in Table 13. Also included are the δD values of mine and surface waters of the Great Bear Lake region. The δD values of inclusion water vary from -48.7 to -135.6 per mil. The δD values of present day waters vary from -146.5 to -165.2 per mil. With the exception of one sample from the Echo Bay deposit (EB/316), the δD values of water in inclusions were found to be quite uniform. The low δD value of sample no. EB/316 may be due to contamination of secondary inclusions.

6.2.3 $^{13}C/^{12}C$ ratios of carbonates

The $\delta^{13}C$ values of carbonates are given in Table 13 and plotted in Figures 23 and 24. Although there is a large range in the $\delta^{13}C$ values, most of the values fall between -3.3 per mil to -6.9 per mil. The calcite samples from the 1st level (sample nos.1L/Cal/SW & 4V/1L/SW) of the Smallwood deposit were found to be most enriched in ^{13}C, while samples 513/82 and 713/82 from vein no. 13 of the Terra deposit, sample no. D/8/D(A)/ED of the Eldorado deposit, and sample no. CL/31 of the Contact Lake deposit were found to be highly depleted in ^{13}C. The $\delta^{13}C$ values of the late carbonate samples from vein no. 13 of the Terra deposit are quite different from the earlier carbonates of the same vein and other veins at this locality. The late carbonates in this vein were probably deposited from a solution of different isotopic composition, or at a later date from a different source. The same arguments could clearly be put forward for the Smallwood, Eldorado and Contact Lake deposits.

6.2.4 Oxygen isotopic composition of the hydrothermal fluids

Oxygen isotopic compositions of hydrothermal minerals are controlled by the isotopic composition of the hydrothermal fluid, by the temperature of crystallization, and by the extent of isotopic exchange. The oxygen isotopic composition of the hydrothermal fluids can be determined directly by measuring the $\delta^{18}O$ of inclusion fluids in a non-oxygen bearing mineral, or indirectly by determining the $\delta^{18}O$ values of an oxygen bearing mineral. If the temperature

of crystallization of the mineral can be determined from an independent source, then the isotopic composition of the fluid which was in equilibrium with the mineral may be determined by choosing the appropriate experimentally determined mineral-water fractionation equation. The latter approach was utilised to calculate the oxygen isotopic composition of the hydrothermal fluids.

The isotopic composition of the hydrothermal fluids was calculated by using the following equations:

dolomite-water (Matthews and Katz, 1977),

$$1000 \ln\alpha = 3.06 \times (10^6/T^2) - 3.24, \text{ and}$$

quartz-water (O'Neil *et al.*, 1973),

$$1000 \ln\alpha = 3.57 \times (10^6/T^2) - 2.73.$$

For calcite-water, the revised version of the original calcite-water equation of O'Neil *et al.* (1969) was used. This equation takes into account the revised value of the equilibrium constant at 25°C between CO_2 and H_2O, which is 1.0412 (Bottinga and Javoy, 1973). The revised equation is:

$$1000 \ln\alpha = 2.78 \times (10^6/T^2) - 2.89.$$

The temperatures used in the above calculations and the calculated isotopic composition of the hydrothermal fluids are presented in Table 13. These temperatures, which represent mean homogenization temperatures for stages I, IV and V mineralization, and mean trapping temperatures for stages II and III mineralization, were determined from fluid inclusions in quartz, dolomite and calcite. Since pressure-correction is less than 25°C, homogenization temperatures have been used for some of these calculations, assuming that it will not significantly affect the trend of argument. In some cases the isotopic composition of the hydrothermal fluids could not be determined as these samples were not suitable for microthermometric experiments. The oxygen isotopic composition of the hydrothermal fluids calculated in this manner were found to vary from -1.1 to 10.0 per mil.

Taylor (1967) discussed the possible effects of impurities on the oxygen isotopic properties of aqueous fluids. It was assumed that high temperature hydrothermal fluids do not deviate significantly from pure water in their oxygen isotopic properties. However, Truesdell (1974) showed that the effects of many common solutes, including NaCl, are appreciable and will increase with temperature up to at least 275°C. He, however, did not carry out experiments on mixed solutions. Hydrothermal fluids on the other hand, are frequently mixtures of NaCl, KCl, $CaCl_2$, etc.. The hydrothermal fluids of the Great Bear Lake deposits have been found to be alkali-chloride solutions as determined by fluid inclusion analyses. Even then the experimental data of Truesdell (1974) cannot be applied in this case, for the salinity of the fluids of the Great Bear Lake deposits is higher than the original experimental range. As the corrections of Truesdell (1974) are approximate and such corrections do not affect the trend of argument, no correction for salinity effects was made.

6.2.5 Carbon isotopic composition of the hydrothermal fluids

The carbon isotopic composition of the hydrothermal fluid may be determined if the temperature of deposition can be estimated and the carbon isotopic composition of the vein carbonates are known. In hydrothermal fluids carbon may be present in different forms, namely, HCO_3^-, CO_3^{2-}, CHaq and H_2CO_3apparent; the latter being the sum of CO_2aq and H_2CO_3 (Ohmoto, 1972). Assuming that the carbon in the hydrothermal fluids was present mainly in the form of H_2CO_3app. (from Robinson and Ohmoto, 1973), which may be approximated to be equal to $\delta^{13}C(CO_2)$[2] (Ohmoto, 1972), the $\delta^{13}C$ of total carbon in the hydrothermal fluid was calculated by using the data of Bottinga (1968). The $\delta^{13}C$ values were found to vary between -3.1 to -8.6 per mil.

---

[2] $CO_2(g)$

6.3 Discussion

According to Taylor (1979) any naturally occurring water can be a potential ore-bearing fluid if it becomes heated as a result of deep circulation in the crust or through its interaction with a magmatic body, especially if it becomes saline in the process. White (1974) defined the following genetic terms for different kinds of water which may be important in forming an ore deposit.

(i) Meteoric--nonmarine water recently involved in atmospheric circulation.

(ii) Ocean--water of the oceans of the time, or recently derived from an ocean.

(iii) Connate--"fossil" water, generally initially ocean water in the interstices of young marine sediments, but out of contact with the atmosphere for an appreciable part of a geologic period.

(iv) Metamorphic--water that is or has been associated with rocks during metamorphism.

(v) Magmatic--water that is in or has come from a magma, regardless of its ultimate origin.

(vi) Juvenile--'new' water that is in or is derived from the mantle and has not previously been part of the hydrosphere.

The $\delta^{18}O$ and δD values of the hydrothermal fluids of the Great Bear Lake silver deposits are plotted in Figure 25. The δD values represent the isotopic composition of the fluid inclusion waters from minerals belonging to stages I, II and III mineralization. δD of fluid inclusion waters from stages IV and V could not be determined because not enough water could be extracted by crushing the samples belonging to these later stages. The $\delta^{18}O$ values represent the $\delta^{18}O$ of the hydrothermal fluids calculated from the $\delta^{18}O$ values of the calcites, dolomites and quartzs. Also plotted are the isotopic ranges of SMOW, magmatic, meteoric and metamorphic waters, and an oil-field brine line for reference. The oil-field brine line represents the isotopic variations of oil-field brines from the Alberta Basin (Hitchon and Friedman, 1969). The calculated $\delta^{18}O$ values of the hydrothermal fluids have a wide range of $\delta^{18}O$ values. This wide range of $\delta^{18}O$ values of the fluids, as was mentioned earlier, were clearly due to variations in the isotopic compositions and temperatures of the fluids. Hence this range in the isotopic composition of the fluids may be attributed to the involvment of two or more types of

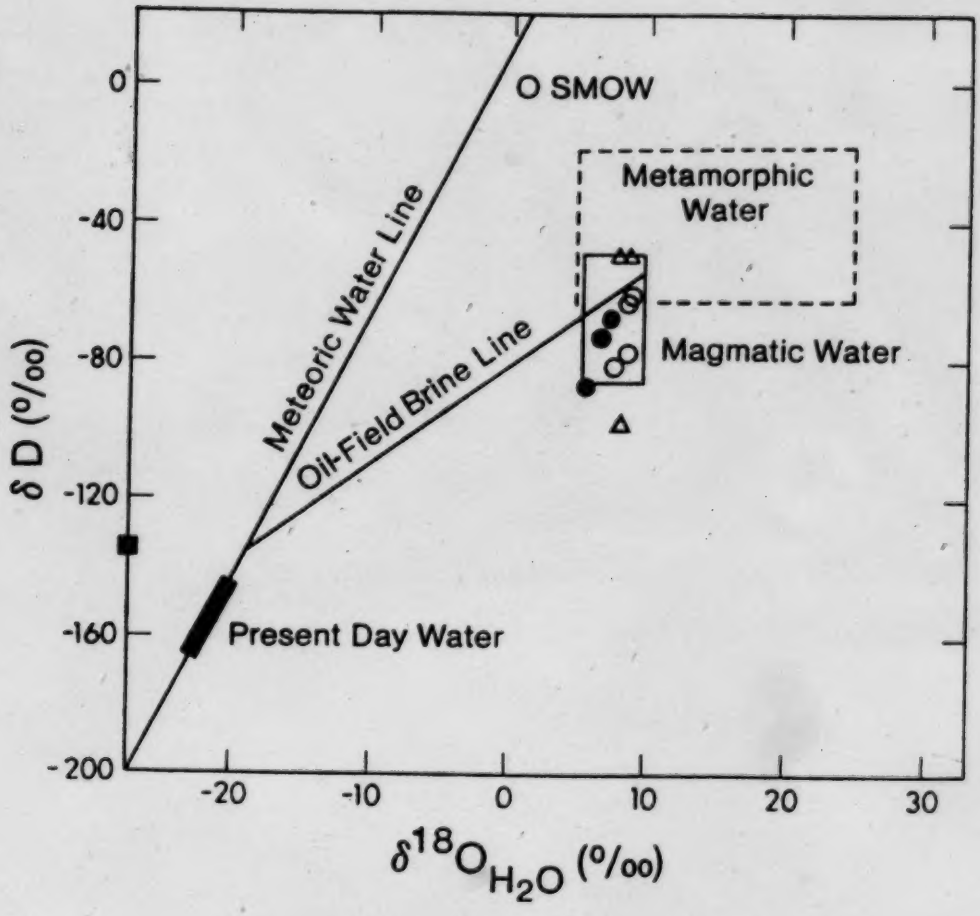

Figure 25. Plot of δD vs $\delta^{18}O$ values of hydrothermal fluids and present day surface and mine waters in the Great Bear Lake region. The δD of fluid inclusion waters in nickeline is plotted on the δD axis because $\delta^{18}O$ value is not available. Open circle - Calcite. Closed circle - Quartz. Open triangle - Dolomite. Closed square - Nickeline. Data listed in Table 13.

fluids during the depositional history of the veins.

The variations in the isotopic composition of the hydrothermal fluids were found to correlate with the paragenetic stages of mineralization. The isotopic composition of fluids belonging to stages I, II and III, in which the arsenides and earlier generations of native silver were deposited, fall within the normal range of magmatic water ($\delta^{18}O$ values of 5.5 to 10.0 per mil, and δD values of -45 to -85 per mil). These fluids were probably derived from a aqueous phase associated with the high level plutons of the batholithic suite. The later fluids, associated with stages IV and V, were considerably lighter ($\delta^{18}O$ values of -1.1 to 4.2 per mil), and were probably the result of subsequent incursion of isotopically lighter water, which could have been either meteoric or marine.

In many instances D/H ratios have been found to be important in determining the origin of many deposits. For example, on the basis of δD values, Ohmoto and Rye (1970) proved that the later stages of mineralization of the Bluebell mine were formed by circulating meteoric water. The δD values of the Great Bear Lake fluids are quite different from those of modern sea water and of present day meteoric waters in the Great Bear Lake region. However, the important question is, what was the isotopic composition of the Precambrian oceans and meteoric water ? It is known that the isotopic composition of meteoric water is controlled by the isotopic composition of the oceans (Taylor, 1979). It has been suggested by Taylor (1979) that the meteoric water line has remained essentially the same for the last 150 million years (± 1.0 per mil for $^{18}O/^{16}O$ and ± 10.0 per mil for D/H), but before that it was probably controlled by the isotopic composition of the oceans. There have been many differences in opinion about the variations in the isotopic composition of the oceans. According to Perry (1967), the Precambrian oceans could have been depleted in $\delta^{18}O$ by as much as 20 per mil. Becker and Clayton (1976) were of the opinion that the Precambrian oceans had a $\delta^{18}O$ of at least -3.5 per mil. Knauth and Epstein (1976) and Kolodny and Epstein (1976) on the other hand, believe that the Precambrian oceans were more or less similar to modern oceans. Beaty and Taylor (1982) have suggested, on the basis of their investigation of the Archean massive

sulphide deposits of the Noranda district, that the $\delta^{18}O$ of the ocean has remained relatively constant at zero per mil throughout at least the past 3 billion years of geologic history.

The present uncertainty regarding the actual isotopic composition of Precambrian sea water precludes any definite conclusions regarding the exact nature of these later fluids. However, the possibility of meteoric components to the systems *sensu lato* cannot be ruled out totally and indeed this is thought to be probable. Robinson and Ohmoto(1973) also suggested such a possibilty. Some of the carbonate and quartz samples from late stage mineralized and unmineralized zones show clear depletion in ^{18}O. The depletion in ^{18}O may well be due to the influence of isotopically lighter meteoric waters, to different temperatures, or to interaction of the hydrothermal fluid with ^{18}O depleted country rocks, which of course, will depend upon the water to rock ratio. Large scale hydrothermal alteration of the intrusive rocks of the region have been reported by Hildebrand (1982). However, no isotopic data for these rocks are currently available to facilitate comment upon the nature of the alteration fluids. Hildebrand (1982) suggested a large scale groundwater:rock interaction based upon the volume of the altered rock.

The source of carbon in the hydrothermal fluids cannot be interpreted unambiguously. In hydrothermal systems the carbon isotopic composition can easily be modified by limestone (Craig, 1953, 1963; Hulston and McCabe, 1962). The isotopic composition of carbon in the hydrothermal fluids of the Great Bear Lake silver veins falls within the range of magmatic carbon (-5.0 ± 2.0 per mil, Deines and Gold, 1973). The late carbonates in these deposits have been found to be depleted in ^{13}C values which correlates well with the oxygen values of these carbonates. Analyses of calcareous siltstones from the Camsell River sector have yielded $\delta^{13}C$ values similar to these late carbonates. These data suggest that the earlier carbonates had a significant contribution of magmatic carbon if not totally. During the later stages, with an increasing incursion of circulating meteoric water, carbon was probably leached from the carbonate beds of the region and its isotopic signature was imprinted into the late stage carbonate gangues.

7. LEAD- AND STRONTIUM- ISOTOPE GEOCHEMISTRY

7.1 Introduction

A preliminary study of lead and strontium isotopes of the vein carbonates and lead isotopes of galena and chalcopyrite was undertaken to see if additional information can be obtained about the origin of the deposits. Although only a few samples were analyzed, the results obtained were found to be interesting, and the results are discussed in the following sections.

7.2 Lead Isotope Study

Lead isotopes have been extensively used in the study of the ore deposits. In addition to determining the age of lead-bearing mineralization, lead isotopes have also been used effectively as tracers. The principles and discussion of lead isotope systematics are extensive in the literature (Russell and Furquhar, 1960; Slawson and Russell, 1967; Kanasewich, 1968; Doe, 1970; Doe and Stacey, 1974; Cumming and Richards, 1975; Stacey and Kramers, 1975; Doe and Zartman, 1979; and others).

The analytical techniques for lead and strontium isotopes are presented in Appendix I.

7.2.1 Results and Interpretations of Lead Data

Samples from five deposits were analyzed. The results are presented in Table 14 and are plotted in Figure 26. Carbonates exhibit the largest variations in isotopic ratios, and may be highly radiogenic. Chalcopyrites are slightly more radiogenic than galenas. The scattered distribution of data points in $^{207}Pb/^{204}Pb$ vs $^{206}Pb/^{204}Pb$ diagram does not lend itself to a simple interpretation. However, the band-like distribution of data points permits some speculation on the timing of mineralization and the nature of ore fluids.

The least radiogenic end of the band is determined by the very steeply trending galena data from Northrim, Silver Bear (or Terra) and Norex deposits. The upper boundary of the band is represented by four carbonate samples from Silver Bear, one carbonate, one chalcopyrite and the most radiogenic galena from Northrim, while the lower boundary is

Table 14

Lead Isotope Data for Hydrothermal Minerals in the Great Bear Lake Silver Deposits, N.W.T.. Data plotted in Figure 26.

Sample Nos.	Mineral	$^{206}Pb/^{204}Pb$	$^{207}Pb/^{204}Pb$	$^{208}Pb/^{204}Pb$
Northrim mine				
AC/32/NR	Galena	15.978	15.441	35.876
AC/31/NR	Galena	15.935	15.377	35.666
AC/44/NR	Galena	15.905	15.355	35.614
AC/42/NR	Galena	15.918	15.365	35.647
AC/41/NR	Galena	15.927	15.366	35.670
AC/45/NR	Galena	15.912	15.363	35.646
AC/33/NR	Galena	15.922	15.361	35.652
AC/C2/NR	Chalcopyrite	16.818	15.474	35.978
AC/C1/NR	Chalcopyrite	16.700	15.513	36.202
NR/1	Dolomite	16.990	15.540	36.626
Terra mine				
713(B)/SB	Calcite	20.457	15.855	39.690
711/SB	Dolomite	19.860	15.812	38.858
513/82(B)/SB	Calcite	17.734	15.607	37.416
AC/L1/SB	Galena	15.981	15.405	35.766
2V/1L/SB	Dolomite	23.930	16.254	43.646
1/7V/3L/SB	Calcite	18.723	15.680	38.423

Norex mine				
AC/N1/NX	Galena	15.967	15.431	35.826
2/3V/3L/NX	Dolomite	16.228	15.431	35.712
Eldorado mine				
5/5V/250/ED	Dolomite	19.655	15.707	37.039
9/5V/500/ED	Dolomite	16.576	15.453	35.901
4/5V/800/ED	Dolomite	20.552	15.816	39.561
Smallwood mine				
9/4V/2L/SW	Dolomite	23.822	16.252	44.126

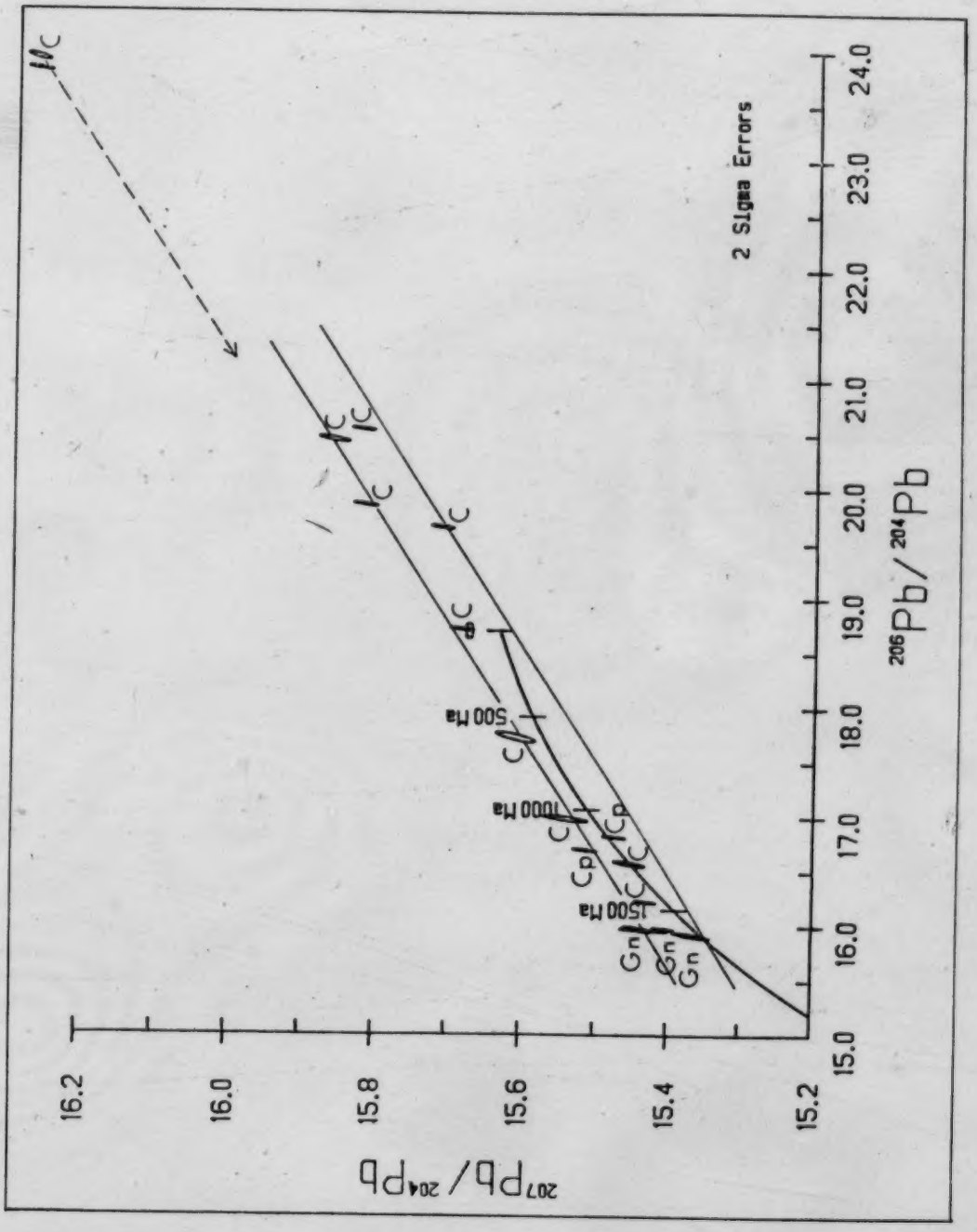

Figure 26. $^{207}Pb/^{204}Pb$ vs $^{206}Pb/^{204}Pb$ plot for hydrothermal minerals in the Great Bear Lake silver deposits. Gn - Galena. Cp - Chalcopyrite. C - Carbonates. Stacey and Kramers (1975) growth curve is shown. Data listed in Table 14.

occupied by three carbonates from Eldorado, and the least radiogenic galena from Northrim. The central part of the band consists of a carbonate sample from Norex and a chalcopyrite sample from Northrim. The two most radiogenic samples appear to be slightly outside the band.

Statistical treatment of upper and lower boundary data (Cumming, 1969; Cumming *et al.*, 1972) yields two essentially parallel lines whose slope suggests a mineralization age of approximately 1500 Ma. Due to the limited number of samples available, this age is somewhat speculative, and should only be considered as a preliminary one. μ values ($^{238}U/^{204}Pb$) of this band-like distribution vary between 9.8 and 10.2 (and possibly greater if the two radiogenic points follow the same pattern as the rest of the samples in the band).

The galena data are an indication of the isotopic composition of the mineralizing fluids during the emplacement, while the carbonate and chalcopyrite leads are a reflection of the radiogenic lead addition, resulting from the decay of uranium present in the mineral since its formation. The steeply trending distribution of the galena points precludes the possibility of a closed system three stage evolution model of lead in the mineralizing fluids. Rather, it implies that the mineralizing fluids had nonuniform isotopic ratios, thereby suggesting that the lead was most likely derived from different sources and incompletely homogenised, or that its isotopic ratios were selectively modified through mixing of fluids and/or by interactions with wall-rocks during upward migration.

Based upon the limited number of data from each deposit presented herein, it appears that the fluids which formed the Eldorado deposit derived their lead from a predominantly lower μ source, while fluids which formed the Silver Bear, and possibly the Smallwood deposits, derived their lead from a generally higher μ source. Data from the Northrim deposit exhibit the largest variation in isotopic ratios (covering the width of the band), possibly suggesting extensive interactions of the fluids.

The combined lead isotope data of Thorpe (1974) and Jory (1964), yield model ages of 1626 and 1767 Ma, using revised decay constants (Miller, 1982b), for vein galenas from

different deposits of the region, and the conformable sulfide zone at the Terra mine in the Camsell River sector respectively. The sulfide zone was probably an exhalite associated with volcanic activity in the region, and hence, this age would represent an older period of mineralization. Thorpe (1974) rejects the model lead age of 1626 Ma for the galenas, on the basis that galenas predates pitchblende mineralization in the veins, which was dated at 1445 ± 20 Ma by the U-Pb method (Jory, 1964). Miller's (1982b) analyses of pitchblende from the SHORE occurrence, on Achook island, about 25 km north of Port Radium, combined with the data of Jory (1964) from the Port Radium deposit (also known as Eldorado), gave a mineralization age between 1500 ± 10 and 1429 ± 29 Ma. According to Miller (1982b), the 1626 Ma age is the result of a mixing of older 1767 Ma lead with 1392±48 Ma lead from a diabase sheet which is exposed adjacent to the Echo Bay deposit. The mineralization age of around 1500 Ma suggested in this study is in agreement with the age of pitchblende mineralization (Jory, 1964; Miller, 1982b). Hence, a model age of 1626 Ma (Thorpe, 1974) is not in agreement.

A lack of whole-rock lead data from the region at present precludes any definite conclusions concerning the source(s) of lead in the silver-bearing veins. However, the distribution of data points suggests that lead was derived from several sources having variable isotopic compositions.

7.3 Strontium Isotope Study

In recent years, in addition to radiometric dating, strontium isotopes have been applied as tracers in mineral deposits. Although several papers have come out in the last few years, the use of strontium isotope geochemistry in delineating the genesis of an ore deposit is still in its infancy. The first published source of strontium isotopic compositions of gangue minerals from hydrothermal veins was that of Reesman (1968). Since then, strontium isotopes in delineating the source of Sr in mineral deposits have been successfully applied by many workers, namely, Brookins *et al.* (1977); Barbieri *et al.* (1982, 1984); Norman (1978); Kesler and Jones (1981);

Kessen *et al.* (1981); Ruiz *et al.* (1981,1985); Kesler *et al.* (1983); Norman and Landis (1983); Lange *et al.* (1983); Farrell and Holland (1983); Medford *et al.* (1983); Hofmann and Baumann (1984) and Metz *et al.* (1985). In geothermal systems, strontium isotopic investigations have been carried out by Stettler (1977) and Stettler and Allegre (1978). They investigated the effects on strontium isotope systematics by mineral dissolution and isotopic exchange processes. They concluded that $^{87}Sr/^{86}Sr$ can be used as a tracer for hydrothermal fluids. Norman (1978) and Norman and Landis (1983) analyzed waters extracted from fluid inclusions for $^{87}Sr/^{86}Sr$.

7.4 Rubidium-Strontium Isotope Study in the Great Bear Lake Region

Few Rb-Sr analytical data are available from the Great Bear Lake region. Robinson (1971) and Robinson and Morton (1972) analyzed the tuffs and lavas of the Echo Bay Group which gave an isochron age of 1770 ± 30 Ma, with an initial $^{87}Sr/^{86}Sr$ of 0.702 ± 0.003. Rb-Sr analyses of the diabase sill adjacent to the Echo Bay deposit, by Thorpe (1978) gave an isochron age of 1345 ± 48 Ma with an initial $^{87}Sr/^{86}Sr$ ratio of 0.7084 ± 0.0010. He attributed the high initial ratio to contamination of the source magma during emplacement. Hildebrand (1982) analyzed samples from the Rainy Lake Intrusive Complex, adjacent to the Terra deposit. According to him, the upper part of the Complex was not closed to Rb and/or Sr, and hence the rocks cannot be dated by this method.

7.4.1 Results and Interpretations of Strontium Data

The analytical results are presented in Table 15 and plotted in Figure 27. The high $^{87}Sr/^{86}Sr$ ratios in the samples cannot be explained by the decay of ^{87}Rb because the concentrations of rubidium were found to very small to account for the high ratios. The $^{87}Sr/^{86}Sr$ ratios, therefore, actually represents the ratios at the time of crystallization of the minerals.

The source of strontium in the carbonates of the veins cannot be explained by leaching of strontium and the associated metals from the volcanics by circulating sea-water as proposed

Table 15

Rubidium and Strontium Isotope Data for Hydrothermal Minerals in the Great Bear Lake Silver Deposits, N.W.T.. Plotted in Figure 27.

Sample nos.	Mineral	Rb (ppm)	Sr (ppm)	$^{87}Rb/^{86}Sr$	$^{87}Sr/^{86}Sr$
Terra mine					
713(B)/SB	Calcite	0.5785	75.34	0.0222	0.71965
1/7V/3L/SB	Calcite	0.5645	36.78	0.0444	0.71369
711/SB	Dolomite	0.4320	44.51	0.0281	0.71435
513/82(B)/SB	Calcite	0.4232	39.59	0.0309	0.71418
Eldorado mine					
5/5V/250/ED	Dolomite	0.1297	24.84	0.0151	0.71175
4/5V/800/ED	Dolomite	0.1305	28.62	0.0131	0.70925
Contact Lake					
CL/9	Dolomite	0.0524	48.71	0.0031	0.70983
Smallwood mine					
9/4V/2L/SW	Dolomite	0.2706	46.50	0.0168	0.71339
Northrim mine					
NR/1	Dolomite	0.1269	28.39	0.0135	0.71083
Norex mine					
2/3V/3L/NX	Dolomite	0.1839	52.30	0.0101	0.71522

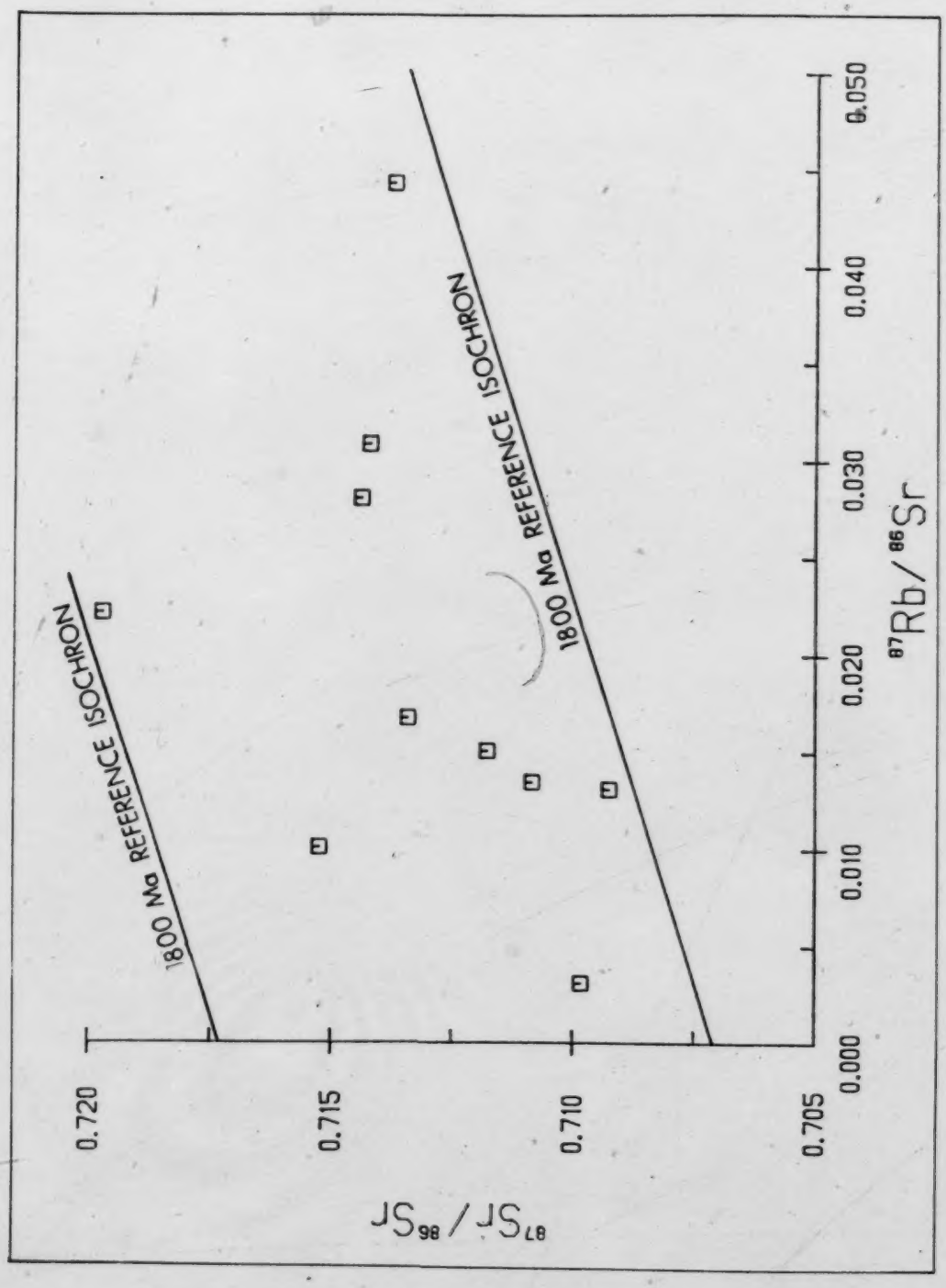

Figure 27. $^{87}Sr/^{86}Sr$ vs $^{87}Rb/^{86}Sr$ plot for hydrothermal carbonates in the Great Bear Lake silver deposits. Data listed in Table 15.

by Robinson (1971) and Robinson and Ohmoto (1973), or by direct derivation from a magmatic source as proposed by Badham (1973, 1975). In order to postulate a leaching model by sea-water, the strontium isotopic composition of the volcanics and sea-water at that time must be known. The volcanics in the Echo Bay sector have an initial $^{87}Sr/^{86}Sr$ ratio of 0.702 ± 0.003 (Robinson, 1971; Robinson and Morton, 1972). Very little is known about the actual strontium isotopic composition of Precambrian sea-water. Most of the data of Precambrian sea-water have been furnished by Veizer and co-workers and were derived from sedimentary carbonates. According to Veizer and Compston (1976), the Archean sea-water probably had $^{87}Sr/^{86}Sr$ values compatible with contemporaneous upper mantle, followed by a strong increase in the radiogenic component during the 2.5 - 2.1 Ga period, and a less pronounced increase during the remaining portion of the Proterozoic and a decrease during the Phanerozoic. According to their data, the $^{87}Sr/^{86}Sr$ value of sea-water between 2.0 - 1.5 Ga was between 0.705 and 0.706. Meinzes and Seyfried (1979) have experimentaly demonstrated that $^{87}Sr/^{86}Sr$ ratio of sea-water is lowered when reacted with basalts depending upon the water to rock ratio and temperature. If we assume an average $^{87}Sr/^{86}Sr$ value of 0.709 of the volcanics of the Echo Bay region around 1500 Ma (the time of mineralization), then the strontium isotopic composition of the evolved fluid should have been between 0.706 and 0.709 depending upon the water to rock ratio. These values, however, are not reflected in the suite of samples investigated. Alternatively, the high values of the carbonates, may be explained by selective leaching of radiogenic Sr from the volcanics. However, mixtures of two components having different $^{87}Sr/^{86}Sr$ ratos and strontium concentrations form hyperbolas in coordinates of $^{87}Sr/^{86}Sr$ and the strontium concentrations (Faure, 1977). Such a relationship was not observed in the samples from the Great Bear Lake veins. It is very unlikely that strontium was derived solely from the 1800 Ma magma (Robinson and Morton, 1972). It is therefore postulated that strontium in the carbonates of the Great Bear Lake silver-bearing veins might have been derived from quite different sources, which had different isotopic compositions. Such a hypothesis is supported by the results of the lead isotope analyses in the same suite.

8. TRANSPORT AND DEPOSITION OF METALS

8.1 Introduction

Ore deposits occur in a wide variety of environments. An understanding of the physico-chemical conditions of ore formation is one of the important aspects of ore genesis. The knowledge of understanding the nature of ore forming fluids has been enhanced in recent years by the analyses of fluid inclusions in ore and gangue minerals, from investigations of modern geothermal systems, and by interpretation of the mineral assemblages. To form an ore deposit under hydrothermal conditions, the metals must be transported from a single source or different sources and deposited in a suitable site under favourable conditions. One of the major problems of understanding the formation of ore deposits is how were the metals transported? The solubilities of common ore minerals, as simple ions, are inadequate for the transportation of metals (Barnes, 1979). Colloidal transport was also put forward in some cases from the textural evidences of the ore minerals. However, the behaviour of colloids at high temperature is little known, and the stability of colloids in concentrated electrolyte solutions is questionable (Krauskopf, 1979). According to Krauskopf (1979), colloidal transport may be important in some cases, but it cannot be generalised.

The ineffectiveness of simple ions and colloids led to the conclusion that metals in hydrothermal systems are transported as complex ions. The ligands which were found to be important for ore transport include Cl^-, sulfur species, OH^-, NH_3, F^-, CO^{2-}, etc.. Barnes (1979) has summarised the importance of some of these complexing agents. Chloride, sulphide, and hydroxide complexes are the most important agents under hydrothermal conditions. Ammine and fluoride complexes may be important at temperatures of around 250°C, and at low temperatures, CO_3^{2-}, CN^- and organic ligands may be important. Thus the transportation of ore metals not only depends upon the concentration of the metals in the solution but also upon the presence of the ligands in sufficient quantities to associate with the metals. According to Barnes (1979), the availability of a ligand to form a metal carrying aqueous complex depends upon the following:

(i) the total concentration of the ligand,

(ii) temperature,

(iii) the ionic strength of the solution,

(iv) the extent of ion pairing of the ligand with other species in the solution,

(v) acidity (pH) of the solution, and

(vi) the oxidation state of the solution.

The above factors vary from deposit to deposit.

Deposition of ore and gangue minerals from solutions may occur by a variety of mechanisms. These mechanisms may be changes in temperature (cooling), in pressure, in pH through interactions with the wall rocks, mixing of fluids, decrease in the activities of the complex forming ligands, etc. (Barnes, 1979; Vaughan and Craig, 1978). The various mechanisms of deposition of ore and non-ore minerals have been discussed by Barnes (1979) and by Holland and Malinin (1979).

8.2 Environment of Ore Deposition in the Great Bear Lake Silver Deposits

The physico-chemical conditions of formation of an ore deposit may be theoretically estimated if the temperature, pressure and other thermodynamic data of the mineral assemblage under investigation, are available. The temperature and pressure of deposition can be obtained from fluid inclusions in associated gangue or transparent ore minerals (e.g. sphalerite), from stable isotopes or from mineral stability studies. Once the temperature and pressure have been determined, the other parameters such as fO_2, fS_2, pH, etc. may be determined from the available thermodynamic data. The applications of thermodynamics in the study of ore deposits can be found in Holland (1959, 1965); Helgeson (1964, 1969); Froese (1981); Greenwood (1977), and Henley *et al.* (1984).

Although a large number of minerals have been identified in the veins of the Great Bear Lake silver deposits, paucity of thermodynamic data for many of the minerals precludes the estimation of physico-chemical conditions of deposition for all the stages of mineralization. However, an attempt was made to determine the range in these conditions from the available

data.

Uraninite in stage I mineralization, occurs in association with hematite, pyrite and quartz. Although considerable research has been done on the low temperature aspect of uranium transport and deposition (Garrels, 1955; Garrels and Christ, 1959; Hostetler and Garrels, 1959; Langmuir, 1978a, 1978b; and others), there are very few data available on the solubility of uranium at high temperature. Most of the experimental work in this aspect has been done by Russian investigators. Recently the research group at the Centre de Recherches Petrographiques et Geochimiques, Nancy, France, have started working on the behaviour of uranium under hydrothermal conditions. Rich *et al.* (1977) have summarized the investigation carried out by Lemoine (1975) in this respect.

In the present investigation the conditions of formation of uraninite have been estimated from the high temperature thermodynamic data of uranium species compiled by Roxlo (1980) using the methods and data of Helgeson (1969), Criss and Coble (1964a, 1964b) and Robie *et al.* (1978). The methods used for the construction of these diagrams are given in Barnes and Kullerud (1961), Garrels and Christ (1965), Vaughan and Craig (1978) and Barton and Skinner (1979). The reactions used in the construction of these diagrams are given in Table 16. The stability fields of uraninite, hematite, and pyrite with respect to fO_2 and fS_2 are plotted in Figure 28 at 200°C. The absence of magnetite in the mineral assemblage defines the lower limit of the fO_2. It also indicates that the fO_2 and fS_2 of the hydrothermal fluids during stage I mineralization were above the pyrite, magnetite and hematite triple-point. The upper limit of fO_2 is defined by the upper stability of uraninite. The upper limit of fS_2 cannot be determined from the assemblage. It probably did not exceed 10^{-4} bars. The fCO_2 is assumed to be between 10^{-2} and 10^{2} bars which is the normal range for hydrothermal ore deposits (Holland, 1965).

The different uranium species are plotted in Figures 29 and 30 at 150° and 200°C. The reactions used in the construction of the diagram are given in Table 16. Also plotted are the stability fields of uraninite, pyrite, pyrrhotite, hematite, magnetite and the important sulfur species. A lack of any pH buffered assemblage in this stage precludes the calculation of pH at

Table 16

Reactions used in the construction of phase diagrams (Figures 28, 29 and 30).

Reactions	Log K 150°C	Log K 200°C
1. $UO_2CO_3^0 + CO_2(g) + H_2O = UO_2(CO_3)_2^{2-} + 2H^+$	-12.30	-13.10
2. $UO_2(CO_3)_2^{2-} + H_2O + CO_2(g) = UO_2(CO_3)_3^{4-} + 2H^+$	-18.44	-20.15
3. $UO_2 + CO_2(g) + 0.5O_2(g) = UO_2CO_3^0$	10.97	7.75
4. $UO_2^{2+} + CO_2(g) + H_2O = UO_2CO_3^0 + 2H^+$	-9.79	-9.87
5. $UO_2 + 0.5O_2(g) + 2CO_2(g) + H_2O = UO_2(CO_3)_2^{2-} + 2H^+$	-1.33	-5.35
6. $UO_2 + 3CO_2(g) + 2H_2O + 0.5O_2(g) = UO_2(CO_3)_3^{4-} + 4H^+$	-19.77	-25.50
7. $UO_2 + 0.5O_2(g) + 2H^+ = UO_2^{2+} + H_2O$	18.30	15.43
8. $UO_2^{2+} + H_2O = UO_2OH^+ + H^+$	-4.45	-3.87
9. $UO_2 + 0.5O_2(g) + H^+ = UO_2OH^+$	13.85	11.56
10. $UO_2OH^+ + CO_2(g) = UO_2CO_3^0 + H^+$	-2.88	-3.81
11. $UO_2 + SO_4^{2-} + 2H^+ + 0.5O_2(g) = UO_2SO_4^0 + H_2O$	24.82	22.90
12. $UO_2 + 2HPO_4^{2-} + 2H^+ + 0.5O_2(g) = UO_2(HPO_4)_2^{2-} + H_2O$	37.54	34.81
13. $3Fe_2O_3 = 2Fe_3O_4 + 0.5O_2(g)$	-22.07	-18.95
14. $FeS_2 + 1.5O_2(g) = Fe_2O_3 + 2S_2(g)$	34.66	31.72
15. $3FeS_2 + 2O_2(g) = Fe_3O_4 + 3S_2(g)$	40.95	38.11
16. $FeS_2 = FeS + 0.5S_2(g)$	-10.25	-8.48
17. $3FeS + 2O_2(g) = Fe_3O_4 + 1.5S_2(g)$	71.57	63.30

18. $H_2S(aq) = H^+ + HS^-$	-6.72	-6.96
19. $HS^- = H^+ + S^{2-}$	-10.62	-9.57
20. $H_2S(aq) + 2O_2(g) = HSO_4^- + H^+$	83.05	71.62
21. $HSO_4^- = H^+ + SO_4^{2-}$	-3.74	-4.49
22. $H_2S(aq) + 2O_2(g) = 2H^+ + SO_4^{2-}$	79.31	67.13
23. $S^{2-} + 2O_2(g) = SO_4^{2-}$	96.68	83.74
24. $HS^- + 2O_2(g) = H^+ + SO_4^{2-}$	86.03	74.09
25. $2FeS + 2H_2S + O_2(g) = 2FeS_2 + 2H_2O$	60.12	46.60
26. $2H^+ + 2HS^- + 2FeS + O_2(g) = 2FeS_2 + 2H_2O$	67.79	65.23
27. $Fe_3O_4 + 6H^+ + 6HS^- + O_2(g) = 3FeS_2 + 6H_2O$	125.77	107.85
28. $3FeS_2 + 11O_2(g) + 6H_2O = Fe_3O_4 + 12H^+ + 6SO_4^{2-}$	387.94	330.19
29. $2FeS_2 + 7.5O_2(g) + 4H_2O = Fe_2O_3 + 8H^+ + 4SO_4^{2-}$	266.17	226.35
30. $3FeS + 3H_2O + 0.5O_2(g) = Fe_3O_4 + 3H^+ + 3HS^-$	-12.05	-10.23
31. $3FeS + 3H_2O + 0.5O_2(g) = Fe_3O_4 + 6H^+ + 3S^{2-}$	-45.07	-47.60

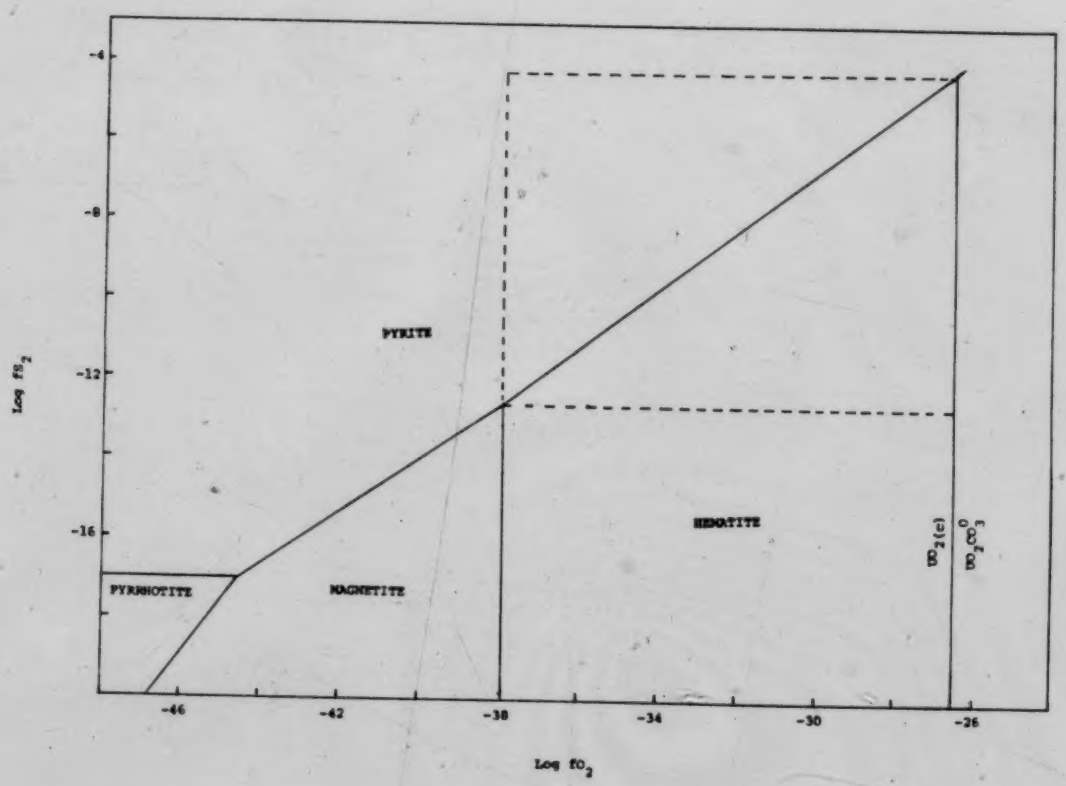

Figure 28. An fO_2 - fS_2 diagram for the system Fe-S-O at 200°C. Possible range of fO_2 - fS_2 for solutions depositing uranium is shown by the dashed lines.

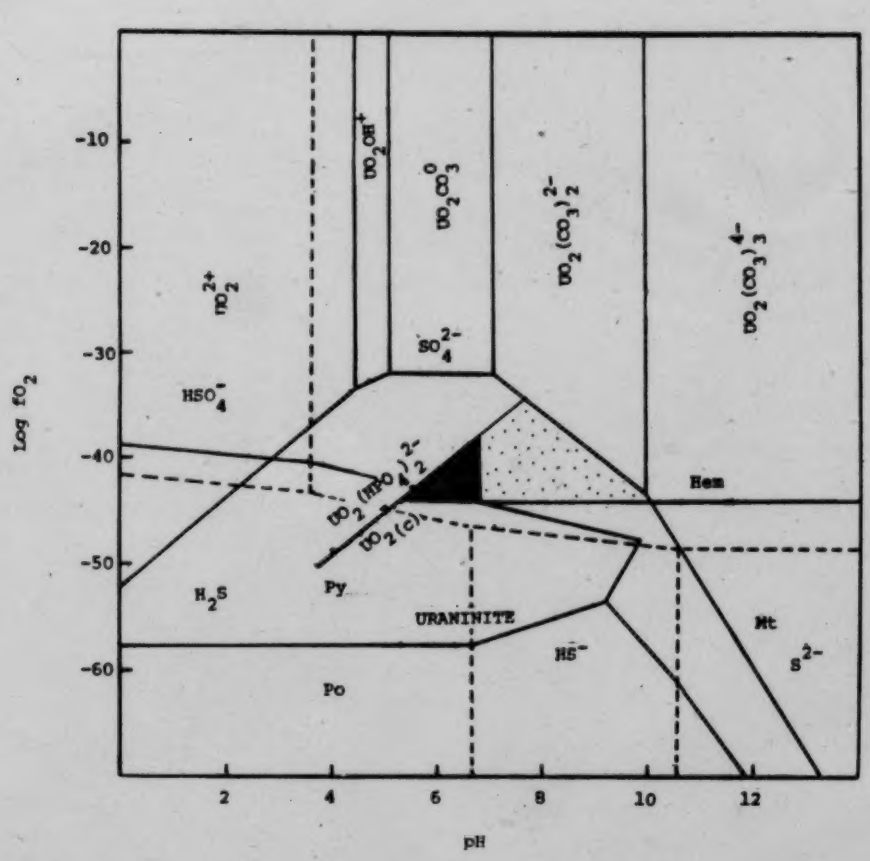

Figure 29. An fO_2 - pH diagram for the system UO_2 - CO_2 - H_2O at 150°C. Also plotted are the stability fields of different sulfur species, pyrite (Py), magnetite (Mt), pyrrhotite (Po), uraninite and hematite (Hem). Possible solution composition for deposition of uranium is shown by the black triangle. U = 10^{-7}m, $\Sigma P = 10^{-4}$m. $\Sigma S = 10^{-2}$m.

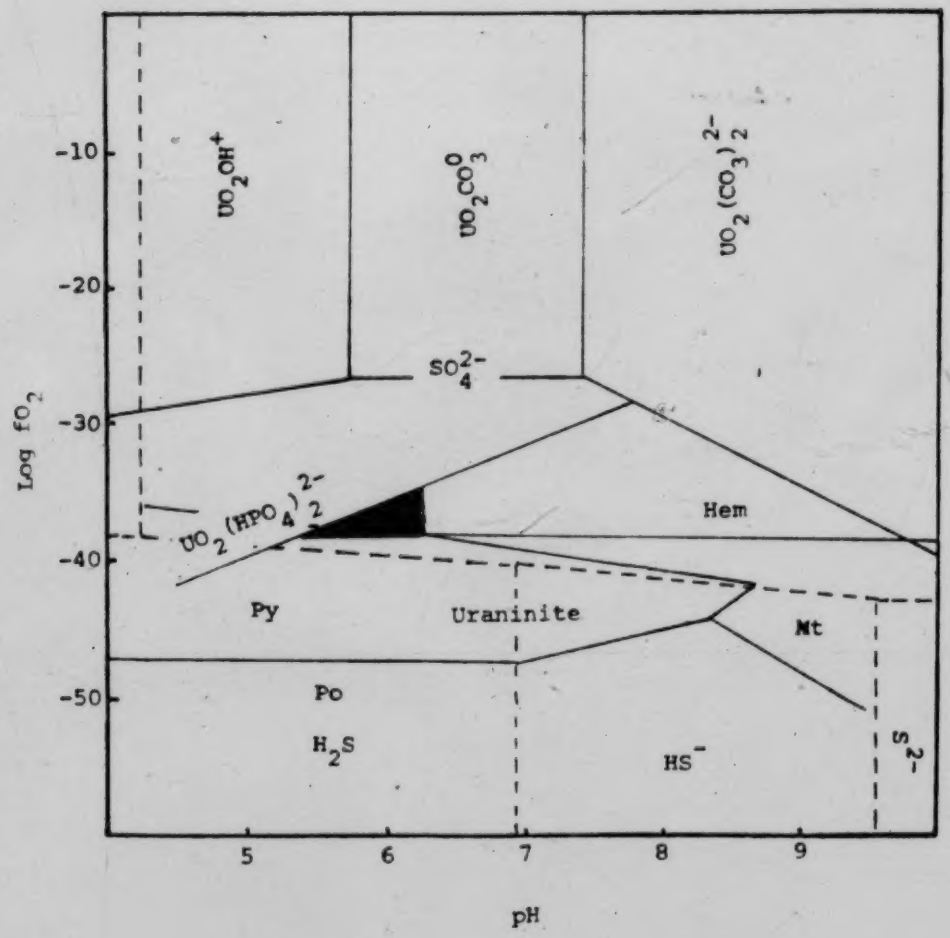

Figure 30. An fO_2 - pH diagram for the system UO_2 - CO_2 - H_2O at 200°C. Also plotted are the stability fields of different sulfur species, pyrite (Py), magnetite (Mt), pyrrhotite (Po), uraninite and hematite (Hem). Possible solution composition for deposition of uranium is shown by the black triangle. U = 10^{-7}m, $\Sigma P = 10^{-6}$m. $\Sigma S = 10^{-2}$m.

the time of mineralization. The stippled area in the diagram covers a wide range in the pH. However, the coexistence of hematite and pyrite, along with uraninite, narrows down the pH range. The dark triangle in the diagram represents the possible range of pH and fO_2 during the deposition of stage I mineralization.

It is a well established fact that uranium is transported in the uranyl state (U^{6+}) and deposited in the uranous state (U^{4+}). Low temperature studies have revealed that uranium is transported as carbonate, fluoride, hydroxyl, phosphate or sulphate complexes under different conditions of Eh and pH. The importance of each of these complexes in transporting uranium at 25°C have been discussed by Langmuir (1978a, 1978b). Naumov (1961) discussed the physico-chemical characteristics of the behaviour of uranium in hydrothermal solutions. According to him, carbonate and fluoride complexes are the important transporting agents of uranium under hydrothermal conditions. Naumov and Miranova (1969) are also of the opinion that uranyl carbonate complexes are important at the temperature range of 100° to 200°C.

Fluid inclusion studies have shown that the hydrothermal fluids at Great Bear Lake were moderate to high in salinity. This makes the chloride ion a possible complexing agent for transporting uranium. However, according to Naumov (1961), the formation of complexes of tetravalent and hexavalent uranium with chlorine is negligible. Sulphate and fluoride uranium complexes may be important, but they become less stable toward higher temperatures (Rich *et al.*, 1977). Moreover, these complexes affect uraninite stability only at low pH (Shrier and Parry, 1982). Hence it is very likely that uranium in the Great Bear Lake silver deposits was transported as uranyl carbonate or uranyl hydroxyl complexes or as both, depending upon the concentration of these ligands. At near neutral to slightly alkaline conditions (the possible conditions for the stage I mineralization), the predominant uranyl carbonate complexes are $UO_2CO_3^0$ and $UO_2(CO_3)_3^{2-}$. $UO_2(OH)_2^0$ is the predominant hydroxyl complex under neutral conditions.

The reduction of U^{6+} to U^{4+} is considered to be the dominant mechanism for precipitating uraninite. Loss of CO_2, due to boiling, has also been put forward as a possible

mechanism by Poty *et al.* (1974). Temperature and pH are not considered very important in the precipitation of uraninite, in comparison to redox reactions. The main reductants are graphite, organic matter, reduced sulfur in sulphides, and ferrous iron in silicates, sulphides or oxides.

The reduction of U^{6+} to U^{4+} and a decrease in temperature were probably the important factors for precipitating the stage I minerals. The deposition of uraninite could have taken place in the following ways depending upon the predominance of the individual complexes :

(i) $UO_2CO_3^0 + H_2O + 2Fe_3O_4 = UO_2 + 3Fe_2O_3 + H_2CO_3$

(ii) $UO_2CO_3^0 + Fe^{2+} + 2HS^- = UO_2 + FeS_2 + H_2CO_3$

(iii) $UO_2(CO_3)_2^{2-} + Fe^{2+} + 2H_2S = UO_2 + FeS_2 + 2H_2CO_3$

(iv) $UO_2(CO_3)_2^{2-} + 2Fe_3O_4 + H_2O = UO_2 + 3Fe_2O_3 + 2HCO_3^-$

(v) $UO_2(OH)_2^0 + 2Fe^{2+} + 2HS^- = UO_2 + FeS_2 + 2H_2O$

(vi) $UO_2(OH)_2^0 + 2Fe_3O_4 = UO_2 + 3Fe_2O_3 + H_2O$

(vii) $UO_2(CO_3)_2^{2-} + H_2O = UO_2 + 0.5O_2 + 2HCO_3^-$

Stage II mineralization in the Great Bear Lake veins comprises of the arsenides, native silver, carbonates, quartz and occasionally fluorite and native bismuth. At present there are no solubility data on the arsenides. This precludes the determination of the physico-chemical conditions of deposition of the mineral assemblage in which the arsenides are associated. Textural studies have shown that native silver in this stage precipitated both before and after the arsenides were deposited. The absence of acanthite (argentite) or bismuthinite or any other sulfur rich phase, indicates that the sulfur fugacity was quite low (less than 10^{-12} bars). The oxygen fugacity was also probably low.

Silver in hydrothermal solutions may be transported as chloride, sulphide or ammine complexes. The $Ag(HS)_2^-$ complex may be important in near neutral hydrothermal solutions (Melent'yev *et al.*, 1970). The amminosilver species, $Ag(NH_3)_2^+$ and $Ag(NH_3)_2Cl^0$, as well as the species $AgHCO_3^0$ may be important in the transport and deposition of silver but there are no data available at elevated temperatures (Seward, 1976). The importance of chloride complexes of silver in the transport and deposition of silver has been demonstrated by Seward

(1976). Helgeson's (1969) suggestion of $AgCl_4^{3-}$ being the important complex in concentrated solutions at elevated temperatures has been contradicted by Seward (1976). According to him at temperatures greater than 275°C, transport of silver as chloride complexes in ore-forming hydrothermal fluids (containing ubiquitous chloride ligands) would involve only $AgCl^0$ and $AgCl_2^-$ with $AgCl_2^-$ predominating in concentrated brines.

The high salinity of the hydrothermal fluids at the Great Bear Lake deposits suggests the predominance of chloride ligands. The absence of any sulfur-rich phases suggests that the total sulfur content of the hydrothermal fluids were quite low to account for the transport of silver by sulfur ligands. Silver in the hydrothermal fluids was probably transported as chloride complexes and thus the formation of silver chloride complexes can be summarized as follows :

(i) $2Ag(c) + 2H^+ + 2Cl^- + 0.5O_2 = 2AgCl^0 + H_2O$

(ii) $2Ag(c) + 2H^+ + 4Cl^- + 0.5O_2 = 2AgCl_2^- + H_2O$

It is obvious from the above reactions that pH, concentration of chloride, fO_2 and temperature are factors which control the solubility of silver. Changes in these factors can lead to the deposition of silver from the hydrothermal fluids. Fluid inclusions in minerals belonging to stages II and III have indicated that the fluids were occasionally boiling or were close to boiling. Boiling has been found to have a profound effect upon mineral precipitation from hydrothermal fluids (Nash, 1973; Drummond and Ohmoto, 1985). It is an effective mechanism for increasing the pH of the hydrothermal fluids, and this could result in the precipitation of the metals. The sequence of mineral deposition (in the order of most to least) due to increase in pH as the result of boiling of hydrothermal fluids, is given by Drummond and Ohmoto (1985) as follows : oxides (e.g., Fe_3O_4, SnO_2), simple metal sulphides (ZnS, AgS), native metals (chlorides complexed, e.g., Ag^0, Au^0), carbonates (e.g., $CaCO_3$), sulphides with intermediate sulfur valence (e.g., $CuFeS_2$, FeS_2), sulphides of the Me_2S class (e.g., Ag_2S, Cu_2S), native metals (bisulphide complexed, e.g., Au^0), and sulfates (e.g., $CaSO_4$, $BaSO_4$). Thus it is likely that boiling played an important role in the precipitation of native silver, native bismuth, quartz, fluorite and the carbonates in the Great Bear Lake veins.

Stages IV and V mineralization are represented by sulfur-rich phases, which include the Cu-, Fe-, Zn-, Ag-, Pb- and Bi- sulphides and sulphosalts. This clearly indicates an increase in the sulfur content of the hydrothermal fluids during the later stages of the depositional history of the veins. The sulfur fugacity was high enough to prevent the deposition of native bismuth and native silver, and instead acanthite (argentite) and bismuthinite and other Ag-Bi sulphosalts were deposited. It was mentioned earlier that fluid mixing was one of the factors in the later stages of mineralization to account for the wide variations in the salinity of the hydrothermal fluids. This factor was probably also one of the major factors responsible for the precipitation of the metals.

In summary, the metals in the Great Bear Lake silver deposits were transported by moderate to high salinity hydrothermal fluids as complexes. Uranium was either transported as carbonate or hydroxyl complexes, whilst the other metals were probably transported mainly as chloride complexes. The effect of other complexes was probably minimal. The metals were deposited in dilatant zones due to decrease in temperature, pressure, boiling or mixing of two different types of fluids.

9. GENESIS OF THE DEPOSITS

9.1 Introduction

Vein-type deposits occur in a wide variety of environments. They have been found to occur within unmetamorphosed to highly metamorphosed terranes. There are many theories pertaining to the origin of the vein-type deposits. The controversies involving the nature of the ore-bearing fluids and the origin of these deposits have been resolved by stable isotopic and fluid inclusion studies. The ore-bearing fluids have been found to be either meteoric, metamorphic, magmatic, connate, or mixture of two or more types of fluids. Important examples of vein type deposits in which different types of ore bearing fluids were involved include :

(i) meteoric - the Au-Ag deposits of southwestern United States (Taylor, 1973; O'Neil *et al.*, 1973; Casadevall and Ohmoto, 1977),

(ii) magmatic - Casapalca Ag-Zn-Cu deposit, Peru (Rye and Sawkins, 1974),

(iii) metamorphic - Glenorchy Au-W-Sb deposit, New Zealand (Paterson, 1982), Au deposits in the Abitibi Greenstone Belt (Kerrich, 1983),

(iv) connate - Ag-Co-Ni arsenide veins in the Cobalt-Gowganda area (Strong and Scott, 1984), and

(v) two or more types of fluids - Pasto Bueno tin-tungsten deposit, Peru (Landis and Rye, 1974; Norman and Landis, 1983), Renison Bell cassiterite sulphide deposit (Patterson *et al.*, 1981) and Finlandia Pb-Zn-Ag-Au deposit, Colqui District, Peru (Kamilli and Ohmoto, 1977).

The metals in these deposits were either derived from magmatic sources or were leached from the country rocks during metamorphism or by convective hydrothermal fluids.

9.2 The Ag - Co - Ni - As ± Bi ± U Association

The Ag - Co - Ni - As ± Bi ± U deposits have been found to occur in complex environments in different parts of the world. Kongsberg (Norway), Jachymov (Czechoslovakia), Erzgebirge (Germany) and the deposits of the Cobalt-Gowganda region,

Ontario, are some of the important deposits belonging to this category. The origin of these deposits still remains an enigma because of their occurrence in a wide variety of geological settings. The metals in the Kongsberg veins which cross-cut 'fahlbands', are believed to be derived by leaching from the 'fahlbands'. Pavlu (1972) ascribed the origin of the Jachymov deposits to the late Variscan granitoids. Ypma (1972) considered the Chalanches deposits, France, to be similar to Kongsberg and Cobalt (Ontario).

There have been differences in views on the origin of the Cobalt-Gowganda deposits. According to Jambor (1971), the Nipissing diabase was the source for the metals. Scott (1972) also attributed the origin of the Siscoe deposit, Gowganda, to the cooling of the Nipissing diabase. Halls and Stumpfl (1969) and Boyle and Dass (1971), on the other hand, proposed a leaching model. Boyle and Dass (1971) suggested that the ore and gangue elements were derived by diffusion from the Keewatin interflow sedimentary beds, with minor contributions from certain volcanic flows. Recent stable isotopic, fluid inclusion and geochemical studies by Andrews *et al.* (1984) and fluid inclusion studies by Strong and Scott (1984) suggest that formation waters of the Huronian sediments were responsible for the mineralization. The Nipissing diabase served as the heat source for mobilization and circulation of fluids.

The Great Bear Lake deposits are similar to the above mentioned deposits in many respects. As was mentioned earlier the origin of these deposits has also been a subject of controversy. In this chapter, a brief review of the earlier views on the origin is given, and the possible origin of the deposits is discussed in the light of the new data obtained in this study, combined with the field and analytical data furnished by the earlier workers.

9.3 A Brief Review on the Geneses of the Great Bear Lake Silver Deposits

Prior to Robinson (1971), the origin of the deposits of the Echo Bay sector had been linked with the magmatic activity of the region. Robinson (1971), Badham *et al.* (1972), Robinson and Ohmoto (1973) and Robinson and Badham (1974), however, on the basis of their investigation postulated a 'lateral secretion' model, in which the metals were leached by

brines, which were believed to be evolved sea water. The leaching model of Robinson (1971) and Robinson and Ohmoto (1973) was based upon sulfur, oxygen, carbon isotopic and trace element studies. Their samples for sulfur and fluid inclusion studies were taken from the later stages of mineralization. Using a temperature of 200° ± 30°C (obtained from fluid inclusions in dolomite), they calculated the oxygen isotopic composition of stage 5 fluids from the $\delta^{18}0$ values of dolomites to be 1.0 ± 2.5 per mil. Clayton and Epstein (1958) analyzed three samples of quartz, hematite and calcite, collected by L.T. Jory from the Eldorado deposit. According to them the relative temperatures indicated by quartz-iron oxide fractionations were in the same order as the quartz-calcite temperatures. However, calcites in the Eldorado deposit, do not occur in association with quartz-hematite of stage 1 mineralization (Jory, 1964; Mursky, 1973; this study). Thus, it is not known how this conclusion was reached. Robinson and Ohmoto (1973) used the data of Clayton and Epstein (1958), and calculated the temperature of crystallization and oxygen isotopic composition of stage 1 fluids to be 135° ± 15°C and 1.9 to -0.6 per mil respectively. On the basis of the oxygen isotopic composition of stages 1 and 5 fluids, they concluded that the oxygen isotopic composition of the hydrothermal fluids was essentially constant throughout the depositional stages of Echo Bay and at Eldorado. They also calculated the temperatures of deposition for stages 3 and 4 fluids at 115° ± 30°C and 120° ± 20°C respectively. The sulphides of of stages 4 and 5 showed a $\delta^{34}S$ range of about 50.0 per mil (CDT). The carbonates showed a $\delta^{13}C$ range of -4.0 to -1.5 per mil (PDB). The $\delta^{34}S(\Sigma S)$ and $\delta^{13}C(\Sigma C)$ of the ore-forming fluids during stages 3 and 4 were calculated at approximately 25.0 per mil (CDT) and -5.0 per mil (PDB) respectively. Badham *et al.* (1972) concluded on the basis of their oxygen and carbon isotopic investigation, that the metalliferous components of the ore deposits originated within the Echo Bay volcanics and were probably transported by brines into the fracture zones during post-Hudsonian regional faulting. Robinson and Badham (1974) analyzed the carbonates and sulphides from some of the deposits of the Camsell River sector for $^{18}O/^{16}O$, $^{13}C/^{12}C$ and $^{34}S/^{32}S$ respectively. They reported wide variations in the $\delta^{18}O$ (7.0 to 22.0 per mil, SMOW) and $\delta^{13}C$ (-2.1 to -9.8 per mil, PDB) of the carbonates, and $\delta^{34}S$

of the sulphides around 1.0 per mil (CDT). The oxygen isotopic composition of the hydrothermal fluids was calculated using an average $\delta^{18}O$ value of 15.0 per mil of the carbonates from all the stages, and an average temperature of 200°C. A $\delta^{18}O$ value of 2.0 per mil (SMOW) was calculated for the ore bearing fluids. Although the $\delta^{34}S$ values of the sulphides suggested a magmatic sulfur source, they presented an equilibrium model, whereby the sulfur was derived from Precambrian sea water sulfate. Badham (1973, 1975) refuted his earlier views on the Echo Bay volcanics being the source of the metals and the sea water being the source of sulfur. He argued that the sulfur and the metals were magmatic, for the following reasons :

(i) The sulfur isotope values for vein and host rock sulphides were found to be closely similar. The host rock sulphides are clearly of magmatic origin.

(ii) The distinct Ag-arsenide ore-type occurs in such a variety of geological settings around the world that a general case magmatic origin is more reasonable than a series of special case origins (Halls and Stumpfl, 1969; Badham, 1975).

(iii) To test Robinson's hypothesis of 'lateral secretion', he combined his analyses of 38 samples of different rock types from the Camsell River sector with that of 284 samples of Mursky (1963) from the northern part (Hunter Bay) of the Echo Bay sector. The values of many metals and the Ni/Co ratios were found to be typical of calc-alkaline suites (Taylor, 1968). No differences in trace elements were found between the rocks of the Camsell River sector and the area sampled by Mursky (1963). The rocks around the Echo Bay deposit were found to be anomalous, and exhibited variable Ni/Co ratios. Anomalous enrichment of the ore elements in the host rocks up to 1400 m from the veins, led Badham to conclude that the ore elements migrated away from the veins and not vice versa.

Shegelski (1973) concluded on the basis of proximity and of the lateral zoning of the arsenide minerals away from the intrusive body, that the latter was responsible for the mineralization. Thorpe (1974) concluded on the basis of lead isotopes that the ordinary leads in the galena samples were probably related to the diabase sheet in the Echo Bay sector. He,

however, did not conclude about the anomalous leads in the veins. Although Miller (1982a, 1982b), did not investigate the deposits of the Echo Bay (except for few dump samples from the Eldorado mine) and Camsell River sectors, he suggested on the basis of his investigation of other uranium occurrences in the Great Bear batholith and investigations of previous workers, that U and Ag may have been derived from different plutons.

Morton and Changkakoti (1985) have looked into the possibilty of the relation between polymetallic element associations of the Great Bear Lake deposits and metalliferous sedimentary protoliths, incorporated during anatexis into S-type granitic rocks. Since this interesting hypothesis do not actually form part of this investigation, it will not be discussed any further in this chapter. However, detailed description of this new hypothesis is given in Appendix II.

9.4 Genesis of the Deposits

The following discussion is primarily a synthesis of results obtained in this study and results obtained by earlier workers. The complex nature of the deposits makes it difficult to propose a definite genetic model applicable to all the deposits of the region. Mineralogical, fluid inclusion and isotopic data obtained in this study clearly suggest the complexity of the hydrothermal fluids which formed the deposits.

The earlier controversies involving the nature of the hydrothermal fluids responsible for the different stages of mineralization have been resolved in this study by detailed fluid inclusion, oxygen, carbon and hydrogen isotopic investigations. In the earlier investigations, temperature data for all the stages were not available. The isotopic composition of the hydrothermal fluids were calculated on the basis of limited temperature data. Fluid inclusion analyses in this study have revealed a wide variation of homogenization temperatures between each stage of mineralization. Shegelski and Scott (1975) have also reported a wide range in the temperature of the hydrothermal fluids. Since temperature is an important factor which controls the isotopic fractionation between mineral and water, invalid assumptions may lead to

erroneous conclusions. The earlier workers reported a uniform isotopic composition of the hydrothermal fluids, and little change in the temperature, except for the last stage, which was reported to be below 100°C.

Significant variations have been found in the isotopic composition of the hydrothermal fluids between different stages of mineralization. The $\delta^{18}O$ and δD values for stages I, II and III waters have been found to be consistent with magmatic waters and were probably derived from an aqueous phase of a cooling pluton. Isotopically lighter fluids were introduced into the veins during the later stages of mineralization. Meteoric water circulation has been reported by Hildebrand (1982, 1983) and other workers. During the later stages of mineralization, the permeability of the rocks were probably increased by fracturing to facilitate influx of surficial waters.

Although the oxygen and hydrogen isotopes point towards a magmatic origin for the stages I, II and III mineralization, it is difficult to explain the exact source for the fluids and the metals. Kieller (1962) suggested that the Eldorado ore originated from unexposed rocks, perhaps closely related to the exposed mafic dykes. Shegelski (1973) and Hoffman *et al.* (1976) suggested that the ore metals were derived from either the Rainy Lake Intrusive Complex or the Balachey Lake Pluton (Fig. 3). Although Badham (1973, 1975, 1976) suggested a magmatic source for the metals, he did not mention which pluton was responsible for the mineralization.

The major problems confronting the genetic link between the mineralization and the plutons of the region are :

(i) the difference in age between the mineralization and the plutonic rocks;

(ii) the occurrence of a mixture of 'felsic' and 'basic' elements in the veins.

Recent geochronological studies have revealed the age of the plutonic and volcanic rocks to be between 1850 and 1875 Ma (Van Schmus and Bowring, 1980; Bowring and Van Schmus, 1982). The age of the mineralization, on the other hand, has been found to be between 1500 and 1400 Ma (Miller, 1982; this study). Hence it is very unlikely that a cooling pluton will be active for more than 200 million years.

The association of the 'felsic' and the 'basic' elements is another enigma. The association of uranium mineralization with basic rocks is very rare. Leblanc and Billaud (1982) reported the occurrence of uranospinite ($Ca(UO_2)(AsO_4).10H_2O$) along with Ni-, Co- arsenide minerals in ophiolites in the Bou Azzer deposit (Morocco). This may be an exceptional case because all previous uranium mineralization in igneous environments has been found to be associated with felsic intrusive bodies. Badham (1976) proposed a model for the Ag-Ni-Co-As-U association, in which the granitic hydrothermal fluids were trapped inside the consolidated outer margin of the batholith. The 'basic' elements were later introduced into the trapped hydrothermal reservoir. The 'mixed' ore association was then released during faulting of the batholith.

It is very tempting to accept the views put forward by Badham (1973, 1976), in the absence of any exposed intrusives having similar age relationships with the mineralization of the region. However, there is evidence of wide-scale igneous activity in the region during the time of mineralization, e.g., the swarms of diabase dykes and sills and the Great Quartz veins. The Giant Quartz veins which have been found to be mineralized sporadically, have not been linked to any of the exposed plutons. The areal distribution and the enormous volume of silica deposited in these veins led Furnival (1935) to suggest that the source must have been a magma corresponding to an acidic rock such as granite and a magma reservoir of large size. According to Mursky (1973) and Badham (1973), uranium mineralization in these deposits occurred as a late stage of the Giant Quartz vein emplacement. Pitchblende (which post-dates the quartz), from the Rayrock vein, about 200 km southeast of the Terra deposit, was dated at 511 ± 86 Ma by Miller (1982a). He suggested that the veins are likely to extend to great depth, and may have been formed after the batholith had been fractured during a continental collision.

Thus, it can be postulated from the geologic events (as deduced by field-relations and geochronological studies) that the region was magmatically active to account for the origin of the deposits. The fluid inclusion, isotope and geologic data fit a model whereby the silver-bearing veins originated from a series of hydrothermal systems which involved the

influence of two or more different types of hydrothermal fluids during the depositional history of the veins. Figure 31 illustrates a generalised model for the origin of these deposits.

It is likely that uranium and silver were derived from different sources at different times. Uranium was probably derived from a source similar to the one which formed the Giant Quartz veins. The deposition of uranium was followed by a period of quiescence (the exact time-gap between each stage of mineralization is not known). Renewed fault movements, accompanied by the reopening of the earlier formed vein-systems, resulted in the deposition of native silver and the associated arsenide minerals from fluids having a different magmatic source, probably a more basic magmatic body. During the later stages of mineralization the influence of meteoric water became more pronounced. The meteoric waters circulated to depth and mixed with ascending magmatic waters to form distinct hydrothermal fluids. The metals in these later stages were probably derived from the magmatic source and the country rocks, being leached by the circulating meteoric waters.

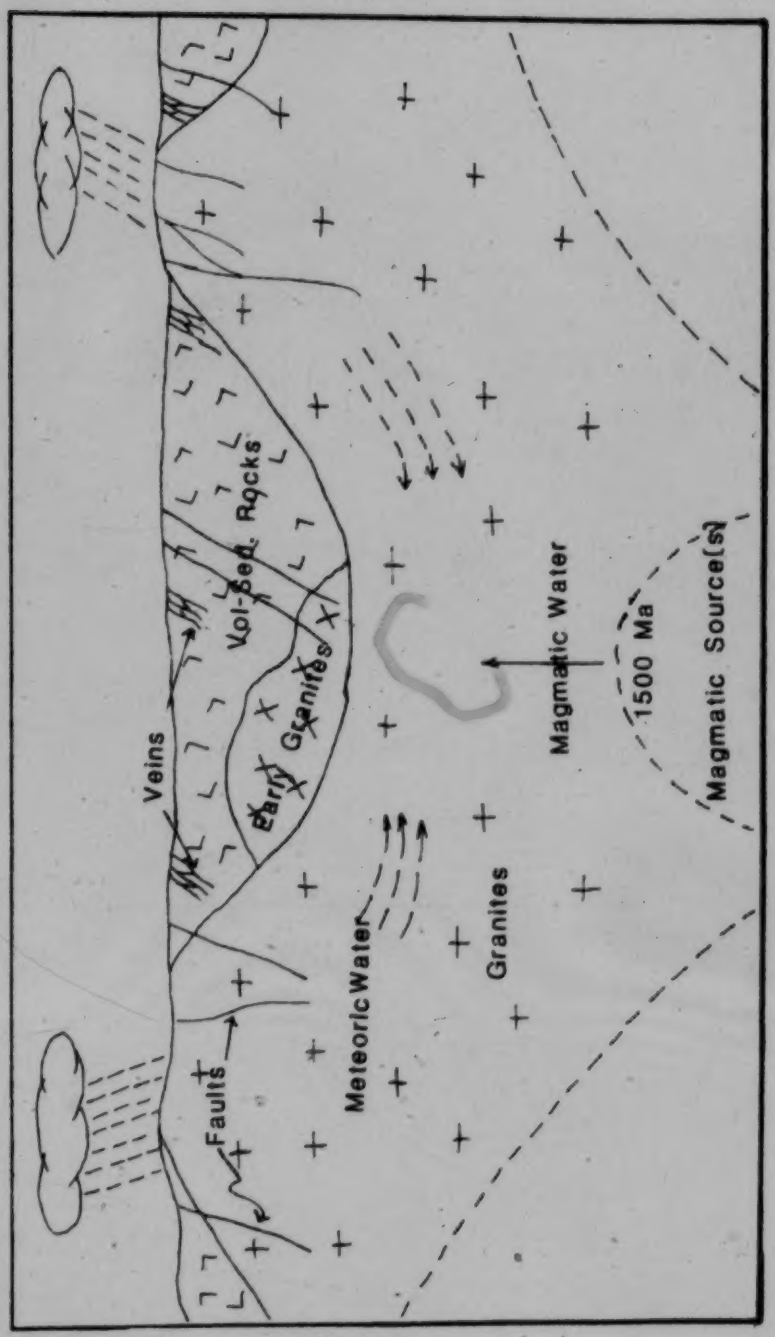

Figure 31. A model illustrating the origin of the Great Bear Lake silver deposits.

10. CONCLUSIONS

The complex nature of the Great Bear Lake silver deposits is obvious from this study and from previous investigations. Although some of the earlier controversies involving the nature and composition of the hydrothermal fluids have been resolved in this study, there is still scope for further research towards a better understanding of the formation of these classical deposits. At present there are no stable isotope data on the country- and host-rocks to compare the nature of the hydrothermal fluids which might have circulated through these rocks with those of the hydrothermal fluids which deposited the metals in the veins. Similarly, detailed lead and strontium isotopes of the rocks might throw new light into the source of the metals.

The detailed mineralogical study of the veins carried out in this investigation has revealed a wide variety of opaque phases. Native silver, which is the most important mineral in these deposits, occurs in association with various types of arsenides, sulpharsenides, uraninite (which is not ubiquitous to all the deposits), sulphosalts, sulphides and native bismuth. The principal gangue minerals include quartz, calcite and dolomite with minor fluorite, chlorite, siderite, rhodochrosite, K-mica and K-feldspar. Five main stages of mineralization have been recognized from microscopic and hand specimen studies. These are:

Stage I : Quartz - hematite ± uraninite

Stage II : Arsenides - Ag - carbonates - quartz ± fluorite

Stage III : Ag - Bi - carbonates - quartz

Stage IV : Sulphosalts - sulphides - carbonates - quartz

Stage V : Sulphides - carbonates - quartz

Electron microprobe analyses of native silver and the arsenides have revealed regional variations in the chemical compositions of some of the minerals. The variations in the compositions of nickelines, cobaltites, gersdorffites and native silvers may be attributed to any of the following reasons :

(i) There were differences in the physico-chemical conditions between the two sectors during ore deposition.

(ii) The minerals in the two sectors formed at different times under different conditions.

(iii) There were changes in the compositions during upward migration of the fluids.

Fluid inclusion studies of the gangue minerals associated with opaque minerals indicate a wide range of homogenization temperatures and salinities. The salinities of the fluids range from about 15 to 35 wt.% NaCl equivalent. The homogenization temperatures range from 150° to 250°C for stage I fluids; 220° to 480°C for stage II fluids; 250° to 350°C for stage III fluids; 150° to 250°C for stage IV fluids and 90° to about 250°C for stage V fluids. The coexistence of liquid-rich and vapour-rich inclusions in minerals of stages II and III suggest that the hydrothermal fluids were boiling or effervescing. The coexistence of saturated and unsaturated inclusions in stages III and IV may be due to effervescence of a less saline fluid, whilst for stages IV and V it may be due to mixing of a highly saline fluid with a less saline fluid, or due to alternation of hydrostatic and lithostatic pressures at the time of trapping of the inclusions.

Stable isotopic studies indicate the involvment of two or more types of hydrothermal fluids. The isotopic composition of fluids belonging to stages I, II and III, in which the arsenides and earlier generations of native silver were deposited were probably derived from an aqueous phase of a cooling pluton. The later fluids, associated stages IV and V, were considerably lighter, and were probably the result of subsequent incursion of isotopically lighter water, which could have been either meteoric or marine. Carbon in these deposits, for the most part, was probably derived from magmatic sources. However, the contribution of carbon from other sources, mainly carbonate beds, became important during the late stages of hydrothermal activity.

The lead isotope data suggest mineralization age of around 1500 Ma. Both the lead and strontium isotope data suggest a multi-source derivation of Pb and Sr components in the vein minerals.

The metals were transported by moderate to high salinity hydrothermal fluids as complexes. Uranium was either transported as carbonate or as hydroxyl complexes, whilst the other metals were probably transported mainly as chloride complexes. The role of other

complexes was probably minimal. The metals were deposited in dilatant zones due to decrease in temperature, pressure, boiling or mixing of different types of fluids. Finally, it is suggested that uranium, and silver and the other metals, were derived from different sources.

11. REFERENCES

Ahmad, S.N., and Rose, A.W., 1980, Fluid inclusions in porphyry and skarn ore at Santa Rita, New Mexico: Econ. Geol., v. 75, p. 229-250.

Andrews, A.J., Kerrich, R., and Owsiacki, L., 1984, Petrographic and geochemical studies of the Ag-Ni-Co arsenide vein deposits, Cobalt-Gowganda, Ontario: GAC/MAC, Program with Abstracts, v. 9, p. 42.

Badham, J.P.N., 1973, Volcanogenesis, Orogenesis and Metallogenesis, Camsell River, N.W.T., Canada: Ph.D Thesis, Univ. of Alberta, 363p.

---------- 1975, Mineralogy, paragenesis and origin of the Ag-Ni, Co arsenide mineralization, Camsell River, N.W.T., Canada: Mineral. Deposita, v. 10, p. 153-175.

---------- 1976, Orogenesis and metallogenesis with reference to the silver-nickel-cobalt arsenide ore association: In: Metallogeny and Plate Tectonics, ed., D.F. Strong, p. 559-572.

Badham, J.P.N., Robinson, B.W., and Morton, R.D., 1972, Geology and genesis of the Great Bear silver deposits: Proceedings of the 24th International Geological Congress (Montreal), Section 4, p. 541-547.

Barbieri, M., Masi, U., and Tolomeo, L., 1982, Strontium geochemistry in the epithermal barite deposits from the Apuan Alps (Northern Tuscany, Italy): Chem. Geol., v. 35, p. 351-356.

---------- 1984, Strontium geochemical evidence for the origin of the barite deposits from Sardinia, Italy: Econ. Geol., v. 79, p. 1360-1365.

Barnes, H.L., 1979, Solubilities of ore minerals. In : Geochemistry of Hydrothermal Ore Deposits: Ed. : H.L. Barnes, 2nd edition. A Wiley-Interscience Publication, p. 404-460.

Barnes, H.L., and Kullerud, G., 1961. Equilibria in sulfur-containing aqueous solutions in the system Fe-S-O, and their correlation during ore deposition: Econ. Geol., v. 56, p. 648-688.

Barton, P.B. Jr., and Skinner, B.J., 1979, Sulphide mineral stabilities: In : Geochemistry of Hydrothermal Ore Deposits, ed., H.L. Barnes, A Wiley-Interscience Publication, p. 278-403.

Bastin, E.S., 1949, Deposition and resolution of native silver at Gowganda, Ontario: Econ. Geol., v. 44, p. 437-444.

---------- 1950a, Interpretations of ore textures: Geol. Soc. Am. Mem., no. 45.

---------- 1950b, Significant replacement textures at Cobalt and South Lorraine, Ontario, Canada: Econ. Geol., v. 45, p. 808-817.

Bayliss, P., 1969, X-ray data, optical anisotropism, and thermal stability of cobaltite, gersdorffite, and ullmanite: Min. Mag., v. 37, p. 26-33.

Bayliss, P., 1982, A further crystal structure refinement of cobaltite: Amer. Mineral., v. 67, p.

1048-1057.

Beaty, D.W., and Taylor, H.P.Jr., 1982, Some petrologic and oxygen isotopic relationships in the Amulet Mine, Noranda, Quebec, and their bearing on the origin of Archean massive sulphide deposits: Econ. Geol., v. 77, p. 95-108.

Becker, R.H., and Clayton, R.N., 1976, Oxygen isotope study of a Precambrian banded iron-formation, Hammersley Range, Western Range, Western Australia: Geochim. Cosmochim. Acta, v. 40, p. 1153-1165.

Bennett, J.N., and Grant, J.N., 1980, Analyses of fluid inclusions using a pulsed laser microprobe: Min. Mag., v. 43, p. 945-947.

Bigeleisen, J., 1965, Chemistry of isotopes: Science, v. 147, p. 463-471.

Bigeleisen, J., and Mayer,M.G., 1947, Calculation of equilibrium constants for isotopic exchange reactions: J. Chem. Phys., v. 15, p. 261.

Bodnar, R.J., 1983, A method of calculating fluid inclusion volumes based on vapour bubble diameters and P-V-T-X properties of inclusion fluids: Econ. Geol., v. 78, p. 535-542.

Bottinga, Y., 1968, Calculation of fractionation factors for carbon and oxygen isotopic exchange in the system calcite-carbon dioxide-water: Jour. of Chemistry, v. 72, p. 800-808.

Bottinga, Y., and Javoy, M., 1973, Comments on oxygen isotope geothermometry: Earth Planet. Sci. Letters, v. 20, p. 250-265.

Bowring, S.A., and Van Schmus, W.R., 1982, Age and duration of igeous events in the Wopmay Orogen, Northewest Territories, Canada: Geol. Soc. America, Abstracts with Programs, v. 12, p. 540.

Boyle, R.W., 1968, The geochemistry of silver and its deposits: Geol. Surv. Canada Bulletin, v. 160, 264p.

Boyle, R.W., and Dass, A.S., 1971, The origin of the native silver veins at Cobalt, Ontario: Can. Min., v. 11, p. 414-417.

Broderick, S.J., and Ehret, W.F., 1931, An x-ray study of the alloys of silver with bismuth, antimony and arsenic : Part I: J. Phys. Chem., v. 35, p. 2627-2636.

Broecker, W.S., and Oversby, V.M., 1970, Chemical equilibria in the earth: McGraw-Hill, New York.

Brookins, D., Metz, M., and Rosenberg, P., 1971, Strontium geochemistry of some quartz-fluorite-carbonate veins from western Montana: EOS, v. 52, p. 364.

Campbell, D.D., 1955, Geology of the pitchblende deposit of Port Radium, Great Bear Lake, N.W.T.: Ph.D. Thesis, Calif. Inst. Tech., 323p.

---------- 1957, Port Radium Mine: In : Structural geology of Canadian ore deposits (vol. II), 6th Comm. Min. Metall. Congr., p. 177-189.

Casadevall, T., and Ohmoto, H., 1977, Sunnyside mine, Eureka mining district, San Juan County, Colorado : geochemistry of gold and base metal ore deposition in a volcanic

environment: Econ. Geol., v. 72, p. 1285-1320.

Clark, A.H., 1972, Mineralogy of the Alacran deposit, Pampa Larga, Chile. VII. Native arsenian silver: Neues Jb. Miner. Mh., v. 11, p. 500-505.

Clark, L.A., 1960, The Fe-As-S system : Phase relations and applications: Econ. Geol., v. 55, p. 1345-1381 and p. 1631-1652.

Clayton, R.N., and Epstein, S., 1958, The relationship between O^{18}/O^{16} ratios in coexisting quartz, carbonate and iron oxides from various geological deposits: J. Geol., v. 66, p. 352-373.

Clayton, R.N., and Mayeda, T.D., 1963, The use of bromine pentafluoride in the extraction of oxygen from oxides and silicates for isotopic analysis: Geochim. Cosmochim. Acta, v. 27, p. 43-52.

Craig, H., 1953, The geochemistry of the stable carbon isotopes: Geochim. Cosmochim. Acta, v. 3, p. 53-92.

----------1963, The isotopic composition of water and carbon in geothermal areas: In: Nuclear Geology on Geothermal areas. Tongiorgi, E., ed., Spoleto: Pisa, Consiglio Nazionale della Richerche, Laboratorio de Geologia Nucleare, p. 17-53.

Craig, J.R., and Vaughan, D.J., 1981, Ore microscopy and ore petrography: A Wiley-Interscience Publication.

Crawford, M.L., 1981, Phase equilibria in aqueous fluid inclusions. In Short Course in Fluid

Inclusions: Applications to Petrology, eds., L.S. Hollister and M.L. Crawford: Min. Assoc. of Canada, v. 6, p. 75-97.

Criss, C.M., and Cobble, J.W., 1964a, The thermodynamic properties of high temperature aqueous solutions. IV. Entropies of the ions up to 200°C and the correspondence principle: J. Am. Chem. Soc., v. 86, p. 5385-5390.

---------- 1964b, The thermodynamic properties of high temperature aqueous solutions. V. The calculation of high temperature ionic heat capacities up to 200°C : Entropies and heat capacities above 200°C: J. Am. Chem. Soc., v. 86, p. 5390-5392.

Cumming, G.L., 1969, A recalculation of the age of the solar system: Can. Jour. Earth Sci., v. 6, p. 719-735.

Cumming, G.L., Rollett, J.S., Rossotti, E.J.C., and Whewell, R.J., 1972, Statistical methods for the computation of stability constants. Part I. Straight line fitting of points with the correlated errors: Jour. Chem. Soc., Dalton Transactions, p. 2652-2658.

Cumming, G.L., and Richards, J., 1975, Ore lead isotope ratios in a continuously changing earth. Earth Planet. Sci. Letters, v. 28, p. 155-171.

Deines, P., and Gold, D.P., 1973, The isotopic composition of carbonatite and kimberlite carbonates and their bearing on the isotopic composition of deep-seated carbon: Geochim. Cosmochim. Acta, v. 37, p. 1709-1733.

Dhamelincourt, P., Beny, J.M., Dubessy, J., and Poty, B., 1979, Analyses of fluid inclusions

by the Raman microprobe MOLE: Bull. Mineral., v. 102, p. 600-610 (in French).

Doe, B.R., 1970, Lead Isotopes: Springer-Verlag.

Doe, B.R., and Stacey, J.S., 1974, The application of lead isotopes to the problems of ore genesis and ore prospect evaluation : A review: Econ. Geol., v. 69, p. 757-776.

Doe, B.R., and Zartman, R.E., 1979, Plumbotectonics, The Phanerozoic. In : Geochemistry of Hydrothermal Ore Deposits. Ed. : H.L. Barnes, 2nd edition: A Wiley-Interscience Publication, p. 22-70.

Dolomanova, E.I., Bogoyavlenskaya, I.V., Boyarskaya, R.V., Loseva, T.I., and Guntau, M., 1974, Data on the conditions of formation of the Ehrenfriedersdorf tin-ore deposit (German Dem. Repub.) by means of gas-liquid inclusions: Z. Angew. Geol., v. 20, p. 352-363 (in German).

Drummond, S.E., and Ohmoto, H., 1985, Chemical evolution and mineral deposition in boiling hydrothermal systems: Econ. Geol., v. 80, p. 126-147.

Edwards, A.B., 1947, Textures of the ore minerals: Aust. Inst. of Min. and Metall., Melbourne.

Ellis, A.J., and Golding, R.M. 1963. The solubility of carbon dioxide above 100°C in water and in sodium chloride solutions: Am. J. Sci., v. 261, p. 47-60.

Farrell, C.W., and Holland, H.D., 1983, Strontium isotope geochemistry of the Kuroko deposits. In : The Kuroko and Related Volcanogenic Massive Sulphide Deposits:

Econ. Geol. Monograph 5, p. 302-319.

Faure, G., 1977, Principles of Isotope Geology: New York, Wiley.

Feniak, M., 1947, The geology of the Dowdell Peninsula, Great Bear Lake, N.W.T.: Geol. Surv. Canada Sp. Rep., 14p.

Fraser, J.A., Hoffman, P.F., Irvine, T.N., and Mursky, G., 1972, The Bear Province. In Variations in Tectonic Styles in Canada. Eds. : R.A. Price and R.J.W. Douglas: Geol. Assoc. Can. Spec. Paper 11, p. 454-503.

Friedman, I.I., 1953, Deuterium content of natural waters and other substances: Geochim. Cosmochim. Acta, v. 4, p. 89-103.

Froese, E., 1981, Applications of thermodynamics in the study of mineral deposits: Geol. Surv. Canada Paper 80-28, 38p.

Furnival, G.M., 1935, The large quartz veins of Great Bear Lake: Econ. Geol., v. 30, p. 843-850.

---------- 1939, A silver-pitchblende deposit at Contact Lake, Great Bear Lake area, Canada: Econ. Geol., v. 34, p. 739-776.

Garrels, R.M., 1955, Some thermodynamic relations among the uranium oxides and their relation to the oxidation states of the uranium ores of the Colorado Plateau: Am. Min., v. 40, p. 1004-1021.

Garrels, R.M., and Christ, C.L., 1959, Behaviour of uranium minerals during oxidation: U.S. Geol. Surv. Prof. Paper 320, 236p.

---------- 1965, Solutions, Minerals, and Equilibria: Harper and Row, New York.

Gonfiantini, R., 1978, Standards for stable isotope measurements in natural compounds: Nature, v. 271, p. 534.

Grappin, C., Saliot, P., Sabouraud, C., and Touray, J.C., 1979, Variations of the Cl/Br, Na/Br, and K/Br ratios in fluid inclusions of quartz in the Bramans-Termignon evaporites, Vanoise, French Alps: Chem. Geol., v. 25, p. 41-52 (in French).

Greenwood, H.J., 1977, Application of thermodynamics to petrology and ore deposits: Min. Assoc. Canada, v. 2, 231p.

Guilhaumau, N., Dhamelincourt, N.P., Touray, J.C., and Barbillat, J., 1978, Raman microprobe analysis of gaseous inclusions in the system N_2-CO_2 (abstr.): Compt. Rend. Acad. Sci. Paris, 287, Series D, p.1317-1319 (in French).

Haas, J.L. Jr., 1971, The effect of salinity on the maximum thermal gradient of a hydrothermal system at hydrostatic pressure: Econ. Geol., v. 66, p. 940-946.

Halls, C., and Stumpfl, E.F., 1969, Geology and ore deposition, Western Kerr Lake Arch, Cobalt, Ontario: Inst. Min. Met., 9th Commonwealth Min. and Met. Cong., 1969, pap. 18.

Helgeson, H.C., 1964, Complexing and hydrothermal ore deposition: New York-London, Pergamon Press.

---------- 1969, Thermodynamics of hydrothermal systems a elevated temperatures and pressures: Am. J. Sci., v. 267, p. 729-804.

Henley, R.W., Truesdell, A.H., and Barton, P.D.Jr., 1984, Fluid-mineral equilibria in hydrothermal systems: Reviews in Econ. Geol., v. 1, 267p.

Hildebrand, R.S., 1981, Early Proterozoic Labine group of Wopmay Orogen : Remnant of continental volcanic arc developed during oblique convergence. In Campbell, F.H.A., ed., Proterozoic basins of Canada: Geol. Surv. Canada Paper 81-10, p. 133-156.

---------- 1982, An early Proterozoic continental volcanic arc at Great Bear Lake, Northwest Territories: Ph.D. Thesis, Memorial Univ. of Newfoundland, 237p.

---------- 1983, Geology of the Rainy Lake and White Eagle Falls map areas, District of MacKenzie : Early Proterozoic cauldrons, stratovolcanoes and subvolcanic plutons: Geol. Surv. Canada Paper 83-20, 42p.

---------- 1984, Continental inta-arc depressions : A nonextensional model for their origin, with a Proterozoic example from Wopmay Orogen: Geology, v. 12, p. 73-77.

Hitchon, B., and Friedman, I., 1969, Geochemistry and origin of formation waters in the Western Canada sedimentary basin - I. Stable isotopes of hydrogen and oxygen: Geochim. Cosmochim. Acta., v. 36, p. 1337-1349.

Hoefs, J., 1980, Stable Isotope Geochemistry. 2nd edition. Springer-Verlag, Berlin.

Hoffman, P.F., 1973, Evolution of early Proterozoic continental margin : The Coronation geosyncline and associated aulacogens of the northwestern Canadian shield: Royal Soc. Lon. Phil. Trans., ser. A, v. 273, p. 547-581.

---------- 1978, Geology of the Sloan River map-area (86K), District of MacKenzie: Geol. Surv. Canada, Open File 535.

---------- 1980, Wopmay Orogen : A Wilson cycle of early Proterozoic age in the northwest of the Canadian Shield. In : Strangway, D.W., ed., The continental crust and its mineral deposits: Geol. Assoc. Canada Special Paper 20, p. 523-549.

---------- 1982, The northern internides of Wopmay Orogen: Geol. Surv. Canada, Open File Map 832.

Hoffman, P.F., and Bell, I.R., 1975, Volcanism and plutonism, Sloan River map-area (86K), Great Bear Lake, District of MacKenzie: in Report of Activities, Part A, Geol. Surv. Canada Paper 75-1A, p. 331-337.

Hoffman, P.F., and McGlynn, J.C., 1977, Great Bear Batholith : A volcano-plutonic depression. In Baragar, W.R.A., Coleman, L.C. and Hall, J.M., eds., Volcanic Regimes in Canada: Geol. Assoc. Canada Special Paper 16, p. 170-192.

Hoffman, P.F., Bell, I.R., and Tirrul, R., 1976, Sloan River map-area (86K), Great Bear Lake, District of MacKenzie; in Report of Activities, Part A, Geol. Surv. Canada Paper 76-1A, p. 353-358.

Hoffman, P.F., St-Onge, M.R., Easton, R.M., Grotzinger, J., and Schulze, D.L., 1980, Syntectonic plutonism in north-central Wopmay Orogen (early Proterozoic), Hepburn Lake area, District of MacKenzie: in Current Research, Part A, Geol. Surv. Canada, Paper 80-1A, p.171-177.

Hofman, R., and Baummann, A., 1984, Preliminary report on the Sr isotopic composition of hydrothermal vein barites in the Federal Republic of Germany: Mineral. Deposita, v. 19, p. 166-169.

Holland, H.D., 1959, Some applications of thermochemical data to problems of ore deposition. I. Stability relations among the oxides, sulphides, and carbonates of ore and gangue minerals: Econ. Geol., v. 54, p. 184-233.

---------- 1965, Some applications of thermochemical data to problems of ore deposition. II. Mineral assemblages and the composition of ore forming fluids: Econ. Geol., v. 60, p. 1101-1166.

Holland, H.D., and Malinin, S.D., 1979, The solubility and occurrence of non-ore minerals. In : Geochemistry of Hydrothermal Ore Deposits. Ed. : H.L. Barnes , 2nd edition. A Wiley-Interscience Publication, p. 461-508.

Hollister, L.S., and Crawford, M.L., 1981, Short Course in Fluid Inclusions : Applications to Petrology: Min. Assoc. Canada, v. 6, 304p.

Holmes, R.J., 1947, Higher mineral arsenides of cobalt, nickel and iron: Bull. Geol. Soc. Amer., v. 55, p. 299-392.

Hostetler, P.B., and Garrels, R.M., 1962, Transportation and precipitation of uranium and vanadium at low temperatures, with special reference to sandstone-type uranium deposits: Econ. Geol., v. 57, p. 137-167.

Hulston, J.R., and McCabe, W.J., 1962, Mass spectrometer measurements in the thermal areas of New Zealand, part II. Carbon isotopic ratios: Geochim. Cosmochim. Acta, v. 26, p. 398-410.

Irving, E., Donaldson, J.A., and Park, J.K., 1972, Paleomagnetism of the Western Channel diabase and associated rocks, N.W.T.: Can. Jour. Earth Sci., v. 9, p. 960-971.

Jambor, J.L., 1971, Origin of the silver veins of the CobaltGowganda region: Can. Min., v. 11, p. 402-413.

Jory, L.T., 1964, Mineralogical and isotopic relations in the Port Radium pitchblende deposit, Great Bear Lake, Canada: Ph.D. Thesis, Cal. Inst. Tech., 275p.

Kalogeropoulos, S.I., 1984, Composition of arsenopyrite from the Olympias Pb-Zn massive sulphide, Chalkidiki Peninsula, N. Greece: Neues Jb. Miner. Mh., v. 7, p. 296-300.

Kamilli, R.J., and Ohmoto, H., 1977, Paragenesis, zoning, fluid inclusion, and isotopic studies of the Findlandia Vein, Colqui district, Central Peru: Econ. Geol., v. 72, p. 950-982.

Kanasewich, E.R., 1968, The interpretation of lead isotopes and their geological significance. In Radiometric Dating for Geologists. Eds.: E.I. Hamilton and R.M. Furquhar. Interscience, New York, p. 147-223.

Keevil, N.B., 1942, Vapour pressures of aqueous solutions at high temperatures: J. Am. Chem. Soc., v. 64, p. 841-850.

Kelly, W.C., and Turneaure, F.S., 1970, Mineralogy, paragenesis and geothermometry of the tin and tungsten deposits of the Eastern Andes, Bolivia: Econ. Geol., v. 65, p. 609-680.

Kerrich, R., 1983, Geochemistry of gold deposits in the Abitibi Greenstone Belt: Can. Min. Met., Sp. Vol. 27, 75p.

Kesler, S.E., and Jones, L.M., 1981, Sulfur and strontium isotopic geochemistryof celestite, barite, and gypsum from the Cretaceous basins of northeatern Mexico: Chem. Geol., v. 31, p. 211-224.

Kesler, S.E., Ruiz, J., and Jones, L.M., 1983, Strontium isotopic geochemistry of fluorite mineralization (Coahuila, Mexico): Isot. Geosci., v. 1, p. 65-75.

Kessen, K.M., Woodruff, M.S., and Grant, N.K., 1981 Gangue mineral $^{87}Sr/^{86}Sr$ ratios and the origin of Mississippi Valley type mineralization: Econ. Geol., v. 76, p. 913-920.

Khaibullin, I.Kh., Novikov, B.Ye., Copeliovich, A.M., and Besedin, A.M., 1980, Phase diagrams for steam solutions and caloric properties of two- and three component systems : H_2O-NaCl, H_2O-Na_2SO_4 and H_2O-NaCl-Na_2O_4. In : Water and Steam. Eds., J. Straub and K. Scheffler, Pergamon Press, New York, p. 641-647.

Kidd, D.F., 1931, Great Bear Lake-Coppermine River Area, MacKenzie District, N.W.T.: Geol. Surv. Canada, Summ. Rep., Part C, p. 47-69.

---------- 1932, A pitchblende-silver deposit, Great Bear Lake, Canada: Econ. Geol., v. 27, p. 145-159.

---------- 1933, Great Bear Lake area, Northwest Territories: Geol. Surv. Canada, Summ. Rep., 1932, Part C, p. 1-36.

Kidd, D.F., and Haycock, M.H., 1935, Mineragraphy of the ores of the Great Bear Lake: Geol. Surv. Am. Bull., v. 46, p. 879-960.

Kieller, B.J., 1962, Mineralogy of the no.2 zone Eldorado mine, Port Radium, Northwest Territories: M.Sc. Thesis, Univ. of Alberta, 106p.

Klemm, D.D., 1965, Synthesen und Analysen in den Dreieckdiagram FeAsS-CoAsS-NiAsS und FeS_2-CoS_2-NiS_2: Neues Jahr. fur Mineral. Abh., v. 103, p. 205-255.

Knauth, L.P., and Epstein, S., 1976, Hydrogen and oxygen isotope ratios in nodular bedded cherts: Geochim Cosmochim. Acta, v. 40, p. 1095-1108.

Kolodny, Y., and Epstein, S., 1976, Stable isotope geochemistry of deep sea cherts: Geochim. Cosmochim. Acta, v. 40, p. 1195-1209.

Krauskopf, K.B., 1979, Introduction to geochemistry. 2nd edition. McGraw-Hill, New York.

Kretschmar, U., and Scott, S.D., 1976, Phase relations involving arsenopyrite in the system Fe-As-S and their application: Can. Miner., v. 14, p. 364-386.

Landis, G.P., and Rye, R.O., 1974, Geologic, fluid inclusion, and stable isotope studies of the

Pasto Bueno tungsten-base metal ore deposit, Northern Peru: Econ. Geol., v. 69, p. 1025-1059.

Lange, S., Chaudhuri, S., and Clauer, N., 1983, Strontium isotopic evidence for the origin of barites and sulphides from the Mississippi Valley type ore deposits in Southeast Missouri: Econ. Geol., v. 78, p. 1255-1261.

Langmuir, D., 1978a, Uranium solution-mineral equilibria at low temperatures with applications to sedimentary ore deposits: Geochim. Cosmochim. Acta, v. 42, p. 547-569.

---------- 1978b, Uranium solution-mineral equilibria at low temperatures with applications to sedimentary ore deposits. Short Course in Uranium Deposits : Their Mineralogy and Origin. Ed. : M.M. Kimberly: Min. Assoc. Canada Short Course Handbook, v. 3, p. 17-55.

Leblanc, M., and Billaud, P., 1982, Cobalt arsenide orebodies related to an upper Proterozoic ophiolite: Bou Azzer (Morocco): Econ. Geol., v. 77, p. 162-175.

Lemmlein, G.G., and Klevtsov, P.V., 1961, Relations among the principal thermodynamic parameters in a part of the system H_2O-NaCl: Geochemistry, no. 2, p. 148-158.

Lemoine, A., 1975, Contribution a l'etude du comportement de UO_2 en milieu aqueux a haute temperature et haute pression: unpub. doctoral thesis, Nancy, 111p.

Lowell, G.R., and Gasparrini, C., 1982, Composition of arsenopyrite from topaz greisen veins in southeastern Missouri: Mineral. Deposita., v. 17, p. 229-238.

Luckscheiter, B., and Parekh, P.P., 1979, A new method for the determinations of dissolved elements in fluid inclusions: N. Jb. fur Minerl. Mh., p. 135-144.

Matthews, A., and Katz, A., 1977, Oxygen isotope fractionation during dolomitization of calcium carbonate: Geochim. Cosmochim. Acta., v. 41, p. 1431-1438.

McCrea, J.M., 1950, The isotopic chemistry of carbonates and paleotemperature scale: J. Chem. Phys., v. 18, p. 849-857.

Medford, R., Maxwell, R.J., and Armstrong, R.L., 1983, $^{87}Sr/^{86}Sr$ ratio measurements on sulphides, carbonates, and fluid inclusions from Pine Point, Northwest Territories, Canada : An $^{87}Sr/^{86}Sr$ ratio increase accompanying the mineralizing process: Econ. Geol., v. 78, p. 1375-1378.

Meinzes, M., and Seyfried, W.E.Jr., 1979, Basalt-seawater interaction : trace element and strontium isotopic variations in experimentally altered glassy basalt: Earth Planet. Sci. Letters, v. 44, p. 463-472.

Melent'yev, B.N., Ivanenko, V.V., and Pamfilova, L.A., 1970, Solubility of some ore-forming sulphides under hydrothermal conditions: Geochem. Int., v. 7, p. 416-460.

Metz, M.C., Brookins, D.G., Rosenberg, P.E., and Zartman, R.E., 1985, Geology and geochemistry of the Snowbird deposit, Mineral County, Montana: Econ. Geol., v. 80, p. 394-409.

Metzger, F.W., Kelly, W.C., Nesbitt, B.E., and Essene, E.J., 1977, Scanning electron microscopy of daughter minerals in fluid inclusions: Econ. Geol., v. 72, p. 141-152.

Miller, R., 1982a, The Metallogeny of Uranium in the Great Bear Batholith Complex, Northwest Territories: Ph.D. Thesis, Univ. of Alberta, 271p.

---------- 1982b, The geochronolgy of uranium deposits in the Great Bear batholith, Northwest Territories: Can. Jour. Earth Sci., v. 19, p. 1428-1448.

Misra, K.C., and Fleet, M.E., 1975, Textural and compositional variations in a Ni-Co-As assemblage: Can. Min., v. 13, p. 8-14.

Morton, R.D., and Changkakoti, A., 1985, Magmatogene silver-bearing vein deposits - possible protolithic precursors: In Can. Jour. Earth Sciences.

Murck, B.W., Burruss, R.C., and Hollister, L.S., 1978, Phase equilibria in fluid inclusions in ultramafic xenoliths: Am. Min., v. 63, p. 40-46.

Mursky, G., 1963, Mineralogy, petrology and geochemistry of the Hunter Bay area, Great Bear Lake, N.W.T.: Ph.D. Thesis, Stanford University.

---------- 1973, Geology of the Port Radium map area, District of MacKenzie: Geol. Surv. Canada Memoir 374, 40p.

Nambu, M., 1980, The analysis of fluid inclusions in microgram range with an ion microanalyzer: 26th Int. Geol. Cong.(abs), v. 1, p. 67.

Nambu, M., Sato, T., Hayakawa, N., and Ohmori, Y., 1977, On the microanalysis of fluid inclusions with the ion microanalyzer (abs). Mining Geology (Japan), v. 27, p. 40.

Nash, J.T., 1973, Geochemical studies in the Park City District : I : Ore fluids in the Mayflower Mine: Econ. Geol., v. 68, p. 34-51.

Naumov. G.B., 1961, Some physicochemical characteristics of the behaviour of uranium in hydrothermal solutions: Geochemistry, no. 2, p. 127-147.

Naumov, G.B., and Mironova, O.F., 1969, Migration of uranium in hydrothermal carbonate solutions (according to physicochemical data). In Khitarov, N.I., ed., Problems of Geochemistry, p. 166-175.

Norman, D.I., 1978, Analysis of Rb, Sr and Sr isotopes in fluid inclusion waters : Inst. Min. Met. Trans., sec. B, v. 87, p. 34-35.

Norman, D.I., and Landis, G.P., 1983, Source of mineralizing components in hydrothermal ore fluids as evidenced by $^{87}Sr/^{86}Sr$ and stable isotope data from the Pasto Bueno deposit, Peru: Econ. Geol., v. 78, p. 451-465.

Oen, I.S., Burke, E.A.J., Kieft, C., and Westerhof, A.B., 1971, Ni-arsenides, Ni-rich loellingite and (Fe, Co)-rich gersdorffite in Cr-Ni-ores from Malaga Province, Spain: Neues Jb. Miner. Abh., v. 115, p. 123-139.

Ohmoto, H., 1972, Systematics of sulfur and carbon isotopes in hydrothermal ore deposits: Econ. Geol., v. 67, p. 551-578.

Ohmoto, H., and Rye, R.O., 1970, The Bluebell Mine, British Columbia. I. Mineralogy, paragenesis, fluid inclusions, and the isotopes of hydrogen, oxygen, and carbon: Econ. Geol., v. 65, p. 417-437.

Ohmoto, H., and Rye, R.O., 1979, Isotopes of sulfur and carbon. In : Geochemistry of Hydrothermal Ore Deposits, ed. : H.L. Barnes, A Wiley-Interscience Publication, 2nd edition, p. 509-567.

O'Neil, J.R., Clayton, R.N., and Mayeda, T., 1969, Oxygen isotope fractionation in divalent carbonates: Jour. Chem. Phys., v. 51, p. 5547-5558.

O'Neil, J.R., Silberman, M.L., Fabbi, B.P., and Chesterman, C.W., 1973, Stable isotope and chemical relations during mineralization in the Bodie Mining District, Mono County, California: Econ. Geol., v. 68, p. 765-784.

Palache, C., Berman, H., and Frondel, C., 1944, Dana's System of Mineralogy. I. Elements, sulphides, Sulfosalts. J. Wiley and Sons, New York.

Parsons, W.H., 1948, Camsell River map area: Geol. Surv. Canada Paper 48-19.

Park, C.F., and MacDiarmid, R.A., 1970, Ore deposits. 2nd edition, W.H. Freeman and company.

Paterson. C.J., 1982, Oxygen isotopic evidence for the origin and evolution of a scheelite ore-forming fluid, Glenorchy, New Zealand: Econ. Geol., v. 77, p. 1672-1687.

Patterson, D.J., Ohmoto, H., and Solomon, M., 1981, Geologic setting and genesis of cassiterite-sulphide mineralization at Renison Bell, western Tasmania: Econ. Geol., v. 76, p. 393-438.

Pavlu, D., 1972, Ag-As-Bi-Co-Ni association in Jachymov ore district, Krusne Hory

Mountains: Int. Geol. Cong., 24th session, Sec. 4, p. 526.

Perry, E.G., 1967, The oxygen isotope chemistry in ancient cherts. Earth Planet. Sci. Letters., v. 3, p. 62-66.

Petruk, W., Cabri, L.J., Harris, D.C., Stewart, J.M., and Clark, L.A., 1970, Allargentum, redefined: Can. Min., v. 10, p. 163-172.

Petruk, W., Harris, D.C., and Stewart, J.M., 1971, Characteristics of the arsenides, sulpharsenides, and antimonides: Can. Min., v. 11, p. 150-186.

Potter, R.W., 1977, Pressure corrections for fluid inclusion homogenization temperatures based on the volumetric properties of the system NaCl-H_2O: U.S. Geol. Surv. J. Res., v. 5, p. 603-607.

Potter, R.W., and Brown, D.L., 1975, The volumetric properties of aqueous sodium chloride solutions from 0° to 500°C at pressures up to 2000 bars based on a regression of the available literature: U.S. Geol. Surv. Open File Rept. No. 75-636, 31p.

Poty, B.P., Leroy, J., and Cuney, M., 1974, Les inclusions fluides dans les minerais des gisements d'uranium intragranitiques du Limousin et du Forez (Massif Central, France): in Formation of Uranium Deposits, Int. Atomic Ener. Agency, Vienna, p. 569-582.

Radcliffe, D., 1968, Structural formula and composition of skutterudite: Can. Min., v. 9, p. 559-563.

Radcliffe, D., and Berry, L.G., 1968, The safflorite-loellingite solid solution series: Am. Min., v. 53, p. 1856-1881.

Ramdohr, P., 1980, The ore minerals and their intergrowths. 2nd edition. Pergamon Press.

Rayson, H.W., and Calvert, L.D., 1958, Solid solutions of mercury in silver and gold: J. Inst. Metals, v. 87, p. 88-90.

Rich, R.A., Holland, H.D., and Petersen, U., 1977, Hydrothermal Uranium Deposits. Elsevier Scientific Pub. Co., New York.

Reesman, R.H., 1968, Strontium isotopic compositions of gangue minerals from hydrothermal vein deposits: Econ. Geol., v. 63, p. 731-736.

Robie, A.R., Hemingway, B.S., and Fisher, J.R., 1978, Thermodynamic properties of minerals and related substances at 298.15 K and 1 bar (10^5 Pascals) pressure and at higher temperatures: Geol. Surv. Bull., v. 1452, 456p.

Robinson, B.W., 1971, Studies on the Echo Bay Silver Deposits,N.W.T.: Ph.D. Thesis, Univ. of Alberta, 256p.

Robinson, B.W., and Morton, R.D., 1972, The geology and geochronology of the Echo Bay area, Northwest Territories, Canada: Can. Jour. Earth Sci., v. 9, p. 158-169.

Robinson, B.W., and Ohmoto, H., 1973, Mineralogy, fluid inclusions and stable isotopes of the Echo Bay U-Ni-Ag-Cu deposits, Northwest Territories, Canada: Econ. Geol., v. 68, p. 635-656.

Robinson, B.W., and Badham, J.P.N., 1974, Stable isotope geochemistry and the origin of the Great Bear Lake silver deposits, Northwest Territories, Canada: Can. J. Earth Sci., v. 11, p. 698-711.

Robinson, H.S., 1933, Notes on the Echo Bay District, Great Bear Lake, Northwest Territories: Can. Min. Met. Bull., v. 26, p. 609-628.

Roedder, E., 1962, Studies of fluid inclusions I : Low temperatures application of a dual-purpose freezing and heating stage: Econ. Geol., v. 57, p. 1045-1061.

---------- 1963, Studies of fluid inclusions II : Freezing data and their interpretations: Econ. Geol., v. 58, p. 167-211.

---------- 1967, Fluid inclusions as samples of ore fluids. In H.L. Barnes, ed., Geochemistry of Hydrothermal Ore Deposits. 1st edition, Holt, Rinehart & Winston, New York. p. 515-574.

---------- 1981, Origin of fluid inclusions and changes that occur after trapping. In Short Course in Fluid Inclusions: Applications to Petrology, eds., L.S.Hollister and M.L. Crawford: Min. Assoc. of Canada, v. 6, p. 101-129.

---------- 1984, Fluid Inclusions: Reviews in Mineralogy, Min. Soc. of America, Series Editor: Paul H. Ribbe, v. 12, 644p.

Roedder, E., and Bodnar, R.J., 1980, Geologic pressure determinations from fluid inclusion studies: Ann. Rev. Earth Planet. Sci., v. 8, p. 263-301.

Rogers, P.S.Z., and Pitzer, K.S., 1982, Volumetric properties of aqueous sodium chloride solutions: J. Phys. Chem. Ref. Data, v. 11, p. 15-81.

Rojkovic, I., 1971, Cobalt-nickel arsenides and sulpharsenides of some U-Co-Ni-Bi-Ag veins at Great Bear Lake, Canada. Geologicky zbornik slovenska akademia vied, v. 22, no. 1, p. 79-96.

---------- 1973, Silver mineralization at Great Bear Lake, Canada: Geologicky zbor. slov. akad. vied, v. 24, p. 325-338.

Rosasco, G.J., and Roedder, E., 1979, Application of a new Raman microprobe spectrometer to nondestructive analysis of sulfate and other ions in individual phases in fluid inclusions in minerals: Geochim. Cosmochim. Acta, v. 43, p. 1907-1915.

Roseboom, E.H., 1962, Skutterudites $(Co,Ni,Fe)As_3$: Compositions and cell dimensions: Am. Min., v. 47, p. 310-327.

---------- 1963, Co-Ni-Fe diarsenides : Compositions and cell dimensions: Am. Min., v. 48, p. 271-299.

Roxlo, K.S., 1980, Uranium geochemistry of the Roosevelt Hot Springs thermal area, Utah: M.S. Thesis, Univ. of Utah, 62p.

Rudashevskii, N.S., Ioffe, P.A., and Grigoriev, D.P., 1979, Chemical composition and zoning of rammelsbergite, safflorite, and loellingite crystals: Min. Abstracts, 79-748, p. 70.

Ruiz, J., Kesler, S.E., and Jones, L.M., 1981, Strontium isotope geochemistry of fluorite

mineralization in northern Mexico: Geol. Soc. Am., Abs. with Programs, v. 13(7), p. 542.

---------- 1985, Strontium isotope geochemistry of fluorite mineralization associated with fluorine-rich igneous rocks from the Sierra Madre Occidental, Mexico : Possible exploration significance: Econ. Geol., v. 80, p. 33-42.

Russell, R.D., and Furquhar, R.M., 1960, Lead Isotopes in Geology: Interscience, New York.

Rye, R.O., and Ohmoto, H., 1974, Sulfur and carbon isotopes and ore genesis: A review: Econ. Geol., v. 69, p. 826-842.

Rye,R.O., and Sawkins, F.J., 1974, Fluid inclusion and stable isotope studies on the Casapalca Ag-Pb-Zn-Cu deposit, Central Andes, Peru: Econ. Geol., v. 69, p. 181-205.

Scott, S.D., 1972, The Ag-Co-Ni-As ores at the Siscoe Metals of Ontario mine, Gowganda, Ontario, Canada: Int. Geol. Cong., 24th session, Sec. 4, p. 528-538.

---------- 1983, Chemical behaviour of sphalerite and arsenopyrite in hydrothermal and metamorphic environments: Min. Mag., v. 47, p. 427-436.

Seward, T.M., 1976, The stability of chloride complexes of silver in hydrothermal solutions up to 350°C: Geochim. Cosmochim. Acta, v. 40, p. 1329-1341.

Sharma, T., and Clayton, R.N., 1965, Measurement of $^{18}O/^{16}O$ ratios of total carbonates: Geochim. Cosmochim. Acta, v. 29, p. 1347-1353.

Shegelski, R.J., 1973, Geology and Mineralogy of the Terra Silver Mine, Camsell River, N.W.T.: M.Sc Thesis, Univ. of Toronto, 169p.

Shegelski, R.J., and Scott. S.D., 1975, Geology and mineralogy of the silver-uranium-arsenide veins of the Camsell River District, Great Bear Lake, N.W.T.: Abstracts with Programs, Geol. Soc. Am., v. 7, p. 857-858.

Shelton, K., 1983, Composition and origin of ore-forming fluids in a carbonate hosted porphyry copper and skarn deposit : a fluid inclusion and stable isotope study of Mines Gaspe, Quebec: Econ. Geol., v. 78, p. 387-421.

Sheppard, S.M.F., 1981, Stable isotope geochemistry of fluids. In : Chemistry and Geochemistry of Solutions at High Temperature and Pressure. Physics and Chemsitry of the Earth, v. 13 & 14, p. 419-445.

Shrier, T., and Parry, W.T., 1982, A hydrothermal model for the North Canning Uranium Deposit, Owl Creek Mountains, Wyoming: Econ. Geol., v. 77, p. 632-645.

Slawson, W.F., and Russell, R.D., 1967, Common lead isotope abundances. In : Geochemistry of Ore Deposit. Ed.: H.L.Barnes. 1st edition. Holt, Rinehart and Winston, Inc., p. 77-108.

Smith, D.G.W., Gold, C.M., Tomlinson, D.A., and Wynne, D.A., 1981, EDATA 2. A Fortran IV programme for processing energy and or wavelength dispersive data from microbeam instruments to quantitative compositional results. Datum Geo-Services, Edmonton.

Sourirajan, S., and Kennedy, G.C., 1962, The system H_2O-NaCl at elevated temperatures and pressures. Am. Jour. Sci., v. 260, p. 115-141.

Stacey, J.S., and Kramers, J.D., 1975, Approximation of terrestrial lead evolution by a two-stage model. Earth Planet. Sci. Letters, v. 26, p. 207-221.

Stanton, R.L., 1972, Ore petrology: McGraw-Hill, Inc..

Stettler, A., 1977, $^{87}Sr/^{86}Sr$ systematics of a geothermal water-rock associations in the Massif Central, France : Earth Planet. Sci. Letters, v. 34, p. 423-438.

Stettler, A., and Allegre, C.J., 1978, $^{87}Sr/^{86}Sr$ studies of waters in a geothermal area : The Cantal, France: Earth Planet. Sci. Letters, v. 38, p. 364-372.

Strong, D.F., and Scott, S.D., 1984, Fluid inclusions of Ag-Co-Ni arsenide veins in the Cobalt-Gowganda area, Ontario: GAC/MAC, Program with Abstracts, v. 9, p. 108.

Taylor, H.P., 1967, Oxygen isotope studies of hydrothermal mineral deposits: in Geochemistry of Hydrothermal Ore Deposits, H.L. Barnes, ed., New York: Holt, Rinehart and Winston, 1st edition, p. 109-142.

---------- 1973, O^{18}/O^{16} evidence for meteoric hydrothermal alteration and ore deposition in the Tonopah, Comstock Lode, and Goldfield mining districts, Neveda: Econ. Geol., v. 68, p. 747-764.

---------- 1974, The application of oxygen and hydrogen isotope studies to problems of hydrothermal alteration and ore deposition: Econ. Geol., v. 69, p. 843-883.

---------- 1979, Oxygen and hydrogen isotope relationships in hydrothermal mineral deposits. In: Geochemistry of Hydrothermal Ore Deposits, H.L. Barnes, ed., A Wiley-Interscience Publication, 2nd edition, p. 236-277.

Taylor, M., Kesler, S.E., Cloke, P.L., and Kelly, W.C., 1983, Fluid inclusion evidence for fluid mixing, Mascot-Jeffferson City Zinc District, Tennessee: Econ. Geol., v. 78, p. 1425-1439.

Taylor, S.R., 1968, Geochemistry of the andesites. In: Origin and distribution of the elements, ed., L.H. Ahrens. Oxford: Pergammon Press.

Thompson, M., Rankin, A.H., Walton, S.J., Halls, C., and Foo, B.N., 1980, The analysis of fluid inclusion decrepitate by inductively-coupled plasma atomic emission spectroscopy : an exploration study: Chem. Geol., v. 30, p. 121-133.

Thorpe, R.I., 1974, Lead isotope evidence on the genesis of the silver-arsenide vein deposits of the Cobalt and Great Bear Lake areas, Canada: Econ. Geol., v. 69, p. 777-791.

---------- 1978, Sill of Western Channel diabase, Port Radium, District of Mackenzie: In: Wanless, R.K. and Loveridge, W.D., 1978. Rubidium-strontium isochron age studies, report 2, Geol. Surv. Canada Paper 77-14, p. 4-6.

Tirrul, R., 1976, The geology of the Rainy Lake Igneous Complex, District of Mackenzie, Northwest Territories: B.Sc. Thesis, Queen's University, 115p.

Touray, J.C., 1976, Activation analysis for liquid inclusions : a brief review, Bull. Soc. franc. Mineral. Cristallogr., v. 99, p. 162-164.

Truesdell, A.H., 1974, Oxygen isotope activities and concentrations in aqueous salt soloution at elevated temperatures : consequence for isotope geochemistry: Earth Planet. Sci. Lett., v. 23, p. 387-396.

Tsui, T.F., and Holland, H.D., 1979, The analysis of fluid inclusions by laser microprobe: Econ. Geol., v. 74, p. 1647-1653.

Urey, H.C., 1947, The thermodynamic properties of isotopic substances: Chem. Soc. Jour., p. 562-581.

Urusova, M.A., 1974, Phase equilibria and thermodynamic characteristics of solutions in the systems NaCl-H_2O and NaOH-H_2O at 350-550°C: Geochem. Int., v. 11, p. 944-950.

---------- 1975, Volume properties of aqueous solutions of sodium chloride at elevated temperatures and pressures: Jour. Inorg. Chem., v. 20, p. 1717-1721.

Van Schmus, W.R., and Bowring, S.A., 1980, Chronology of igneous events in the Wopmay Orogeny, Northwest Territories, Canada: Geol. Soc. Am., Abstracts with Programs, v. 14, p. 449.

Vaughan, D.J., and Craig, J.R., 1978, Mineral chemistry of metal sulphides: Cambridge University Press.

Veizer, J., and Compston, W., 1976, $^{87}Sr/^{86}Sr$ in Precambrian carbonates as an index of crustal evolution: Geochim. Cosmochim. Acta, v. 40, p. 905-914.

White, D.E., 1974, Diverse origins on hydrothermal ore fluids: Econ. Geol., v. 69, p. 954-973.

Withers, R.L., 1979, Mineral deposits of the Northrim Mine and a brief enquiry into the genesis of veins of the (Ag, Bi, Ni, Co, As) type: M.Sc. thesis, University of Alberta, 271p.

Ypma, P.J.M., 1972, The multistage emplacement of the Chalanches (France) Ni-Co-Bi-As-Sb-Ag deposits and the nature of the mineralization solutions: Int. Geol. Cong., 24th session, Sec.4, p. 525.

Ypma, P.J.M., and Fujikama, K., 1980, Fluid inclusion and oxygen isotope studies of the Nabarlek and Jabiluka Uranium deposits, Northern Territory, Australia: Proceedings of International Uranium Symposium on the Pine Creek Geosyncline, p. 375-395.

Yund, R.A., 1961, Phase relations in the system Ni-As: Econ. Geol., v. 56, p. 1273-1296.

Yund, R.A., 1962, The system Ni-As-S : phase relations and mineralogical significance: Am. Jour. Sci., v. 260, p. 761-782.

12. APPENDIX I

12.1 Electron Microprobe Analyses of the Arsenides and Native Silver

The electron microprobe analyses performed during this study involved both the energy- and wave- length techniques on an Applied Research Laboratories--EMX microprobe fitted with an Ortec energy dispersive spectrometer. For the arsenides, which were analysed by the energy dispersive technique, synthetic nickel sulphide, synthetic cobalt sulphide and stibnite were used as standards for nickel, cobalt and antimony respectively. Arsenopyrite was used as standard for iron, arsenic and sulphur. An operating voltage of 15 kV and an aperture current of 250 nA were used. Count times of 400 seconds were used for both the standards and the samples. The limit of detection for the elements is 0.05 wt.% and the maximum percentage error is $\pm$0.05% at the 99% confidence level.

Native silver samples were analysed by the wavelength dispersive technique. The analytical X-ray lines chosen were Lβ for Ag; Lα for As, Te, Sb; Mα for Bi, Au, Pb, Hg; Kα for Cu, Ni, Zn, Co and Fe. Silver metal was used as standard for Ag analysis. 'CANMET' synthetic standards were used for Co, Hg, Te, Au and Sb. Sphalerite, chalcopyrite, matildite, arsenopyrite, and millerite were used as standards for the analyses of Zn, Cu, Fe, Bi, As and Ni. An operating voltage of 15k kV and an aperture current of 100 nA were used as operating conditions for the analyses. The limit of detection is 0.01 wt.% and the maximum percentage error is about $\pm$1% at 99% confidence level. The analytical data were processed by the computer program EDATA 2 (Smith *et al.*, 1981) which makes corrections for matrix ("ZAF") effects.

12.2 Fluid Inclusion Analyses

Small chips of quartz, calcite, dolomite and fluorite, belonging to different paragenetic sequences, were selected for investigations. One side of the sample was first polished and the sample mounted on a glass slide with LOC-WAX 40 (high molecular weight glycolpthalate thermoplastic) and left overnight to dry. The plates were then ground to varying thicknesses (less than a millimetre) depending upon the transparency of the minerals. The other side was then polished in a similar manner. The polished plates were then studied under the petrographic

microscope and inclusions suitable for microthermometric work were selected. Microthermometric experiments were carried out in a Chaixmeca model VT2120 heating and freezing stage. The instrument was calibrated for both heating and freezing experiments by using a series of standards supplied by the Centre de Recherches Petrographiques et Geochimiques, Nancy, France. The standards included pure liquid CO_2 inclusions in quartz from Switzerland and a series of Merck Co. solid melting point standards ranging in M.P. from $+70^{\circ}$ to $+398^{\circ}C$. Replicate runs on the same inclusions gave $\pm 0.1^{\circ}C$ for freezing and $\pm 1^{\circ}$ to $\pm 3^{\circ}C$ at higher temperatures for heating.

12.3 Oxygen-, Carbon- and Hydrogen- Isotope Analyses

12.3.1 Oxygen and carbon isotope ratios

Calcites, dolomites, siderite and rhodochrosite from the Great Bear Lake region were analysed for oxygen and for carbon isotopes. The carbonate samples were ground to less than 200 mesh size. About 30 mg of the sample were reacted with 100% phosphoric acid, under vacuum, at 25°C (McCrea, 1950). The calcite samples were reacted for 12 to 24 hours, while the dolomites were reacted for 3 to 6 days. The siderite and rhodochrosite samples were reacted for 10 to 12 days. The technique, based upon the different reaction rates of carbonate minerals, was used to analyse the calcareous siltstones, as it was not possible to separate the carbonate minerals from these rocks. The CO_2 liberated in the first hour was thus assumed to have evolved from calcite, whilst the gas evolved from 4 to 72 hours was assumed to be from dolomite.

The coarse-grained quartz samples were hand picked. The quartz samples which were intergrown with the arsenide minerals were first separated by heavy liquids and then purified using hydrochloric and hydrofluorosilic acids. All the samples were ground to less than 200 mesh size. The technique of Clayton and Mayeda (1963) was used to extract oxygen from the quartz samples. All the analyses were carried out using a VG Micromass 602C isotope ratio

mass spectrometer.

12.3.2 Hydrogen isotope ratios

Water extracted from fluid inclusions in quartz, calcite, dolomite and nickeline was analysed for hydrogen isotope ratios. The samples were cleaned, dried and heated *in vacuo* to remove any adsorbed water. The samples were crushed under vacuum and the released water was collected using a liquid nitrogen trap. The extracted water was next reacted with uranium metal at 750°C (Friedman,1953). The liberated hydrogen was analysed mass spectrometrically. The water samples from the mine sites, the Camsell River and Great Bear Lake were also analysed similarly for hydrogen isotope ratios. The crushing stage and the hydrogen extraction lines are shown in Plates 31 and 32.

12.4 Lead and Strontium Isotope Analyses

The coarse-grained carbonate, galena and chalcopyrite samples were hand picked and were ground to less than 200 mesh size. The carbonates (50 to 100 mg) were dissolved in nitric acid and spiked with a mixed Rb-Sr spike solution. Hydrofluoric acid had to be added to nitric acid to dissolve two samples which contained minor amounts of quartz and native silver. The solutions were left overnight on hot plates for complete dissolution of the samples. The solutions were then converted to nitrates by treating twice with concentrated HNO_3 and in 5 ml HNO_3 solution. $Ba(NO_3)_2$ co-precipitation technique was used for Rb-Sr separation. Sr was separated from the precipitate using ion exchange columns loaded with Dowex 50 8X cation exchange resin and eluted with 2.5 N HCl. The supernatent which contains Rb was dried and treated with HCl. Rb was separated in the similar way as Sr.

For Pb, the procedure was similar to Sr upto $Ba(NO_3)_2$ co-precipitation stage. The precipitate which contained Pb was dissolved in water, and Pb was separated using ion exchange columns loaded with Dowex 50 8X chloride anion exchange resin eluted with 1.5 N HCl. Galena and chalcopyrite were also dissolved in HNO_3. Pb was separated through chloride

COLOURED PICTURES
Images en couleur

Plate 31. The crushing stage for extracting fluid inclusion waters.

COLOURED PICTURES
Images en couleur

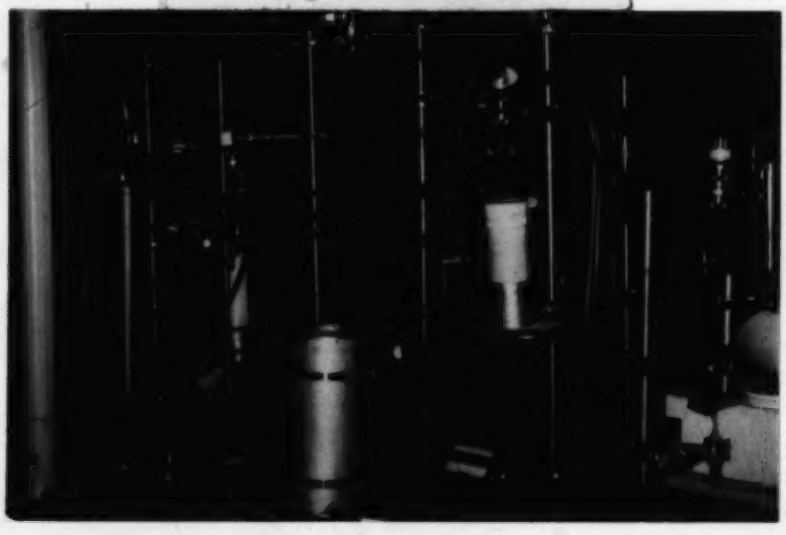

Plate 32. The hydrogen extraction line.

anion exchange columns.

Isotopic compositions were measured by double Re-filaments (for Sr) and single Re-filaments silica gel (for Pb) methods in a micromass MM-30 solid source mass spectrometer. Total blanks were found to be negligible for Rb (less than 5 ng), Sr (less than 2 ng) and Pb (less than 2 ng). The two sigma errors of estimate used for $^{87}Sr/^{86}Sr$ and $^{87}Rb/^{86}Sr$ are 0.03% and 1% respectively. For Pb analysis, estimated one sigma errors used are 0.42 per mil ($^{206}Pb/^{204}Pb$) and 0.60 per mil ($^{207}Pb/^{204}Pb$).

13. APPENDIX II

Magmatogene silver-bearing vein deposits - possible protolithic precursors

ROGER D. MORTON and AMARENDRA CHANGKAKOTI

Department of Geology, Earth Sciences Building, University of Alberta, Edmonton, Alberta T6G 2E3, Canada

ABSTRACT

The origins of the silver-bearing, polymetallic element associations of vein deposits in the Great Bear Lake region might be related to metalliferous sedimentary protoliths, incorporated during anatexis into S-type granitic rocks. Wholesale capture of metals and metalloids by biota and by their remains, during Lower Proterozoic times, might have preceeded or accompanied any increase in oxygen in the Precambrian atmosphere. Organic-rich sedimentary protoliths with captured metals could release polymetallic associations to magmatic/metamorphic hydrothermal systems upon metamorphism and anatexis. The metallogenic effects of a Lower Proterozoic *bioexplosion* could be of great importance and far reaching, in that they might account for the polymetallic signatures of numerous younger, remobilized metalliferous systems.

Introduction

The silver-bearing, bonanza vein deposits of the Great Bear Lake region of Canada's Northwest Territories, discovered in 1930, have been the source of a largess of silver and uranium, and of considerable academic controversy. Work by various researchers (Boyle, 1968; Badham *et al*, 1972; Badham, 1973, 1975; Robinson, 1971; Robinson and Ohmoto, 1973; Shegelski, 1973; Withers, 1979) has failed to elucidate the ultimate origins of the associated metals and metalloids in these polymetallic deposits.

Silver-bearing veins in the Great Bear Lake district are fault-controlled, within roof-pendants suspended in the upper levels of the Proterozoic (Hudsonian) Great Bear batholith and partly in high-level sectors of the batholithic suite. The batholith itself is partly roofed by a remnant cover sequence (represented by mineralized pendants) of Middle Proterozoic, continental, calc-alkalic volcanics and volcaniclastics with minor clastic wedges. The volcanics range in composition from basaltic, through andesitic and dacitic to rhyolitic. The lower part of the sequence contains alkalic basalts, overlain by thick rhyolitic to dacitic ignimbrites and associated volcaniclastics. This dominantly volcanic cover sequence is cut and

metamorphosed by epizonal, intermediate to felsic plutons which represent magmas in part coeval and consanguineous with the volcanics. Older monzonitic to syenitic plutons are folded and intruded by a younger suite of Hudsonian biotite granites. Hoffman and McGlynn (1977) noted that this trend towards more felsic plutonism "....reflects a progressively greater contribution of melts derived by crustal anatexis". The increasing destruction of a suite of older, perhaps Lower Proterozoic, supracrustals is inferred.

Within the cover, now represented by the roof pendants, a marked regional, northeast-trending, structural anistropy is imparted by quasi-vertical fault systems, diabase dykes and by giant quartz veins. North-east trending, en-echelon fault sets carry the polymetallic veins which are characterised by U, Ag, Ni, Co, As, Pb, Cu, Zn, Au, Hg, Sb, Fe, Mn, Bi, Ba, S, Se and Te mineralization.

The Great Bear Lake region constitutes a metallogenic province in which polymetallic veins appear to be related to hydrothermal activity within the higher levels of a plutonic complex and its cover rocks. Thus Badham (1975, 1976) concluded that the deposits belong to the *magmatic-hydrothermal* class. The present authors agree, but we wish to examine the fundamental question as to why, this particular polymetallic association occurs elsewhere (e.g. Western Europe and South America) and is commonly associated with high-level, S-type granitic intrusions. These other examples have been documented by such authors as Bernard (1970), Gillerman (1968), Krieger (1935) and Rosler and Bauman (1970).

Previous Hypotheses and their inference

Two major theories on the origins of the Great Bear Lake region polymetallic veins were forwarded by Robinson and Ohmoto (1973) and by Badham (1975, 1976). Robinson and Ohmoto postulated that the veins were emplaced at depths of 2.5 to 4.5 km, from a "uniform" hydrothermal fluid. They also thought that the fluid was a connate, marine brine with a salinity of 35 wt.% NaCl equivalent.

Badham (1975, 1976) postulated a magmatic-hydrothermal origin for the silver-bearing veins. He noted the strong similarity between these deposits, with their association of Ag-Ni-Co-As-Bi-(U), and those of the classic Schneeberg-Joachimsthal type in Europe and in the cordillera of South America, where Ag, Ni, Co, Bi, As and occasionally U, were common associates (Ramdohr, 1980). However, at the same time he emphasized the apparent lack of early Sn, W and Au mineralization commonly observed in the other localities. Thus the deposits presented another enigmatic facet.

We therefore reach a stage where these polymetallic veins are considered as classic magmatic hydrothermal systems related to high level, felsic plutons. If this is the case, then the origin of such polymetallic deposits must be sought in the precursors of the anatectic melts. If such precursors were sediments, the polymetallic element association preserved in the present-day veins would indicate *black shale* protoliths (i.e. pelitic rocks with metal-organic compounds in abundance), or organic sediments akin to coal (Valkovic, 1983). The apparent lack of Sn, W, and Au might be explained by the high-level situation of the Great Bear Lake veins postulated by Robinson and Ohmoto (1973), with the vein systems being zoned in depth and richer in Sn, W and Au. Otherwise the metal association might be simply attributable to the unique geochemical signature of the source rocks.

Possible sources of the element associations in the silver-bearing deposits

What are the possible origins of the constituent elements of such polymetallic veins? If the above ideas are correct, one might look to an older Proterozoic sequence of sediments as being likely protoliths. Older, Archean precursors would be less likely to carry the localised, large volumes of organic compounds necessary to explain the quantities of metals contained within the present day, remobilized, vein assemblages. The evolution of the Proterozoic biosphere thus has important implications.

The first prokaryotes, comparable to modern bacteria, had developed by 3500 Ma ago. Their geochemical influence was, for a long time, limited and localized to "sinks" in marginal marine or lacustrine environments. It was not until around 2400 Ma ago that the widespread proliferation of photosynthetic cyanobacterial mats within anoxic, shallow marine waters took place; and this might have resulted in the first wholesale dramatic rise in the oxygen level of the atmosphere (Walker, 1977). It is possible too that at this time the open waters of the sea were populated by significant planktonic communities, both of prokaryotic and possibly of primitive eukaryotic affinity (Vidal, 1984). These primitive eukaryotes were probably unicellular, photosynthetic forms, comparable to modern chroococcoleans. The explosive development of the red-tide like "blooms" of planktonic cyanobacteria could well have been commonplace phenomena in regions where the ancient Archean land surface was releasing floods of nutrient-rich water into nearshore environments or into land-locked lake systems. Such systems might have been hypersaline or mesosaline in character and analagous either to the lakes of the Great Rann of Kutch in western India, Lake Nakuru in Kenya (Hutchinson, 1970) and the Tanatar Lakes of the Kulundu Steppe in the U.S.S.R. (Strakhov, 1970), or to the lagoons of Laguna Ojo de Liebre in Baja California, Laguna Madre in Texas and the Sivash of the southwest Soviet Union. Kirkland and Evans (1981) emphasized the phenomenal potential of stratified mesosaline (4 to 12% salinity) systems for the production and preservation of thick organic deposits which might serve as petroleum source-rocks. Whilst this concept has appeal in explaining the petroleum source-rock potentials of evaporitic sequences, it might equally be applied to the search for organo-metallic precursors of polymetallic mineral associations such as those under discussion here.

The concept of the oxyatmoversion event some 2400 Ma ago (Salop, 1983) implies a profound change in the inorganic geochemistry of such elements as iron and uranium. But what of the equally profound effect of developing biota? Prolific growth of shallow benthic microbial communities could have induced a profound change in the chemistry of metals and

associated elements in solution. For the first time in the Earth's history organometallic[3] and metallorganic[4] compounds would have been synthesized in large volumes and the biota, both during life cycles and after death, would play a major role, (in the form of a *bioexplosion*) in the geochemistry of shallow bodies of water. Metals and metalloids, which for many years had remained in solution or had been locked into insoluble compounds, would be captured and bonded to organic ligands, complexed with carbon compounds, chelated and form salts with organic acids and be reduced by metabolic products such as H_2S, H_2 and CH_4. Hence, large amounts of metals and metalloids would become trapped in organic slimes. Thus an era of biomineralization would commence and the onset of a major role of organic geochemistry in the environment would be seen.

Recent publications (Lowenstam (1981), Fyfe (1984) and Shotyk (1984)), define the major role played by biochemical processes in modern marine, fluvial and lacustrine environments. Not only do some 30% of the elements play bioessential roles (Mertz, 1981), but inadvertantly the organisms and their post-mortem remains often provide key molecules for the precipitation and dissolution of many elements. Thayer (1974) demonstrated the widespread occurence of organic complexes of Fe, Ni, Co, Cu, Hg, Sn, Pb, Sb, Bi, Ga, In, Ge, Tl, As, B, P, Si and Te. We now know that Au will form stable, water-soluble, biomolecular complexes and may be sequestered by bacteria. Certain algae have been shown to methylate As, Se, Te, Hg, Sn and possibly Cd and Pb (Shotyk, 1984). Indeed, such highly toxic metals as U may be precipitated into and incorporated within certain algae (Mann and Fyfe, 1983). The results of this wide spectrum of possible biochemical metal-capture and -precipitation mechanisms have long been evident in the polymetallic signatures of carbonaceous sedimentary rocks such as black shales, coals and crude-oil bearing strata. The "black shale association" of V, Cr, Mn, Co, Ni, Cu, Fe, Zn, Mo, Ag, Pb, U, Ba, Zr, Se, S and As (Bell, 1979) may be compared with that of coals (Vakovic, 1982), which also includes Be, Ba, Sr, B, Sc, Y, the Lanthanides, Zr, V,

---

[3]Complexes involving direct C to metal bonds
[4]A general term for metal ions with coordinate bonds onto organic ligands using non-C donors such as N, S, P, As and O.

Co, Ni, Mo, U, Zn, Ga, Ge, As, Sb, Cd and Sn. Together, these associations illustrate the potential power of organic fractions in sediments for the generation of such polymetallic associations as are today observed in the veins of the Great Bear Lake area.

It is thus not illogical that such a bioexplosion, around 2400 Ma ago, could have been responsible for the wholesale capture and precipitation of a wide spectrum of metals and metalloids to form what today would be classified as typical black shale and/or coal and/or oil associations. The local magnitude of such capture and precipitation during the life of the microorganisms, or in post-mortem diagenesis, might have been immense if one considers the uniformitarian analogy of modern-day red tides and the phenomenal bioproductivity of some evaporative lakes and tropical lagoons around the world. The subsequent burial, metamorphism and anatexis of such Lower Proterozoic metallorganic- and organometallic-rich sediments could then release to fugitive hydrothermal fluid phases, a broad spectrum of elements. Such elements would then migrate to form polymetallic mineral deposits in and above S-type anatectic granitoids.

Conclusions and further inferences

This paper proposes that the silver-bearing polymetallic vein associations, found within the roof-pendants and upper intrusions of the Great Bear batholith, might have originated as biogenic metallorganic- and organometallic-associations within a sequence of Lower Proterozoic sediments. During the Hudsonian orogeny, these organic- and metal-rich strata were metamorphosed and suffered anatexis to generate S-type granitoid melts with associated magmatic-hydrothermal systems. The polymetallic, silver-uranium bearing associations would, in such a case, reflect not only specific magma types and particular geotectonic settings (Badham, 1975, 1976), but geochemical systems dominated by the organic and metal-organic signatures of protoliths.

The implications of such a major metallogenic epoch in the early Proterozoic development of the biosphere, hydrosphere, lithosphere and atmosphere are profound. One

must look to the early Proterozoic bioexplosion as being capable of explaining a number of otherwise "enigmatic" metalliferous associations within Precambrian domains. Not only might the presence of localized prolific biota and their remains explain the common association of U, Ag, Ni, Co, As and Bi, but it might well explain the limited spectral associations of such elements as Co-Au and Ni-Bi, occasionally observed in various localities to the south of the Great Bear Lake area, within the southern sectors of the Slave Province (e.g., the East Arm of Great Slave Lake). Ultimately too, the remobilized deposits of the unconformity associated type found in northern Canada and in northern Australia could probably form a genetic continuum with the deposits discussed herein. If such is the case, the eventual list of elements found in these giant U-Ni deposits should include such "exotic" elements as Sn, Ge, Ga, Be, and Zr.

It is perhaps worth emphasizing that the biogenic origins and processes postulated here are not unique, in that they operated, to some localized degree, prior to the Lower Proterozoic epoch (witness the role of cyanobacterial mats in the generation of some parts of the Witwatersrand Au-U deposits) and continue to do so to the present day. What was probably uniquely non-uniformitarian about the bioexplosion in the Lower Proterozoic epoch was the probable large magnitude of its metallogenic effects.

Acknowledgements

The authors are indebted to W. Padgham of D.I.A.N.D. in Yellowknife who kindly arranged finances for our research program in the Northwest Territories and to C.R. Stelck and H. Baadsgaard who offered critical comments on the original manuscript.

References

Badham, J.P.N. 1973. Volcanogenesis, Orogenesis and Metallogenesis, Camsell River, N.W.T., Canada, Ph.D. Thesis, University of Alberta, 363pp.

---------- 1975. Mineralogy, paragenesis and origin of th Ag-Ni, Co arsenide mineralization, Camsell River, N.W.T., Canada, Mineralium Deposita, 10, pp.153-175.

---------- 1976. Orogenesis and metallogenesis with reference to the silver-nickel, cobalt arsenide ore association. In : Metallogeny and Plate Tectonics, ed. D.F. Strong. Geological Association of Canada, Special Paper, 14, pp.559-571.

Badham, J.P.N., Robinson, B.W. and Morton, R.D. 1972. Geology and genesis of the Great Bear silver deposits. Proceedings 24th International Geological Congress (Montreal), Section 4, pp.541-547.

Bell, R.T. 1978. Uranium in black shales - A review. In : Uranium Deposits : Their mineralogy and origin. Mineralogical Association of Canada Short Course Handbook, volume 3. ed. M.M. Kimberley, pp.307-329.

Bernard, J.H. 1970. Gradual decrease of the spatial relation between the Variscan Granitoid Plutons and the persistent ore-forming hydrothermal mineral associations of the Bohemian massif. International Union of Geological Sciences, volume 2, pp.58-60.

Boyle, R.W. 1968. The geochemistry of silver and its deposits. Geological Survey of Canada, Bulletin 160, 264pp.

Fyfe, W.S. 1984. The geochemical cycle. In : Environmental Geochemistry. Mineralogical Association of Canada. Short Course Handbook, volume 10, May 1984. Editor M.E. Fleet.

Gillerman, E. 1968. Uranium mineralization in the Burro Mountains, New Mexico. Economic Geology, volume 63, pp.239-246.

Hoffman, P.F. and McGlynn, J.C. 1977. Great Bear Batholith : A volcano-plutonic depression. In : Volcanic Regimes in Canada. eds. W.R.A. Baragar, L.C. Coleman and J.M. Hall. Geological Association of Canada, Special Paper, 16, pp.170-192.

Hutchinson, G.E. 1967. A treatise on limnology. Volume 2, Introduction to lake biology and limnoplankton. John Wiley and Sons, New York. 1115pp.

Kirkland, D.W. and Evans, R. 1981. Source-rock potential of evaporitic environment. American Association of Petroleum Geologists Bulletin,volume 65, no.2, pp.181-190.

Krieger, P. 1935. Primary silver mineralization at Sabinal, Chihuahua, Mexico. Economic Geology, volume 30, pp.242-259.

Lowenstam, H.A. 1981. Minerals formed by organisms. Science, 211, pp.1126-1131.

Mann, H. and Fyfe, W.S. 1984. Selective uptake of barium and uranium by algae. Chemical Geology (in press).

Mertz, W. 1981. The essential trace elements. Science, volume 213, pp.1332-1338.

Ramdohr, P. 1980. The ore minerals and their intergrowths. 2nd edition, volume 1, 440pp.

Robinson, B.W. 1971. Studies on the Echo Bay Silver Deposit, N.W.T., Ph.D. Thesis, University of Alberta, 256pp.

Robinson, B.W. and Ohmoto, H. 1973. Mineralogy, fluid inclusions and stable isotopes of the Echo Bay U-Ni-Ag-Cu deposits, N.W.T., Canada. Economic Geology, 68, pp.635-656.

Rosler, H.J. and Bauman, L. 1970. On the different origin of Variscan and post-Variscan mineralizations in Central Europe. International Union of Geological Sciences, volume 2, pp.72-77.

Salop, L.J. 1983. Geological Evolution of the Earth during the Precambrian. Springer Verlag.

Shegelski, R.J. 1973. Geology and Mineralogy of the Terra Silver Mine, Camsell River, N.W.T., M.Sc Thesis, University of Toronto, 169pp.

Shotyk, W. 1984. Metal-organic species in natural waters. In : Environmental geochemistry. Mineralogical Association of Canada, Short Course Handbook, volume 10, May 1984. Editor M.E. Fleet.

Strakhov, N.M. 1970. Principles of lithogenesis. Plenum Press, New York. 577pp.

Thayer, J.S. 1974. Organometallic compounds and living organisms. Journal of Organometallic Chemistry, volume 76, pp. 265-295.

Valkovic, V. 1983. Trace elements in coal. volume 1. Chemical Rubber Company Press, Baton Rouge, 224pp.

Vidal, G. 1984. The oldest eukaryotic cells. Scientific American, volume 250, number 2, pp.48-57.

Walker, J.C.G. 1977. Evolution of the atmosphere. Macmillan, New York, 285 pp.

Withers, R.L. 1979. Mineral deposits of the Northrim Mine and a brief enquiry into the genesis of veins of the (Ag, Bi, Ni, Co, As) type. M.Sc. thesis, University of Alberta, 271pp.